The Pennsylvania State University

The Graduate School

College of Engineering

INVESTIGATING AND EMPLOYING MICROBIAL FUNCTIONS IN BIOELECTROCHEMICAL SYSTEMS FOR BIOENERGY PRODUCTION

A Dissertation in

Environmental Engineering

by

Hengjing Yan

Submitted in Partial Fulfillment
of the Requirements
for the Degree of

Doctor of Philosophy

August 2013

The dissertation of Hengjing Yan was reviewed and approved* by the following:

John M. Regan
Professor of Environmental Engineering
Dissertation Advisor
Chair of Committee

Bruce E. Logan
Evan Pugh and Kappe Professor of Environmental Engineering

William D. Burgos
Professor of Environmental Engineering
Chair of Graduate Program

Jason Kaye
Associate Professor of Soil Biogeochemistry

*Signatures are on file in the Graduate School

ABSTRACT

Microbial fuel cells (MFCs) rely on microbes serving as the biocatalysts for bioenergy recovery from organic feedstocks, such as wastewater. Microbes can work on both the anode and cathode electrodes for electron transfer, or contribute distinct functions combined with bioelectrochemical systems (BESs). For a better understanding and application of microbial functions in BESs, investigations were conducted on anode community behaviors corresponding to different electrochemical conditions, the potential application of clostridia biocathodes for biofuels production, and combined nutrient treatment in MFCs with a nitrifier-enriched mixed community.

Serving as biocatalysts in anode electron transfer, exoelectrogenic bacteria and their co-colonizers on the anode electrode are subject to various changes in the system operating conditions. Anode potentials in BESs were found to affect both the electrochemical performance and the microbial community structures of the systems. The performance of MFCs under both potentiostatic operation and fixed external resistance has been previously studied. To investigate whether setting anode potentials will result in distinct microbial communities from dynamic anode potentials, fixed anode potentials of -250 mV and -119 mV vs SHE (throughout) were picked to match with the negative peak anode potentials obtained from MFCs operated with a fixed external resistance of 1 kΩ and 47 Ω, respectively. Pyrosequence data from two-month time series samples showed hindered enrichment of *Geobacter* spp. in a more diverse anode bacterial community at the lower fixed anode potential (-250 mV) compared to 1 kΩ, though more comparable *Geobacter* abundances in anode biofilms were found between the -119 mV and 47 Ω reactors. Setting the anode potential at the negative peak values results in less energy extraction by the microorganisms for growth, which might have slowed down the development of the whole anode microbial community as well as the enrichment of exoelectrogenic bacteria. In addition, a

possible limitation of potentiostatic operation with a volumetric anode is uncertainty in the actual anode potential due to variable proximity to the reference electrode. This study indicated that a balance between screening exoelectrogenic bacteria and encouraging microbial growth needs to be considered when setting a low anode potential in BESs.

Exoelectrotrophic bacteria contribute to *cathode* electron transfer and are helpful in converting electrical energy to other useful energy carriers or products. Altered electron flow has previously been induced in *Clostridium acetobutylicum* fermentation using electrochemical energy as a source of reducing equivalents in the presence of the electron mediator methyl viologen. Also, *C. acetobutylicum* was demonstrated to produce exclusively hydrogen using cathode-derived electrons under organic-free conditions in the presence of methyl viologen. Recently, *C. acetobutylicum* was demonstrated to generate current in MFC anodes without the addition of redox mediators. The study here was aimed at testing the possibility of using electrical energy *without* exogenous mediator addition to influence the distribution of valuable extracellular products, such as hydrogen, butanol, and ethanol, using *C. acetobutylicum* as the cathode biocatalyst. *C. acetobutylicum* was demonstrated to be exoelectrotrophic with a fixed cathode potential at -400 mV and organic carbon sources. A current uptake of up to 83 mA/m^2 was achieved by *C. acetobutylicum*, with a decreasing trend over time that electrochemical impedance spectroscopy showed was probably due to an increased cathode charge transfer resistance. Control experiments and cyclic voltammetry tests ruled out abiotic electrochemical hydrogen evolution and electron shuttles for electron transfer, suggesting that the cells derived electrons directly from the electrode. Increased yields of more energy dense products (hydrogen and butanol) and decreased yields of butyrate, acetate, and ethanol were found with current uptake by *C. acetobutylicum*. The electron balance indicated that current uptake might have also reduced the biomass production of *C. acetobutylicum*. This study demonstrated the non-mediated exoelectrotrophic phenotype of a solventogenic bacterium. The metabolic flux shift with current

uptake found in this study provides a primary guidance for the potential utilization of a *C. acetobutylicum* biocathode in a BES.

Single-chamber MFCs with nitrifiers pre-enriched at the air cathodes have previously been demonstrated as a passive strategy for integrating nitrogen removal into current-generating BESs. To further define system design parameters for this strategy, the effects of oxygen diffusion area and COD/N ratio in continuous-flow reactors were investigated. Doubling the gas diffusion area by adding an additional air cathode or a diffusion cloth significantly increased the ammonia and COD removal rates (by up to 115% and 39%), ammonia removal efficiency (by up to 134%), the cell voltage and cathode potentials, and the power densities (by up to 124%). When the COD/N ratio was lowered from 13 to 3, up to 244% higher ammonia removal rate but at least 19% lower ammonia removal efficiency were detected. An increase of COD removal rate by up to 27% was also found when the COD/N ratio was lowered from 11 to 3. The Coulombic efficiency (CE) was not affected by the additional air cathode, but decreased an average of 11% with the addition of a diffusion cloth. Ammonia removal by assimilation was also estimated to understand the ammonia removal mechanism in these systems. These results show that the doubling of gas diffusion area enhanced N and COD removal rates without compromising electrochemical performance.

TABLE OF CONTENTS

LIST OF FIGURES

LIST OF TABLES

LIST OF ABBREVIATIONS

Anammox	Anaerobic Ammonia Oxidation
AOA	Ammonia-Oxidizing Archaea
AOB	Ammonia-Oxidizing Bacteria
BES	Bioelectrochemical System
CE	Coulombic Efficiency
CEM	Cation Exchange Membrane
CR	Coulombic Recovery
EIS	Electrochemical Impedance Spectroscopy
HRT	Hydraulic Retention Time
MEC	Microbial Electrolysis Cell
NOB	Nitrite-Oxidizing Bacteria
MFC	Microbial Fuel Cell
PTFE	Polytetrafluoroethylene
WWTP	Wastewater Treatment Plant

ACKNOWLEDGEMENTS

I would like to express my deepest gratitude to my advisor Dr. John M. Regan, for his patient guidance, enthusiastic encouragement, and most importantly, his strong supports to my long-term career goals during my five years graduate study at Penn State. Dr. Regan's mentorship has helped me grow not only as an Environmental Engineer but also a researcher with independent thinking and effective communication skills. His intellectual heft, genuinely good nature, and down-to-earth humility set an academic model for me, and I am truly fortunate to have had the opportunity to work with him.

Besides my advisor, I also would like to offer my special thanks to the rest of my dissertation committee: Dr. Bruce E. Logan, Dr. William D. Burgos, and Dr. Jason Kaye, for their insightful comments and hard questions that have proved this dissertation.

I am particularly grateful for the advices and assistances given by labmates Matt Yates, Dr. Justin Tokash, Dr. Xiuping Zhu, Dr. Fang Zhang, Dr. John Pisciotta, Zehra Zaybak, and Dr. Xiaoyu Zhu on the research projects included here. I would give many thanks to my labmate Hiroyuki Kashima for sharing experiences and advices on my experiment. I am thankful to staff members David Jones, Peggy VanOrnum, Judy Heltman, and Amy Case for accommodating my research and study during this time.

Financial supports from King Abdullah University of Science and Technology (KAUST) through my graduate study and Army Research Office Equipment on part of the research included here are greatly acknowledged.

I am also thankful to my friends, Siqin He, Robert Davis, Yunhui Tan, Wulin Yang, "Reviver" members, and all the rest, for enriching my life and helping me overcome the difficulties during my graduate study. Especially thanks to Dr. Xi Xiong, for his broad understanding and constant supports to my study and life though the past five years.

Finally, none of this would have been possible without the love and understanding of my parents. I want to express my heart-felt gratitude to my parents for being my source of strength and encouraging me throughout this meaningful endeavor.

Hengjing Yan

August 2013

Chapter 1

Introduction

1.1 Global energy consumption and challenges

At the beginning of the 21st century, the global population expanded to 6.1 billion and the total energy consumption reached 4.19×10^{19} J [1]. The energy source for the primary energy use mainly came from oil (35%), coal (23%), and natural gas (22%), with traditional biomass (9.3%), nuclear (6.9%), and hydro (2.3%) constituting most of the non-fossil fuel contributions [1]. New renewable energy sources, including modern biomass (which refers to biomass produced in a sustainable way and used for electricity generation, heat production, and transportation), small hydropower, geothermal energy, wind energy, solar energy, and marine energy, contributed a total of 2.2% to the global primary energy use [1]. Due to the recent discovery of large shale gas reservoirs, it is projected that the U.S. domestic natural gas consumption will remain steady or even slightly increase from 26% of the primary energy use in 2011 to 28% in 2040 [2]. However, with the finite storage of the fossil fuels coal, oil, or natural gas can only supply the energy needs of human society for a limited time [1]. Additionally, conventional utilization of coals, oil, and natural gas contributes a net release of carbon dioxide to the atmosphere, which will accelerate global climate change. Despite positive developments in some countries, global energy-related carbon dioxide emissions increased by 1.4% to reach 3.16×10^{13} kg during 2012 [3]. Therefore, more research efforts are required to investigate a proper and expanded utilization of alternative energy sources for sustainable development.

Two current alternative energy approaches, namely nuclear fission and solar energy, have drawn a lot of attention. While proposed as a carbon-neutral energy source, nuclear fission still

has limitations in application due to the safety concerns of uranium mining and long-term nuclear waste storage. Solar panels can efficiently capture and provide energy during daylight hours, but efficient methods of solar energy storage for nighttime hours are still lacking. “Modern” biomass is a good storage method for solar energy, but the required land area for biomass to meet existing energy demand is not practical [4]. This current situation necessitates further research on these alternative energy capture technologies or expanded investigation on other emerging renewable energy approaches.

1.2 Energy recovery from wastewater

For sanitation purposes, most wastewater treatment plants (WWTPs) spend considerable energy to remove biodegradable organic matter from the wastewater. For example, approximately 1.5% of the electricity use in the U.S. goes to wastewater treatment processes [5]. However, these biodegradable organics contain energy, and this potential energy storage can be eight times greater than the energy required for their treatment [6]. If we could recover part of this energy, we could make the water infrastructure more energy efficient or even self-sufficient [5], which would not only reduce our energy consumption but might also promote enhanced sanitation in countries that cannot afford the energy burden of conventional technologies.

Several technologies of energy recovery from wastewater have been developed to benefit the sustainability of the energy-water nexus, such as anaerobic digestion of wastewater, turbine electricity production from hydraulic head loss, thermal energy extraction, incineration of dry biosolids, and gasification of biosolids. Among these, anaerobic digestion of wastewater is the most mature technology and was applied in over 1000 public wastewater facilities in 2004 [7]. Anaerobic digestion with biogas utilization and biosolids incineration with electricity generation have been widely studied, demonstrated, and proposed to offset the electricity consumption in the

wastewater sector [8]. However, significant methane emission has been reported from both anaerobic digesters and anaerobic wastewater treatment process. For example, in a municipal WWTP with anaerobic digestion in the Netherlands, a major portion (72%) of the total methane emission was found from the anaerobic digestion facility, resulting in a higher methane emission in comparison with other two WWTPs without anaerobic sludge treatment [9]. The amount of dissolved methane in anaerobic reactor effluent was also found significant, with 3.27×10^3 kg dissolved CH_4 per day reported in the wastewater effluent [10]. Since methane has a greater greenhouse gas potential than carbon dioxide [11], a technology is required to economically capture methane emission from traditional anaerobic digestion processes to limit its adverse effect on global climate change. Also, the anaerobic digestion process usually requires a long detention time [5] and ends up with high chemical oxygen demand (COD) and nutrient contents in the effluent that exceed wastewater effluent standards [12, 13]. The removal of both digester heating and siloxanes/hydrogen sulfide from the produced biogas is required for sustainable operation of the electricity generation component [14]. Therefore, new technologies with improved energy recovery efficiency and a carbon-neutral effect on global climate change are required for wastewater treatment processes.

1.3 Microbial fuel cells for bioelectricity generation from wastewater treatment

Bioelectrochemical systems (BESs) are an emerging approach for energy and product recovery from wastewater treatment. Moreover, BESs also produce less sludge than aerobic processes, thus reducing the amount of subsequent solids handling processes [5]. Although the first observation of electricity generation by bacteria was reported a century ago [15], BES technologies were not popularly studied until the late 1990s [16, 17]. In the past decade, intensive

research has been conducted on BESs in terms of their microbiology, electrochemistry, and reactor architecture and operation [18].

The microbial fuel cell (MFC) design platform can directly generate electricity at ambient temperature from the oxidation of the organics in the waste stream [5]. The maximum power density generated by a bench-scale MFC can now reach 2080 W m^{-3} [19], though it varies greatly due to different reactor designs, electrode and membrane types, and substrate levels. Demonstrations of pilot-scale MFCs have also been performed for powering remote devices in seawater [20] or for energy recovery from wastewater [21, 22]. However, additional work needs to be done on system stability, power output, and cost reduction to make MFC applications generally practical.

While existing MFC designs have a small magnitude of power generation relative to other energy technologies, extended applications of BESs have also been developed for alternative or value-added functionality, such as desalination [23, 24], nutrient removal [25] or recovery [26] from wastewater, and caustic production [27]. Chemical storage forms of the bioelectricity generated by MFCs have also been developed such as hydrogen in a microbial electrolysis cell (MEC) [28] and organic matter in microbial electrosynthesis (MES) [29, 30]. The recovery of low-grade thermal energy with MFCs has also been reported as a strategy to enhance energy recovery in these systems [31, 32]. Since microbes play a key role in any BES format, understanding the behavior and the potential applications of microbes in the power generation and treatment processes will greatly benefit the optimization of system performance and innovation of new BES technologies for efficient energy and product recovery from wastewater.

1.4 Objectives

BESs are inherently multidisciplinary and involve many design features, including microbial considerations, materials, electrochemistry, and applications. My Ph.D. dissertation specifically focuses on the investigation and employment of *microbial* functions in BESs for bioenergy and bioproduct recovery, including microbial biofilm community studies on both the anode and cathode electrodes, biocathode utilization for influencing fermentation end products, and incorporating nitrifying bacteria in an air cathode biofilm to achieve simultaneous nitrogen and organics removal in MFCs.

The collective hypotheses of these studies were:

1. The anode microbial community develops differently between MFC reactors with constant anode potential and those with fixed resistances (which have dynamic anode potentials in fed-batch systems);
2. *Clostridium acetobutylicum* is exoelectrotrophic, i.e. can directly receive electrons from cathode electrodes without the addition of an exogenous redox mediator;
3. Cathodic electron supplementation can alter the metabolic flux in *Clostridium acetobutylicum*; and
4. Increasing gas diffusion areas will increase the nitrogen removal ability of single-chamber air-cathode MFCs.

1.5 Organization of this dissertation

This Ph.D. dissertation is organized into six chapters, including this introductory Chapter 1, a literature review of microbes in MFCs in Chapter 2, Chapters 3 through 5 that address the four proposed hypotheses, and a final chapter on future work.

In Chapter 3, I compared the microbial communities in MFCs with constant anode potentials and those with fixed resistances and the resultant dynamic anode potentials. Sets of duplicate reactors were operated at two fixed anode potentials or the corresponding fixed external resistances that gave the same minimum anode potentials. Two-month time series samples of the anode community in each MFC were analyzed by pyrosequencing. Hindered enrichment of *Geobacter* in a more diverse anode bacterial community was found in the lower fixed anode potential systems, in which there is continually less energy available for microbial growth that possibly slows down the evolution of the whole anode microbial community as well as the enrichment of exoelectrogenic bacteria. I did all the reactor preparation, operation, and data collection, the DNA sampling and extraction, metagenomic data analysis, and preparation of the first draft of a manuscript. Matt Yates helped me with the initial implementation of the mother program and provided advice on metagenomic analysis. Dr. Justin Tokash provided advice on potentiostat usage for setting anode potential. The extracted DNA was pyrosequenced by Research and Testing Laboratory at Lubbock, Texas. The manuscript of this work is currently in preparation.

In Chapter 4, I demonstrated that *C. acetobutylicum* is exoelectrotrophic by providing a fixed cathode potential of -400 mV versus Standard Hydrogen Electrode (SHE) and glucose as the organic carbon source. Abiotic electrochemical hydrogen evolution and possible electron shuttles for electron transfer were excluded by negative control experiments and cyclic voltammetry tests. Slightly increased yields of more energy dense products (hydrogen and

butanol) and decreased yields of butyrate, acetate, and ethanol were found with current uptake in a *C. acetobutylicum* biocathode relative to open-circuit systems. The electron balance indicated that current uptake might have also affected the biomass production of *C. acetobutylicum*. In this work, I did all the experiment preparation, reactor operation, and data collection and analysis except that Dr. Xiuping Zhu helped me load prepared samples to the gas chromatograph (GC) and operate the GC. The manuscript of this work is currently in preparation.

In the work presented in Chapter 5, I investigated the effects of gas diffusion area and chemical oxygen demand (COD)/N ratio in continuous-flow reactors. I doubled the gas diffusion area of the MFC system by adding an extra air cathode or diffusion cloth to the original single-chamber air-cathode MFC design, which significantly increased the ammonia and COD removal rates, ammonia removal efficiency, the cell voltage and cathode potentials, and the power densities. The results from this study demonstrated that doubling of gas diffusion area could enhance nitrogen and COD removal rates without compromising electrochemical performance. This work was summarized in a paper by Yan, H. and Regan, J., titled "Enhanced nitrogen removal in single-chamber MFCs with increased gas diffusion areas", and it was published in *Biotechnology and Bioengineering*. I did all the experimental work (including preparation, testing, data collection and analysis) and prepared the first draft of the manuscript. My co-author (my adviser) contributed to the revision and final writing of the paper.

1.6 Literature cited

1. Goldenberg, J. and T. Johansson, World energy assessment: overview 2004 update. *United Nations Development Programme (UNDP)*, 2004: p. 28.
2. EIA, Annual engergy outlook 2013: with projections to 2040, 2013, U.S. Energy Information Administration (EIA). p. 60.

3. IEA, Redrawing the energy-climate map, in *World Engergy Outlook Special Report*2013, International Energy Agency (IEA).

4. Grant, P.M., Hydrogen lifts off - with a heavy load - the dream of clean, usable energy needs to reflect practical reality. *Nature*, 2003. **424**(6945): p. 129-130.

5. Logan, B.E., Microbial fuel cells. 2008: John Wiley & Son, Inc.

6. Shizas, I. and D.M. Bagley, Experimental determination of energy content of unknown organics in municipal wastewater streams. *Journal of Energy Engineering-Asce*, 2004. **130**(2): p. 45-53.

7. NACWA, Renewable energy recovery oppoortunities from domestic wastewater, in *A clear commitment to America's waters*2009, National Association of Clean Water Agencies (NACWA).

8. Stillwell, A., D. Hoppock, and M. Webber, Energy recovery from wastewater treatment plants in the United States: a case study of the energy-water nexus. *Sustainability*, 2010. **2012**(2): p. 945-962.

9. Daelman, M.R.J., et al., Methane emission during municipal wastewater treatment. *Water Research*, 2012. **46**(11): p. 3657-3670.

10. Cakir, F.Y. and M.K. Stenstrom, Greenhouse gas production: a comparison between aerobic and anaerobic wastewater treatment technology. *Water Research*, 2005. **39**(17): p. 4197-4203.

11. Lashof, D.A. and D.R. Ahuja, Relative contributions of greenhouse gas emissions to global warming. *Nature*, 1990. **344**(6266): p. 529-531.

12. Kim, M., Y.H. Ahn, and R.E. Speece, Comparative process stability and efficiency of anaerobic digestion; mesophilic vs. thermophilic. *Water Research*, 2002. **36**(17): p. 4369-4385.

13. Song, Y.C., S.J. Kwon, and J.H. Woo, Mesophilic and thermophilic temperature co-phase anaerobic digestion compared with single-stage mesophilic- and thermophilic digestion of sewage sludge. *Water Research*, 2004. **38**(7): p. 1653-1662.

14. Opportunities for and benefits of combined heat and power at wastewater treatment facilities, 2007, Eastern Research Group and Energy and Environmental Analysis, U.S. Environmental Protection Agency: Washington, DC, USA. p. ii-10.

15. Potter, M.C., Electrical effects accompanying the decomposition of organic compounds. *Proceedings of the Royal Society of London Series B-Containing Papers of a Biological Character*, 1911. **84**(571): p. 260-276.

16. Kim, B.H., et al., Direct electrode reaction of Fe(III)-reducing bacterium, Shewanella putrefaciens. *Journal of Microbiology and Biotechnology*, 1999. **9**(2): p. 127-131.

17. Kim, H.J., et al., A microbial fuel cell type lactate biosensor using a metal-reducing bacterium, *Shewanella putrefaciens. Journal of Bioscience and Bioengineering*, 1999. **9**(3): p. 3.

18. Logan, B.E., Essential data and techniques for conducting microbial fuel cell and other types of bioelectrochemical system experiments. *Chemsuschem*, 2012. **5**(6): p. 988-994.

19. Fan, Y., S.-K. Han, and H. Liu, Improved performance of CEA microbial fuel cells with increased reactor size. *Energy & Environmental Science*, 2012. **5**(8): p. 8273-8280.

20. Tender, L.M., et al., The first demonstration of a microbial fuel cell as a viable power supply: powering a meteorological buoy. *Journal of Power Sources*, 2008. **179**(2): p. 571-575.

21. Jiang, D. and B. Li, Granular activated carbon single-chamber microbial fuel cells (GAC-SCMFCs): a design suitable for large-scale wastewater treatment processes. *Biochemical Engineering Journal*, 2009. **47**(1-3): p. 31-37.

22. Logan, B.E., Scaling up microbial fuel cells and other bioelectrochemical systems. *Applied Microbiology and Biotechnology*, 2010. **85**(6): p. 1665-1671.

23. Cao, X., et al., A new method for water desalination using microbial desalination cells. *Environmental Science & Technology*, 2009. **43**(18): p. 7148-7152.

24. Mehanna, M., et al., Using microbial desalination cells to reduce water salinity prior to reverse osmosis. *Energy & Environmental Science*, 2010. **3**(8): p. 1114-1120.

25. Yan, H., T. Saito, and J.M. Regan, Nitrogen removal in a single-chamber microbial fuel cell with nitrifying biofilm enriched at the air cathode. *Water Research*, 2012. **46**(7): p. 2215-2224.

26. Cusick, R.D. and B.E. Logan, Phosphate recovery as struvite within a single chamber microbial electrolysis cell. *Bioresource Technology*, 2012. **107**: p. 110-115.

27. Rabaey, K., et al., High current generation coupled to caustic production using a lamellar bioelectrochemical system. *Environmental Science & Technology*, 2010. **44**(11): p. 4315-4321.

28. Call, D. and B.E. Logan, Hydrogen production in a single chamber microbial electrolysis cell lacking a membrane. *Environmental Science & Technology*, 2008. **42**(9): p. 3401-3406.

29. Nevin, K.P., et al., Microbial electrosynthesis: feeding microbes electricity to convert carbon dioxide and water to multicarbon extracellular organic compounds. *Mbio*, 2010. **1**(2).

30. Nevin, K.P., et al., Electrosynthesis of organic compounds from carbon dioxide is catalyzed by a diversity of acetogenic microorganisms. *Applied and Environmental Microbiology*, 2011. **77**(9): p. 2882-2886.

31. Kim, Y. and B.E. Logan, Microbial reverse electrodialysis cells for synergistically enhanced power production. *Environmental Science & Technology*, 2011. **45**(13): p. 5834-5839.

32. Cusick, R.D., Y. Kim, and B.E. Logan, Energy capture from thermolytic solutions in microbial reverse-electrodialysis cells. *Science*, 2012. **335**(6075): p. 1474-1477.

Chapter 2

Literature Review

Bioelectrochemical systems (BESs) rely on microbes serving as the catalyst for bioelectrochemical processes at the anode and/or cathode. There are numerous BES formats designed to extract various energy carriers and products. In the microbial fuel cell (MFC) configuration, bioelectricity is a recovered product. Organic substrates are oxidized by bacteria growing on the anode electrode, with electrons delivered to the anode and protons released into the solution. On the cathode electrode, electrons transferred through the outer circuit are consumed and a terminal electron acceptor (such as oxygen) is reduced (Figure 2-1). Microbes can work on both anode and cathode electrodes for electron transfer, or carry out alternative reactions that are complementary or deleterious to the BES.

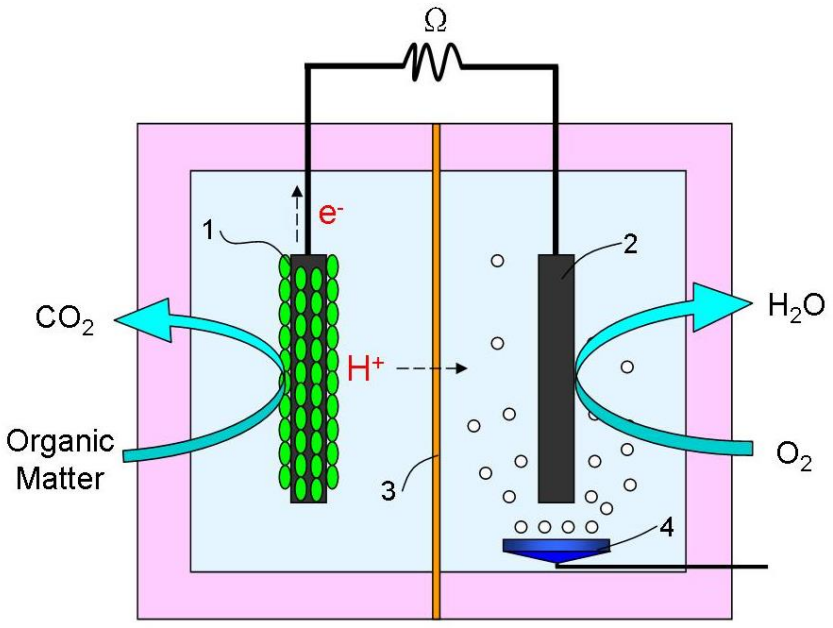

Figure 2-1: Schematic of the basic components of a two-chamber MFC. (1: anode electrode; 2: cathode electrode; 3: ion exchange membrane; 4: air sparger) (Adopted from [1])

On anode electrodes, exoelectrogenic bacteria oxide substrates, e.g., acetate to carbon dioxide. A fraction of the electrons is used by exoelectrogens for cell maintenance and growth; the remaining fraction, detected as current in the circuit, is transferred out of the cell and donated to the anode electrode for energy production [2]. Exoelectrogenic bacteria can be studied in pure culture using a sterile synthetic electrolyte, but in systems inoculated with environmental samples or fed real wastewater they will live in the anode biofilm as part of a mixed-culture microbial community. Understanding the behaviors of exoelectrogenic bacteria in mixed-culture anode biofilms will aid the design and operation of BESs for stable and efficient bioelectricity production.

On the other side of the BES circuit, exoelectrotrophic bacteria can receive electrons directly from the cathode [3]. While microbial catalysts have slower cathode-oxidizing kinetics than inorganic catalysts, there are several advantages of having a biocathode. First is the lower cost compared to noble metal catalysts that are commonly used in electrochemical cells [4]. Second, renewable bioelectricity that is produced in small magnitude can be converted by exoelectrotrophs to other storable energy forms such as potential transportation fuels [5]. Third, a biocathode can use bioelectricity to drive other treatment processes, such as bioremediation [6]. The application of biocathodes can be considered in a variety of fields.

Some other bacteria, although they do not participate in the electron transfer processes, can still grow in MFCs and catalyze other reactions that are of interest in wastewater treatment plants. For example, nitrifying bacteria (ammonia-oxidizing bacteria and nitrite-oxidizing bacteria) can be enriched in the presence of oxygen in a mixed-culture MFC for the oxidation of ammonia to nitrate oxygen [7]. The subsequent activity of denitrifiers can reduce this nitrate to nitrogen gas, thereby fully removing nitrogen from the wastewater.

2.1 Anode biofilm

2.1.1 Anodic electron transfer mechanisms in MFCs

To transfer an electron from a microbial cell to an anode electrode, the electron first needs to be transferred from the inside of the microbial cell membrane to its outside. This can be achieved via the extracellular transfer of reduced compounds, including reduced primary metabolites, or via electron transfer across the membrane between different membrane-bound redox complexes [8]. Once the electron is transferred outside of the cell membrane, it must be further directed to the anode by a redox-active species. This species could be a soluble redox shuttle or a redox protein on the outer membrane [8].

2.1.1.1 Direct electron transfer (DET)

Direct electron transfer (DET) describes a mechanism by which electrons are transferred through physical contact between the bacterial cell membrane and the anode, without the involvement of diffusible redox species [8]. Microbes capable of DET have membrane-bound electron transport proteins that can transfer electrons from the inside of the cell to its outside. From there, the electrons are further transferred to an external electron acceptor (e.g., an MFC anode) *via* an outer-membrane redox protein, such as c-type multiheme cytochromes in exoelectrogenic bacteria like *Geobacter* [9, 10], *Rhodoferax* [11, 12], and *Shewanella* [12, 13] (Figure 2-2A).

DET restricted to only the first monolayer of bacteria in the anode biofilm [11] would limit the current density in MFCs. Recently, it has been proposed that some bacteria, including species of *Geobacter* and *Shewanella*, can reduce an electrode that is not in direct contact with the outer cell membrane *via* electronically conductive molecular pili (nanowires) [14, 15]. These

pili extend from the membrane-bound cytochromes to the electrode surface and are proposed to allow electron transfer from outside of the cell to an electrode at a distance (Figure 2-2B).

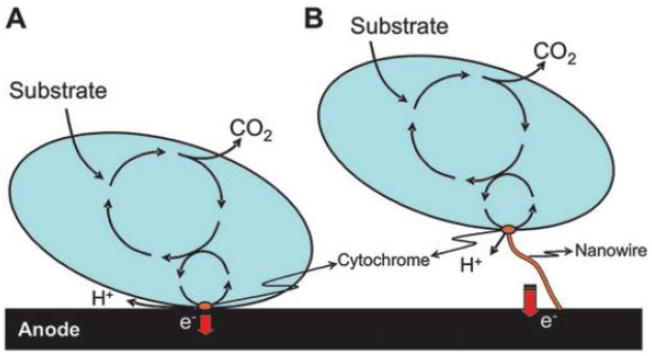

Figure 2-2. Illustration of DET via (A) membrane-bound cytochromes, (B) electronically conductive nanowires [8].

2.1.1.2 Mediated electron transfer (MET)

Generally, MFCs that solely rely on the DET process have higher efficiency in current generation but lower current densities compared to MFCs with mediated electron transfer (MET) processes. MET allows microbes to donate electrons out of the cell *via* mediating redox species, such as exogenously supplied mediators or endogenously produced mediators from secondary metabolites or reduced primary metabolites, representing an effective means to connect the microbial metabolism to the electrode.

With the very limited current generation in early MFC studies, exogenous redox mediators were often introduced to BESs to facilitate the electron transfer from cells to electrodes. Various compounds, such as potassium ferricyanide, benzoquinone, phenazines, phenothiazine, phenoxazines, and quinoes were used as MFC mediators [16-21]. However, even with the exogenous addition of redox mediators, the current densities were still low, and the requirement of a regular addition of the exogenous compound is unfeasible and environmentally questionable. Therefore, this approach has been generally abandoned and more research now

focuses on endogenous redox mediators or primary metabolites that are self-produced by the exoelectrogenic bacteria or the symbiotic bacteria in the same system.

When there are neither available soluble electron acceptors nor directly contacted solid electron acceptors, some bacteria can produce low molecular weight, electron-shuttling compounds via secondary metabolic pathways [22-24]. These shuttling compounds are reversible terminal electron acceptors that can be re-oxidized after transferring electrons from the cell to the electrode (Figure 2-3). For example, bacterial phenazines are secondary metabolites that have been shown to be involved in extracellular electron transfer [22]. Endogenous redox mediators allow electron transfer independent of the presence of exogenous redox shuttles. They are especially effective for current generation in batch cultures, where they can accumulate to appreciable concentrations. However, the identification of endogenous redox mediators is very challenging. Both *Pseudomonas aeruginosa* and *Shewanella* species have been proved or discussed to have pyocyanine, phenazine-1-carboxamide, or quinone-type redox shuttles involved in the electron transfer from cells to the anode [24, 25].

Besides endogenous redox shuttles, reduced metabolites from anaerobic respiration and fermentation can also serve as linking species for electron transfer from bacterial cell to electrode. Theoretically, if a terminal electron acceptor in anaerobic respiration has sufficiently negative redox potentials to that of an oxygen-reducing counter electrode and is reversibly oxidizable and soluble in water in both its reduced and oxidized forms, it can mediate electron transfer from a cell to an electrode (Figure 2-4A). For example, sulfate reduction by *Desulfovibrio desulfuricans* has been adopted in an MFC [26]. However, since sulfate-reducing bacteria are unable to metabolize carbohydrates, they require a co-colonization with fermenting bacteria to provide them with low molecular weight organic acids and alcohols [8]. The fermentation process can also produce energy-rich reduced metabolites (hydrogen, ethanol, or formate) that can be directly oxidized by an electrocatalytic anode (Figure 2-4B). Non-biocatalysts such as platinum and

tungsten carbide [27-29] have been applied to anodes to facilitate the oxidation of those primary metabolites; however, the potential combination of fermentative pre-digestion of carbohydrates and biocatalyzed anode electrodes is of greater practical interest.

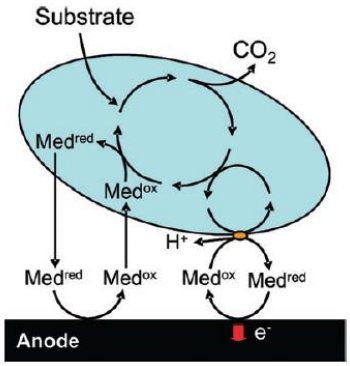

Figure 2-3. Simplified illustration of MET *via* microbial secondary metabolites. Two possible redox mechanisms are shown: shuttling via outer cell membrane cytochromes and *vi*a periplasmic or cytoplasmic redox couples [8].

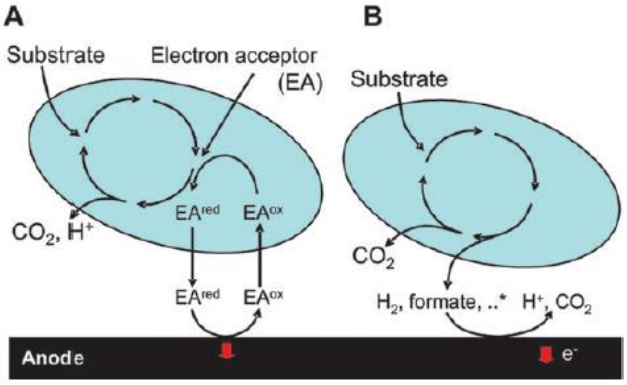

Figure 2-4. Simplified illustration of MET *via* microbial primary metabolites (A) *via* reduced terminal electron acceptors (use of anaerobic respiration), (B) *via* oxidation of reduced fermentation products [8].

2.1.2 The effect of various conditions on microbial community structure in mixed-culture anode biofilms

For most potential applications of MFCs, such as wastewater treatment or other environmental installations, a mixed-culture anode biofilm will be more practical than a pure-culture biofilm. Various experiment conditions including but not limited to substrate, inocula, pH,

and anode potentials might affect the relationship of exoelectrogens with other microbial groups in the anode community.

2.1.2.1 Substrates

Microbial communities in anode biofilms with different substrates have been analyzed in many studies. BESs fed with acetate usually possess a microbial community dominated by *Geobacteraceae* species [30-36], such as *G. sulfurreducens* and *Pelobacter propionicus* [30, 32-36]. With single fermentable substrates that can be directly converted to current, such as lactate, propionate, and butyrate, *Geobacteraceae* species were less dominant in the community, replaced by *P. propionicus*, *Bacillus* species, *Dechloromonas* species, or *Desulfuromonas* species [31, 32, 37].

To practically apply BESs in wastewater treatment, a microbial community in the anode biofilm with diverse phenotypic characteristics is required to convert the complex organics into electrical energy [38]. Many of the predominant exoelectrogenic bacteria have limited metabolic versatility with respect to their electron donor [39], so syntrophic interactions with fermenters are often required for electrical current production from diverse substrates. For example, ethanol and formate could be initially fermented to acetate and hydrogen by acetogenic bacteria and fermenters like *P. propionicus* and *Paracoccus denitrificans*, and then *Geobacter* species can utilize the fermentation by-products for current generation [40, 41]. Similar syntrophic reactions between bacteria capable of fermentation (such as *Rhodopseudomonas* and *Clostridium* species) and *G. sulfurreducens* were also found with glucose or cellulose as the substrate (Figure 2-5), where the consumption of the fermentation by-products by exoelectrogenic bacteria reduced feedback inhibition of glucose or cellulose conversion [42, 43]. However, when the substrate

level is high, fermenters are favored over exoelectrogens, which could lead to low electricity conversion efficiencies [40].

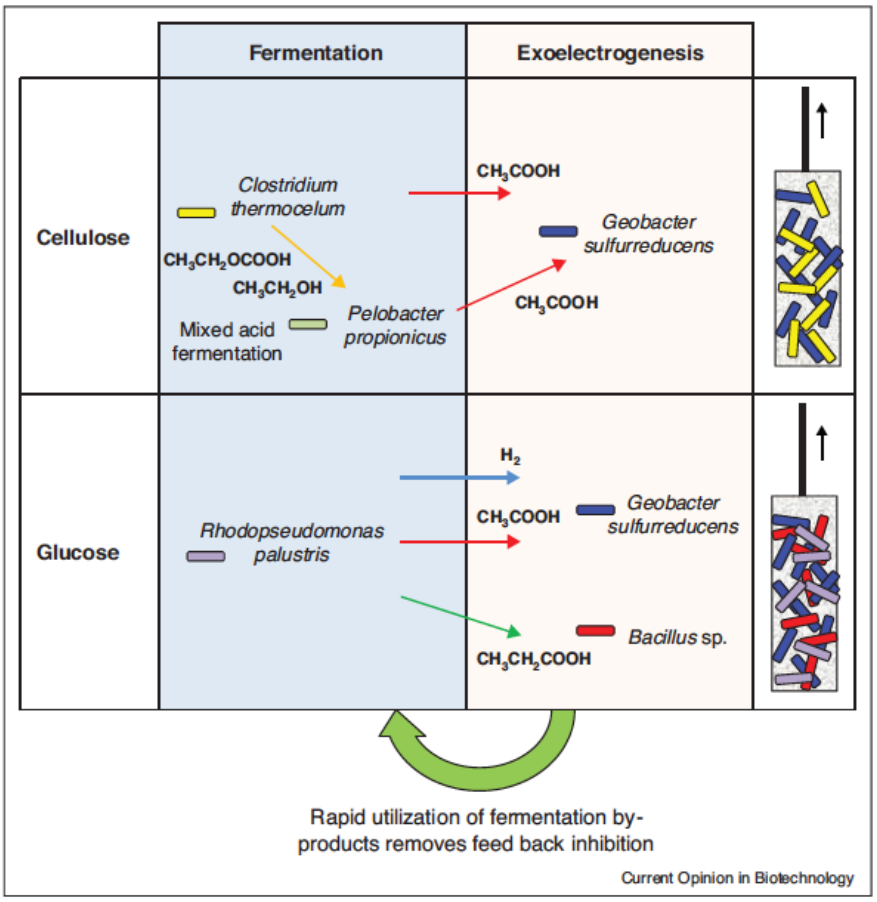

Figure 2-5. Syntrophic microbial interactions allow for increased cellulose hydrolysis and glucose oxidation at the anode of a bioelectrochemical system [38].

The characterization of the anodic community in BESs fed with real wastewaters presented more complex and diverse microbial communities [44], though simpler composition of the substrates in the wastewater or less oxygen intrusion might result in more percentages of *Geobacter* species in the community [45].

2.1.2.2 Inocula

Samples from different natural environments and wastewater streams have been inoculated in various MFCs for the comparison of performances. Anodic communities started with inocula from salt-water marshes or freshwater and marine sediments were all dominated by different bacterial orders belonging to *Deltaproteobacteria* [46], suggesting their possible relations to current production. The performance of MFCs inoculated with different wastewater effluents and natural samples from river or soil were compared [47, 48], but the conclusion varied with different compositions of the wastewaters, and no complimentary community analyses were reported. A recent comparative study on microbial communities in MFCs using inocula from primary clarifier effluent samples from two different wastewater treatment plants and an anaerobic bog sediment suggested that the predominance of *Geobacter* species in acetate-fed systems was consistent with good MFC performance and independent of the inoculum source [49]. This paper also demonstrated that the community analysis method can influence the representation of the microbial community, which may have contributed to previous interpretations.

2.1.2.3 pH

The anodic half-reaction releases electrons to the electrode as well as protons to the biofilm and the solution. Excessive accumulation of protons in an anode biofilm usually leads to anode biofilm acidification, which has been experimentally substantiated by fluorescent detection of the pH gradient in a pure *G. sulfurreducens* system [50]. The acidification of the anode biofilm affects current generation because of the inhibition of low pH on microbial activity [50-52]. For example, a pH decrease from 7 to 5 considerably lowered the growth rate of fumarate-fed *G.*

sulfurreducens [50]. Another well-know exoelectrogenic bacterium, *S. oneidensis*, was also found to produce less riboflavin and power density at pH 5 than with neutral pH [53].

2.1.2.4 Anode potential

Anode potentials in MFCs change with different external resistances or can be directly set and maintained via a potentiostat. Low external resistances lead to more positive anode potentials, and were found to limit methanogenesis in the MFC anode chamber by favoring exoelectrogenesis [30, 54]. Operating MFCs with different external resistances may yield similar electrochemical performance capabilities, particularly in cathode-limited systems, but the anode biofilm architectures and communities varied considerably, with filamentous bacteria dominating the anode biofilm under high external resistances (1000 and 5000 Ω) and more diverse rod-shaped cells forming dense anode biofilms under lower resistances (10, 50, and 265 Ω) [55].

While MFCs operated with fixed external resistances have a dynamic pattern in fed-batch systems, running reactors with fixed anode potentials is another operational approach. The later has been used to remove possible cathode limitation in systems operated with fixed external resistances [56]. The reported effects of setting different anode potentials on the electrochemical performance are sometimes inconsistent with each other [57]. However, anode potentials were found to impose a selective pressure on the anode community composition based on bacteria's affinity for the anode and their maximum substrate utilization rate, as most studies have found that lower anode potentials enriched more known exoelectrogenic bacteria in the anode biofilm, e.g. *G. sulfurreducens* and *Geobacter psychrophilis* [36, 58, 59].

2.2 Biocathode

2.2.1 Biocathode electron transfer mechanisms in MFCs

Although the electron transfer mechanisms in biocathodes have not been as intensely studied as anode electron transfer, there are currently two reported mechanisms, namely direct and indirect electron transfer (Figure 2-6A) [3]. Similar to DET in anode electron transfer, direct electron transfer in a biocathode also requires a physical contact between the bacterial cell membrane and the cathode electrode surface. The linking species for electrons from the electrode being directly transferred to cells are outer membrane redox macromolecules such as cytochromes, which have been reported in *Geobacter* species, *Shewanella putrefaciens*, and mixed cultures [6, 24, 60-65]. It is still not clear whether the exoelectrogenic and exoelectrotrophic processes of one bacterium, e.g., *S. putrefaciens*, have similar mechanisms for direct electron transfer [24, 64, 65]. However, different cytochromes were suggested for *G. sulfurreducens* in biocathode electron transfer and anode DET [61]. Although most of the electrochemically active bacteria in biocathodes have been reported to be Gram-negative, Gram-positive bacteria including *Micrococcus luteus*, *Bacillus subtilis*, and *Staphylococcus carnosus* have also shown the capability of direct electron transfer in cyclic voltammetry tests [66].

During indirect electron transfer, some microorganism can receive electrons from the cathode electrode *via* mobile redox compounds without physically contacting the cathode electrode surface (Figure 2-6B) [3]. The redox compounds can be exogenously added or self-excreted (endogenous) mediators, or a cathodic reduction product (e.g., hydrogen). For example, perchlorate-reducing bacteria like *Dechloromonas agitata*, *D. aromatica*, and *Azospira suillum* can microbially catalyze the reduction of perchlorate by indirectly receiving electrons from a cathodic current in the presence of mediator anthraquinone-2,6-disulfonate. However, the

operational cost and possible toxicity of exogenous mediators is a concern [67]. Perchlorate-reducing bacteria can also use hydrogen produced at the cathode in a half cell with added exogenous redox species [68]. Extracellular electron transfer for cathodic oxygen reduction via self-excreted redox compounds was found in *Acinetobacter calcoaceticus*, which was prevalent in a mixed-culture microbial cathode [37, 69, 70]. It was also suggested that extracellular substances are always involved in the indirect electron transfer between microbes and electrodes in MFCs with naturally occurring microbial communities [71].

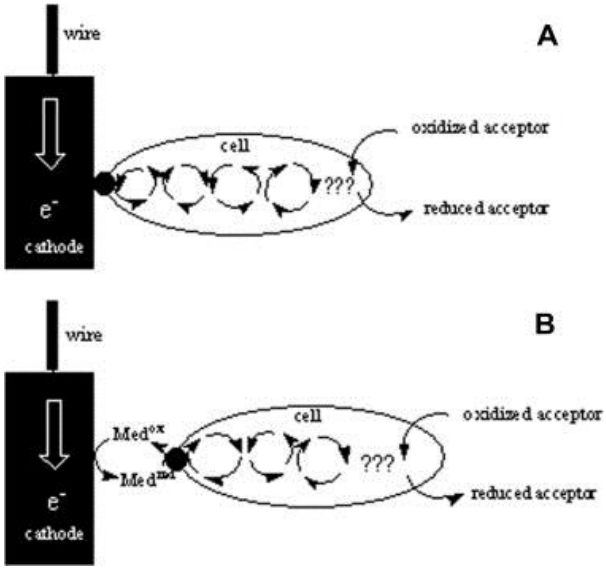

Figure 2-6. Schematics of direct electron transfer mechanism via membrane-bound cytochromes (A) and indirect electron transfer mechanism via added (exogenous) or secreted (endogenous) mediators (B) [3].

2.2.2 Biocathodes for different electron acceptors in MFCs

Biocathodes can be classified as aerobic or anaerobic according to the terminal electron acceptor in the system. With its high redox potential and abundance, oxygen is the most popular terminal electron acceptor for the cathode reaction in MFCs. Many bacteria species are able to catalyze cathodic oxygen reduction [37, 42, 69, 72-77]. In addition, biocathodic oxygen reduction can also be utilized to assist the oxidation of transition metal compounds, such as Mn(II) or

Fe(II), which can be biologically recycled after accepting electrons from electrodes *via* electrochemical reactions and releasing electrons to oxygen [4, 78, 79]. The main drawbacks of aerobic biocathodes are the requirement for dissolved oxygen and the crossover of oxygen from the cathodic to anodic chamber [3].

In the absence of oxygen, biocathodes can use other molecules as terminal electron acceptors, such as nitrate, sulfate, carbon dioxide, H^+, Cr(VI), Fe(III), Mn(IV), U(VI), fumarate, perchlorate, trichloroethene, and tetrachloroethene [3, 6, 60-63, 68, 80-93]. Based on the metabolic activity and redox potentials, nitrate is the most promising terminal electron acceptor in an anaerobic cathode. Nitrate removal by a biocathode has been achieved in various mixed-culture BESs [81, 82, 94-96]. Denitrifying biocathodes with perchlorate-reducing bacteria or other anaerobic cultures have also shown the ability of biological reduction of perchlorate or Cr(VI) [63, 84]. Biocathodic carbon dioxide reduction and fixation by the algal species *Chlorella vulgaris* was found with the presence of methylene blue mediator [92]. With a set potential of less than -0.7 V (vs Ag/AgCl), carbon dioxide can be reduced to methane on a hydrogenophilic methanogenic biocathode [93, 97]. Recently, it was demonstrated that acetogens, such as *Sporomusa ovate*, *Clostridium ljungdahlii*, *Clostridium aceticum*, *Moorella thermoacetica*, *Sporomusa sphaeroides*, and *Sporomusa silvacetica*, can fix carbon dioxide and covert it to organics, mainly acetate, by receiving electrons from the cathode electrode without exogenously added mediators [5, 98].

2.2.3 Alternating electron and carbon flows in the solventogenic *Clostridium acetobutylicum*

The demonstration that a biocathode can convert electric energy into useful organics opened a promising potential application of BESs. Currently acetogens have been shown to be able to microbially electrosynthesize only acetate and a small amount 2-oxobutyrate [5, 98].

Compared to acetate and 2-oxobutyrate, butanol is much more energy dense and is also a useful transportation fuel, with low volatility and low proneness to hydration [99]. The production of butanol *via* fermentation processes in solventogenic bacteria has been intensely studied in the past century. Industrially scaled fermentation processes by *Clostridium* species were built during the earlier part of the past century; however, this approach declined due to the competition from petrochemical synthesis of solvents since the 1960s [100]. The proof of microbial electrosynthesis of organics on biocathodes in BESs introduces the possibility of storing electrical energy in energy dense fermentation products as an alternative means to the petrochemical synthesis route.

As a model bacterium for the acetone-butanol-ethanol (ABE) fermentation process, *Clostridium acetobutylicum* has been thoroughly studied with respect to its biochemical pathways and physiology. In a normal batch culture, *C. acetobutylicum* converts carbohydrates to hydrogen, carbon dioxide, acetate, and butyrate during the initial acidogenic growth phase (Figure 2-7) and results in decreased pH of the culture medium. When the culture enters the stationary growth phase, the cells continue consuming the carbohydrates but their metabolism shifts to acetone, butanol, and ethanol production (solventogenic phase) (Figure 2-7), with a resultant increase in the pH of the culture medium. The influence of pH has been recognized as a key factor for triggering the solventogenic phase, with the initiation of solvent production usually occurring after the bulk pH decreases to around 4.5 to 5.0 [101-104]. However, good levels of solvent production between pH 5.5 and 4.3 have also been reported [105]. High concentrations of organic acids in their undissociated forms (acetic and butyric acids) could result in a total inhibition of all metabolic function in the cell due to its induction of a rapid decrease in the nucleoside triphosphate to diphosphate ratio [106].

As a reduced electron carrier, ferredoxin (a low molecular-weight, iron-sulfur-containing protein) plays a key role in electron distribution in *C. acetobutylicum* cells because it can either

transfer electrons via hydrogenases to generate hydrogen or transfer electrons to the pyridine nucleotides via the appropriate ferredoxin oxidoreductase [100]. It was proposed that the activities of three enzymes, NADH ferredoxin oxidoreductase, NADPH ferredoxin oxidoreductase, and hydrogenase, would affect the electron flow and thus the carbon flow within the cell [107]. For example, carbon monoxide can strongly inhibit hydrogenase activity [108] by reacting with the iron in the active site of the enzyme [104], thus resulting in inhibited hydrogen, carbon dioxide, acetate, and butyrate production but increased butanol and ethanol production. High partial pressure of hydrogen in the medium will also inhibit the flow of electrons from reduced ferredoxin to molecular hydrogen due to the resultant low H^+/H_2 redox potential [107]. Besides the headspace gas composition, altered electron flow has also been found in *C. acetobutylicum* with a low set cathode potential with the presence of the electron mediator methyl viologen, where electrochemically provided reducing equivalents reduced more $NAD(P)^+$ ferredoxin oxidoreductase for increased butanol and decreased acetone yields [109]. Without organic substrate, *C. acetobutylicum* was demonstrated to produce exclusively hydrogen using cathode-derived electrons with methyl viologen [110].

Different from acetogens, most if not all solventogenic bacteria, including *C. acetobutylicum*, do not have the Wood-Ljungdahl pathway for carbon dioxide fixation [111, 112]. Therefore, the exact process of microbial electrosynthesis of organics from carbon dioxide, water, and the electrons from the cathode electrode would not be feasible in *C. acetobutylicum*. However, a compromised approach of converting electric energy to increased solvent production with the presence of an organic carbon source in the biocathode is still worthy of investigation.

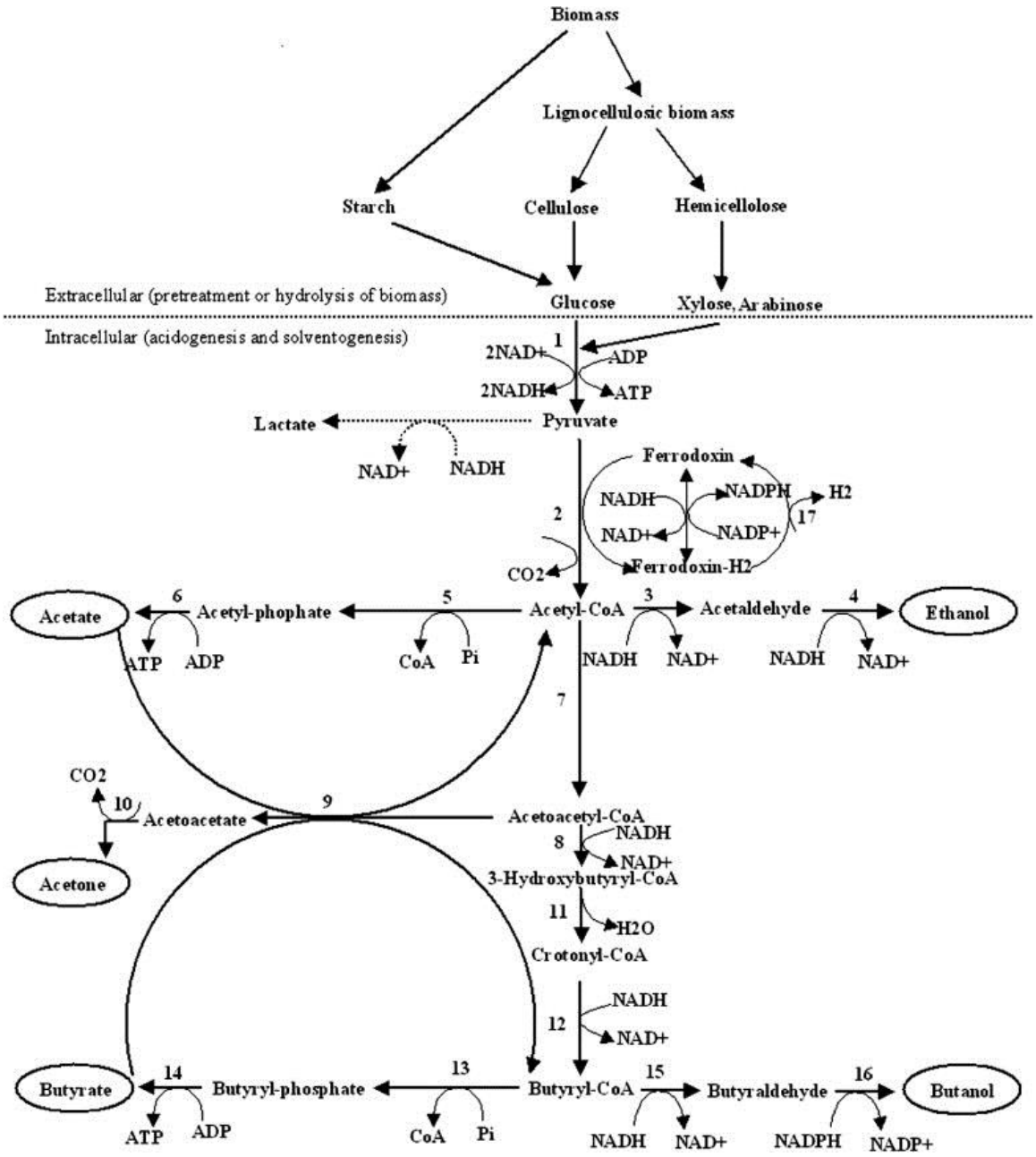

Figure 2-7. Metabolic pathways in *C. acetobutylicum* for the acidogenic and solventogenic phase. (Note: the stoichiometry of post-glycolysis products is per 0.5 mol glucose.) Enzymes are indicated by numbers as follows: (1) enzymes including in glycolysis process (2) pyruvate–ferredoxinoxidoreductase; (3) acetaldehyde dehydrogenase; (4) ethanol dehydrogenase; (5) phosphate acetyltransferase (phosphotransacettylase); (6) acetate kinase; (7) thiolase (acetyl-CoA acetyltransferase); (8) 3-hydroxybutyryl-CoA dehydrogenase; (9) acetoacetyl-CoA: acetate/butyrate:CoA-transferase; (10) acetoacetate decarboxylase; (11) crotonase; (12) butyryl-CoA dehydrogenase; (13) phosphate butyltransferase (phosphotransbutyrylase); (14) butyrate kinase; (15) butyraldehyde dehydrogenase; (16) butanol dehydrogenase; (17) hydrogenase [113].

2.3 Combining nitrogen removal in MFCs

2.3.1 Nutrient removal in traditional wastewater treatment plant (WWTPs)

Excess anthropogenic discharge of nutrient elements such as N and P has led to significant eutrophication in freshwater systems. Therefore, nitrogen removal has become one of the key required processes in most WWTPs. Nitrogen can be removed from wastewater streams by microbial assimilation for synthesis of proteins and nucleic acids, and nitrification coupled with denitrification (Figure 2-8). Nitrification is the primary way to remove only ammonia from wastewater. This process involves the sequential aerobic oxidations of ammonia (herein referring to NH_3 and NH_4^+) to nitrite (NO_2^-) through a hydroxylamine intermediate by ammonia-oxidizing bacteria (AOB), and then nitrite to nitrate (NO_3^-) by nitrite-oxidizing bacteria (NOB) (Table 2-1). The existence of ammonia-oxidizing archaea (AOA) was also discovered in natural systems and WWTPs [114], but their relative contribution to ammonia removal is presently unknown. Under anoxic conditions, certain bacteria can facultatively use nitrate as their electron acceptor, reducing nitrate sequentially to nitrite, nitric oxide (NO), nitrous oxide (N_2O), and nitrogen gas (N_2), which is called the denitrification process (Table 2-1). Recently some bacteria have been discovered that oxidize ammonia anaerobically, using ammonia as an electron donor, nitrite as an electron acceptor, and inorganic carbon as a carbon source. The coupling of partial aerobic ammonia oxidation to nitrite and anaerobic ammonia oxidation (anammox) has become an emerging approach to nitrogen removal in wastewater [115-117]. As only half of the ammonia is aerobically oxidized by AOB and the resultant nitrite is not further oxidized by NOB, theoretically there will be much less oxygen required in the anammox process. However, due to the extremely slow growth of anammox bacteria, the process stability is a big concern. Currently, the practical implementation of this process is still in its infancy.

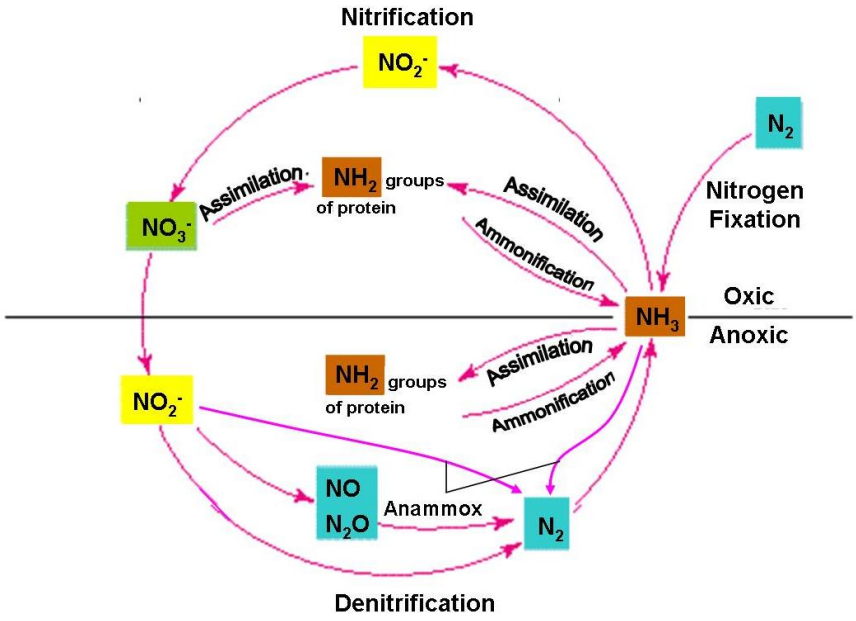

Figure 2-8. Redox cycle for nitrogen [118].

Table 2-1. Chemical formulae of nitrification reactions [1]

Reaction	Chemical Formula
Ammonia Oxidation	$NH_4^+ + \frac{3}{2}O_2 \Rightarrow NO_2^- + H_2O + 2H^+$
Nitrite Oxidation	$NO_2^- + \frac{1}{2}O_2 \Rightarrow NO_3^-$
Total Reaction	$NH_4^+ + 2O_2 \Rightarrow NO_3^- + H_2O + 2H^+$

The oxidation of ammonia to nitrite by AOB is often the rate-limiting step of nitrification because AOB can grow more slowly than NOB and denitrifiers under typical conditions and are more prone to inhibition by low oxygen concentrations. Also, since the ammonia oxidation reaction is an acidification process (Table 2-1), AOB are easily affected by pH in insufficiently buffered systems (Figure 2-9). Due to its slow growth rate, a thick AOB biofilm is difficult to obtain within a short period in ammonia-rich wastewater containing no organic compounds [119].

To enhance biofilm attachment, surface grafting has been adopted to improve the adhesivity of bacteria to a polymer membrane [120]. For example, a porous hollow-fiber membrane with polymer chains containing a diethylamine group immobilized on the pore surface can collect proteins at a high rate and high capacity because of convective transport and multi-layering of proteins [121]. Functionalizing the hollow-fiber membranes with diethylamine groups enhanced the adhesivity of nitrifying bacteria in a continuously fed fluidized bed bioreactor [119, 122, 123]. The nitrifying biofilm also exhibited a much higher nitrification rate per unit area than other biofilm, which might have been due to the positive charge and soft polymer chains on the grafted membrane surface [119, 122, 123].

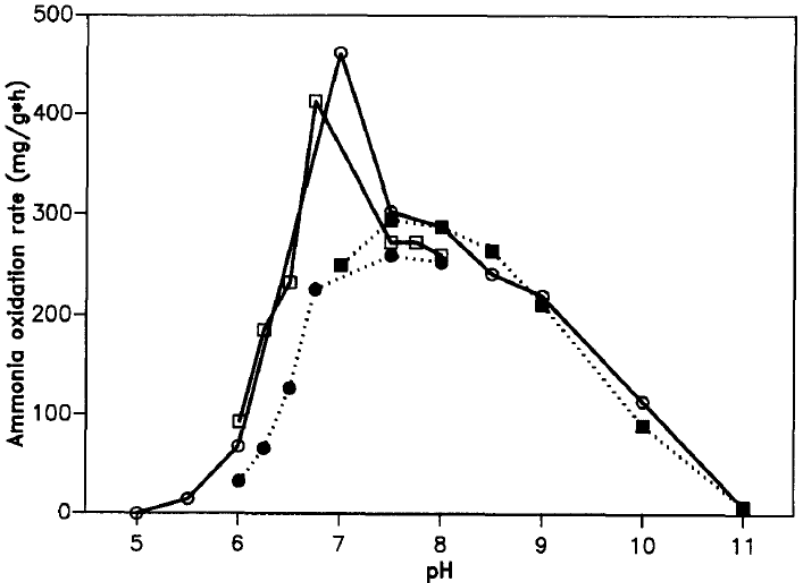

Figure 2-9. Ammonia oxidation rates versus pH at 30 ºC. Open squares and circles: data from two different batches of *Nitrosomonas* biomass incubated with 0.37 mg NH_3-N L^{-1}. Solid symbol: data from incubations with 5 mg NH_3-N L^{-1} [124].

2.3.2 Nutrient removal in BESs

Since both AOB and NOB are aerobic chemolithoautotrophs, oxygen is required in MFCs to remove reduced nitrogen (which is usually in the forms of ammonia and organic

nitrogen) by nitrification. In two-chamber MFC designs for coupled nitrification, oxygen was supplied either inadvertently by diffusion to the anode chamber from an aerated cathode chamber [125-127] (Fig 2-10A) or deliberately in a side-stream aerated nitrifying tank [82] (Figure 2-10B). These approaches incur energy costs for aeration and encountered ammonium leakage from anode to cathode chamber across the proton exchange membrane. Ammonia oxidation associated with electricity production was also reported in a rotating-cathode MFC [128]. However, the very low coulombic efficiency (CE; 0.06% - 0.34%) obtained in this system suggested that the current more likely resulted from heterotrophic exoelectrogenesis sustained by nitrifier-produced organics rather than from direct ammonium oxidation.

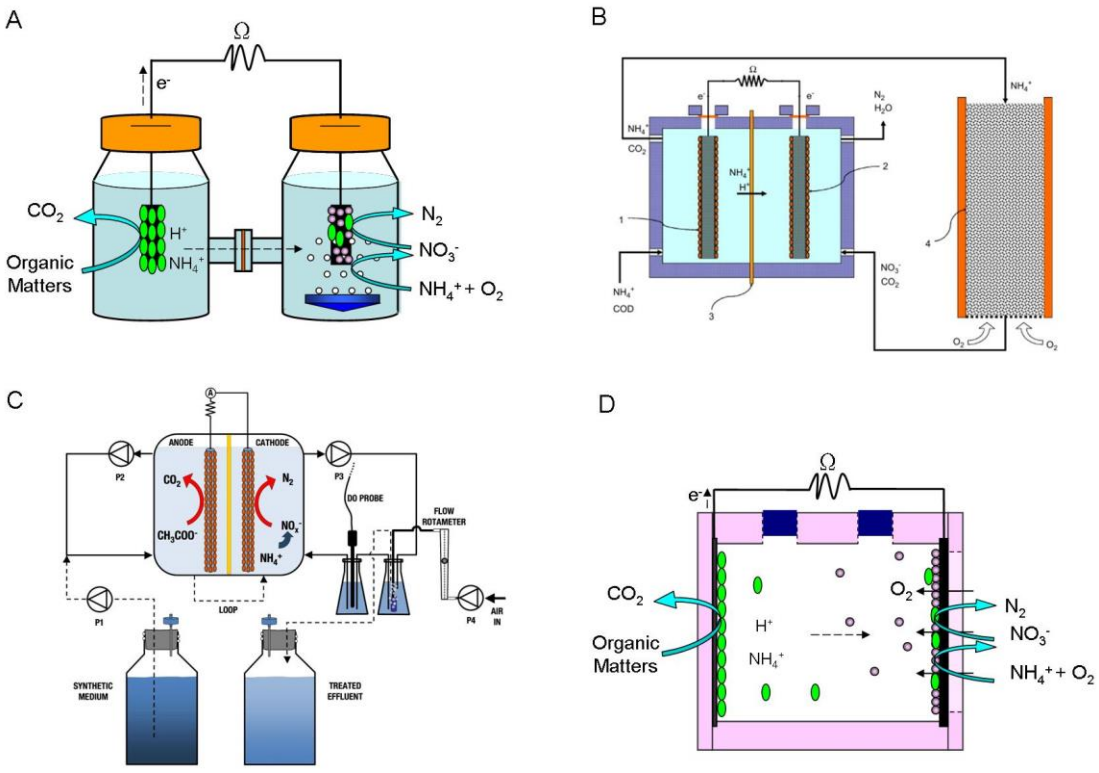

Figure 2-10. Schematic of MFCs for nitrogen removal. (A: two-chamber MFCs with aerated cathode [77], figure adopted from [1]; B: a continuous system of a two-chamber MFC with an aerated nitrification sidestream [129]; C: a continuous system of a two-chamber MFC with an aerated influent for cathode chamber [130]; D: single-chamber air-cathode MFCs (only one PTFE diffusion layer on the cathode [125], figure adopted from [1])

The oxidized nitrogen produced in the nitrification process could be removed in MFCs by the denitrification process, in conjunction with soluble electron donor oxidation or cathode oxidation in biocathodes [81, 82, 131]. To combine both nitrification and denitrification and eliminate the ammonium leakage issue, an aerated cathode chamber or pre-aerated cathode influent was successfully incorporated to MFC designs [130, 132] (Figure 2-10C). However, both approaches still require energy for the aeration. To address the energy concern, single-chamber air-cathode MFCs, which allow atmospheric oxygen to passively diffuse into the solution, were tested for ammonia removal [124, 126] (Figure 2-10D). Subsequent testing demonstrated the ammonia removal in a single-chamber MFC with no buffer solution and only one PTFE layer on the air cathode was mainly due to the volatilization of ammonia at the cathode, which was not significant in a well buffered system [125].

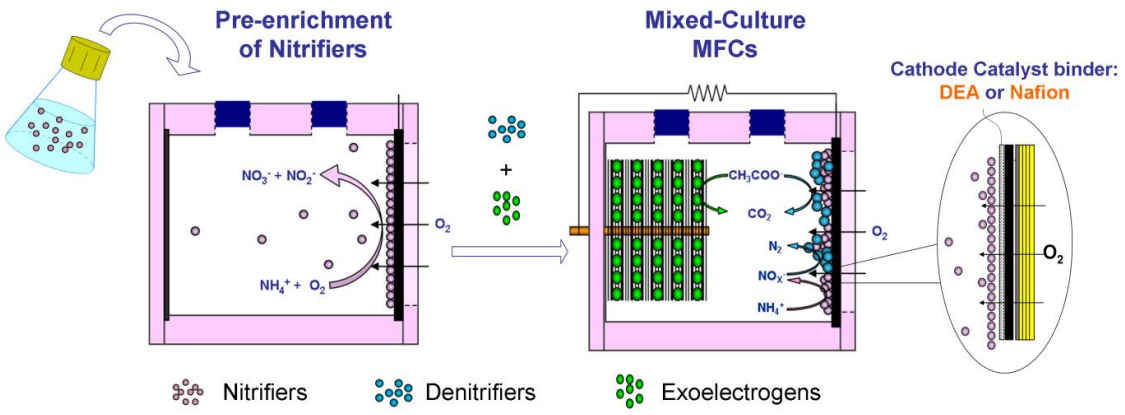

Figure 2-11. Schematic of design highlights of the single-chamber air-cathode MFCs for nitrogen removal [133].

In my recent single-chamber air-cathode MFC design for nitrogen removal, a nitrifier biofilm was pre-enriched on the air cathode, which was coated with four PTFE layers and one Pt catalyst layer with diethylamine-functionalized polymer (DEA) as the binder (Figure 2-11) [7]. Enhanced ammonia removal (up to 98%) and COD removal (up to 100%) and reduced

contribution to ammonia loss from non-nitrification reactions (50%) were achieved in this system relative to Kim et al (2005) and Min et al (2005). The success of using single-chamber air-cathode MFCs with a tailored microbial community at the air cathode opens the possibility of modifying a suitable microenvironment to preferentially retain a higher abundance of the slow-growing nitrifiers. However, since the ammonia-oxidation reaction is the limiting process in nitrification and has a strict demand for oxygen [134], increasing the oxygen diffusion flux in air-cathode MFCs might further enhance the nitrogen removal ability of the system to handle high-strength ammonia and COD influent that might occur in real wastewater treatment plants.

2.4 Outlook

This review covered recent studies of anode and cathode microbial communities and mechanisms for electron transfer as well as the achievements in combining nitrogen removal with MFCs by tailored microbial communities. Uncertain behaviors of anode and cathode communities under different operational conditions raises the concern of the community shifting and impacting the electrochemical performance results from different operational conditions. The potential of converting electrical energy to increased biofuels production makes the study of solventogenic bacteria as biocathode of great interest. Finally, the success of using single-chamber air-cathode MFCs for high efficiency nitrogen removal suggested the need for further improvements of this design for MFCs performing under various working conditions and wastewater compositions.

2.5 Literature cited

1. Yan, H., MS Thesis: Nitrogen removal in a single-chamber microbial fuel cell with nitrifying biofilm enriched at the air cathode, in *Civil and Environmental Engineering*2010, Pennsylvania State University, University Park.
2. Logan, B.E., Microbial fuel cells. 2008: John Wiley & Son, Inc.
3. Huang, L., J.M. Regan, and X. Quan, Electron transfer mechanisms, new applications, and performance of biocathode microbial fuel cells. *Bioresource Technology*, 2011. **102**(1): p. 316-323.
4. He, Z. and L.T. Angenent, Application of bacterial biocathodes in microbial fuel cells. *Electroanalysis*, 2006. **18**(19-20): p. 2009-2015.
5. Nevin, K.P., et al., Microbial electrosynthesis: feeding microbes electricity to convert carbon dioxide and water to multicarbon extracellular organic compounds. *Mbio*, 2010. **1**(2).
6. Gregory, K.B. and D.R. Lovley, Remediation and recovery of uranium from contaminated subsurface environments with electrodes. *Environmental Science & Technology*, 2005. **39**(22): p. 8943-8947.
7. Yan, H., T. Saito, and J. Regan, Nitrogen removal in a single-chamber microbial fuel cell with nitrifying biofilm enriched at the air cathode. *Water Research*, 2012.
8. Schroder, U., Anodic electron transfer mechanisms in microbial fuel cells and their energy efficiency. *Physical Chemistry Chemical Physics*, 2007. **9**(21): p. 2619-2629.
9. van der Meer, J.R., Analytics with engineered bacterial bioreporter strains and systems. *Current Opinion in Biotechnology*, 2006. **17**(1): p. 1-3.
10. Holmes, D.E., et al., Potential role of a novel psychrotolerant member of the family *Geobacteraceae*, *Geopsychrobacter electrodiphilus* gen. nov., sp nov., in electricity

production by a marine sediment fuel cell. *Applied and Environmental Microbiology*, 2004. **70**(10): p. 6023-6030.

11. Chaudhuri, S.K. and D.R. Lovley, Electricity generation by direct oxidation of glucose in mediatorless microbial fuel cells. *Nature Biotechnology*, 2003. **21**(10): p. 1229-1232.
12. Kim, B.H., et al., Direct electrode reaction of Fe(III)-reducing bacterium, Shewanella putrefaciens. *Journal of Microbiology and Biotechnology*, 1999. **9**(2): p. 127-131.
13. Chang, I.S., et al., Electrochemically active bacteria (EAB) and mediator-less microbial fuel cells. *Journal of Microbiology and Biotechnology*, 2006. **16**(2): p. 163-177.
14. Gorby, Y.A., et al., Electrically conductive bacterial nanowires produced by *Shewanella oneidensis* strain MR-1 and other microorganisms. *Proceedings of the National Academy of Sciences of the United States of America*, 2006. **103**(30): p. 11358-11363.
15. Reguera, G., et al., Extracellular electron transfer via microbial nanowires. *Nature*, 2005. **435**(7045): p. 1098-1101.
16. Park, D.H. and J.G. Zeikus, Electricity generation in microbial fuel cells using neutral red as an electronophore. *Applied and Environmental Microbiology*, 2000. **66**(4): p. 1292-1297.
17. Roller, S.D., et al., Electron transfer coupling in microbial fuel cells.1. comparison of redox mediator reduction rates and respiratory rates of bacteria. *Journal of Chemical Technology and Biotechnology B-Biotechnology*, 1984. **34**(1): p. 3-12.
18. Delaney, G.M., et al., Electron-transfer coupling in microbial fuel cells.2. performance of fuel cells containing selected microorganism mediator substrate combinations *Journal of Chemical Technology and Biotechnology B-Biotechnology*, 1984. **34**(1): p. 13-27.
19. Stirling, J.L., et al., Microbial fuel cells. *Biochemical Society Transactions*, 1983. **11**(4): p. 451-453.

20. Bennetto, H.P., et al., Anodic reactions in microbial fuel cells. *Biotechnology and Bioengineering*, 1983. **25**(2): p. 559-568.

21. Park, D.H. and J.G. Zeikus, Utilization of electrically reduced neutral red by *Actinobacillus succinogenes*: physiological function of neutral red in membrane-driven fumarate reduction and energy conservation. *Journal of Bacteriology*, 1999. **181**(8): p. 2403-2410.

22. Hernandez, M.E. and D.K. Newman, Extracellular electron transfer. *Cellular and Molecular Life Sciences*, 2001. **58**(11): p. 1562-1571.

23. Newman, D.K., Microbiology - how bacteria respire minerals. *Science*, 2001. **292**(5520): p. 1312-1313.

24. Newman, D.K. and R. Kolter, A role for excreted quinones in extracellular electron transfer. *Nature*, 2000. **405**(6782): p. 94-97.

25. Rabaey, K., et al., Microbial phenazine production enhances electron transfer in biofuel cells. *Environmental Science & Technology*, 2005. **39**(9): p. 3401-3408.

26. Habermann, W. and E.H. Pommer, Biological fuel cells with sulfide storage capacity. *Applied Microbiology and Biotechnology*, 1991. **35**(1): p. 128-133.

27. Karube, I., et al., Biochemical fuel cell utilizing immobilized cells of *Clostridium butyricum*. *Biotechnology and Bioengineering*, 1977. **19**(11): p. 1727-1733.

28. Suzuki, S., et al., Biochemical energy-conversion by immobilized whole cells. *Annals of the New York Academy of Sciences*, 1983. **413**(DEC): p. 133-143.

29. Niessen, J., et al., Fluorinated polyanilines as superior materials for electrocatalytic anodes in bacterial fuel cells. *Electrochemistry Communications*, 2004. **6**(6): p. 571-575.

30. Jung, S. and J.M. Regan, Comparison of anode bacterial communities and performance in microbial fuel cells with different electron donors. *Applied Microbiology and Biotechnology*, 2007. **77**(2): p. 393-402.

31. Chae, K.J., et al., Effect of different substrates on the performance, bacterial diversity, and bacterial viability in microbial fuel cells. *Bioresource Technology*, 2009. **100**(14): p. 3518-3525.

32. Kiely, P.D., et al., Long-term cathode performance and the microbial communities that develop in microbial fuel cells fed different fermentation endproducts. *Bioresource Technology*, 2011. **102**(1): p. 361-366.

33. Call, D.F., R.C. Wagner, and B.E. Logan, Hydrogen production by *Geobacter* species and a mixed consortium in a microbial electrolysis cell. *Applied and Environmental Microbiology*, 2009. **75**(24): p. 7579-7587.

34. Kiely, P.D., et al., Anode microbial communities produced by changing from microbial fuel cell to microbial electrolysis cell operation using two different wastewaters. *Bioresource Technology*, 2011. **102**(1): p. 388-394.

35. Chae, K.J., et al., Biohydrogen production via biocatalyzed electrolysis in acetate-fed bioelectrochemical cells and microbial community analysis. *International Journal of Hydrogen Energy*, 2008. **33**(19): p. 5184-5192.

36. Torres, C.I., et al., Selecting anode-respiring bacteria based on anode potential: phylogenetic, electrochemical, and microscopic characterization. *Environmental Science & Technology*, 2009. **43**(24): p. 9519-9524.

37. Freguia, S., et al., Microbial fuel cells operating on mixed fatty acids. *Bioresource Technology*, 2010. **101**(4): p. 1233-1238.

38. Kiely, P.D., J.M. Regan, and B.E. Logan, The electric picnic: synergistic requirements for exoelectrogenic microbial communities. *Current Opinion in Biotechnology*, 2011. **22**(3): p. 378-385.

39. Caccavo, F., et al., *Geobacter sulfurreducens* sp.nov, a hydrogen-oxidizing and acetate-oxidizing dissimilatory metal-reducing microorganism. *Applied and Environmental Microbiology*, 1994. **60**(10): p. 3752-3759.

40. Parameswaran, P., et al., Microbial community structure in a biofilm anode fed with a fermentable substrate: the significance of hydrogen scavengers. *Biotechnology and Bioengineering*, 2010. **105**(1): p. 69-78.

41. Ha, P.T., B. Tae, and I.S. Chang, Performance and bacterial consortium of microbial fuel cell fed with formate. *Energy & Fuels*, 2008. **22**(1): p. 164-168.

42. Freguia, S., et al., Syntrophic processes drive the conversion of glucose in microbial fuel cell anodes. *Environmental Science & Technology*, 2008. **42**(21): p. 7937-7943.

43. Ren, Z.Y., T.E. Ward, and J.M. Regan, Electricity production from cellulose in a microbial fuel cell using a defined binary culture. *Environmental Science & Technology*, 2007. **41**(13): p. 4781-4786.

44. Patil, S.A., et al., Electricity generation using chocolate industry wastewater and its treatment in activated sludge based microbial fuel cell and analysis of developed microbial community in the anode chamber. *Bioresource Technology*, 2009. **100**(21): p. 5132-5139.

45. Cusick, R.D., P.D. Kiely, and B.E. Logan, A monetary comparison of energy recovered from microbial fuel cells and microbial electrolysis cells fed winery or domestic wastewaters. *International Journal of Hydrogen Energy*, 2010. **35**(17): p. 8855-8861.

46. Holmes, D.E., et al., Microbial communities associated with electrodes harvesting electricity from a variety of aquatic sediments. *Microbial Ecology*, 2004. **48**(2): p. 178-190.

47. Ieropoulos, I., J. Winfield, and J. Greenman, Effects of flow-rate, inoculum and time on the internal resistance of microbial fuel cells. *Bioresource Technology*, 2010. **101**(10): p. 3520-3525.

48. Jiang, D.Q., et al., Effect of Inoculum types on bacterial adhesion and power production in microbial fuel cells. *Applied Biochemistry and Biotechnology*, 2010. **160**(1): p. 182-196.

49. Yates, M.D., et al., Convergent development of anodic bacterial communities in microbial fuel cells. *Isme Journal*, 2012. **6**(11): p. 2002-2013.

50. Torres, C.I., A.K. Marcus, and B.E. Rittmann, Proton transport inside the biofilm limits electrical current generation by anode-respiring bacteria. *Biotechnology and Bioengineering*, 2008. **100**(5): p. 872-881.

51. Franks, A.E., et al., Novel strategy for three-dimensional real-time imaging of microbial fuel cell communities: monitoring the inhibitory effects of proton accumulation within the anode biofilm. *Energy & Environmental Science*, 2009. **2**(1): p. 113-119.

52. Gil, G.C., et al., Operational parameters affecting the performance of a mediator-less microbial fuel cell. *Biosensors & Bioelectronics*, 2003. **18**(4): p. 327-334.

53. Biffinger, J.C., et al., The influence of acidity on microbial fuel cells containing Shewanella oneidensis. *Biosensors & Bioelectronics*, 2008. **24**(4): p. 900-905.

54. Lee, H.S., et al., Evaluation of energy-conversion efficiencies in microbial fuel cells (MFCs) utilizing fermentable and non-fermentable substrates. *Water Research*, 2008. **42**(6-7): p. 1501-1510.

55. Ren, Z.Y., et al., Characterization of microbial fuel cells at microbially and electrochemically meaningful time scales. *Environmental Science & Technology*, 2011. **45**(6): p. 2435-2441.

56. Logan, B.E., Exoelectrogenic bacteria that power microbial fuel cells. *Nature Reviews Microbiology*, 2009. **7**(5): p. 375-381.

57. Wagner, R.C., D.I. Call, and B.E. Logan, Optimal set anode potentials vary in bioelectrochemical systems. *Environmental Science & Technology*, 2010. **44**(16): p. 6036-6041.

58. Sun, D., et al., Syntrophic interactions improve power production in formic acid fed MFCs operated with set anode potentials or fixed resistances. *Biotechnology and Bioengineering*, 2012. **109**(2): p. 405-414.

59. Commault, A.S., et al., Influence of anode potentials on selection of *Geobacter* strains in microbial electrolysis cells. *Bioresource Technology*, 2013. **139C**: p. 226-234. DOI: 10.1016/j.biortech.2013.04.047.

60. Cao, X., et al., A completely anoxic microbial fuel cell using a photo-biocathode for cathodic carbon dioxide reduction. *Energy & Environmental Science*, 2009. **2**(5): p. 498-501.

61. Dumas, C., R. Basseguy, and A. Bergel, Microbial electrocatalysis with *Geobacter sulfurreducens* biofilm on stainless steel cathodes. *Electrochimica Acta*, 2008. **53**(5): p. 2494-2500.

62. Strycharz, S.M., et al., Graphite electrode as a sole electron donor for reductive dechlorination of tetrachlorethene by *Geobacter lovleyi*. *Applied and Environmental Microbiology*, 2008. **74**(19): p. 5943-5947.

63. Tandukar, M., et al., Biological chromium(VI) reduction in the cathode of a microbial fuel cell. *Environmental Science & Technology*, 2009. **43**(21): p. 8159-8165.

64. Fredrickson, J.K., et al., Towards environmental systems biology of Shewanella. *Nature Reviews Microbiology*, 2008. **6**(8): p. 592-603.

65. Kim, H.J., et al., A microbial fuel cell type lactate biosensor using a metal-reducing bacterium, *Shewanella putrefaciens*. *Journal of Microbiology and Biotechnology*, 1999. **9**(3): p. 365-367.

66. Cournet, A., et al., Electrochemical reduction of oxygen catalyzed by a wide range of bacteria including Gram-positive. *Electrochemistry Communications*, 2010. **12**(4): p. 505-508.

67. Huang, L. and I. Angelidaki, Effect of humic acids on electricity generation integrated with xylose degradation in microbial fuel cells. *Biotechnology and Bioengineering*, 2008. **100**(3): p. 413-422.

68. Thrash, J.C., et al., Electrochemical stimulation of microbial perchlorate reduction. *Environmental Science & Technology*, 2007. **41**(5): p. 1740-1746.

69. Rabaey, K., et al., Cathodic oxygen reduction catalyzed by bacteria in microbial fuel cells. *Isme Journal*, 2008. **2**(5): p. 519-527.

70. Laurinavicius, V., et al., Wiring of PQQ-dehydrogenases. *Biosensors & Bioelectronics*, 2004. **20**(6): p. 1217-1222.

71. Watanabe, K., et al., Electron shuttles in biotechnology. *Current Opinion in Biotechnology*, 2009. **20**(6): p. 633-641.

72. Clauwaert, P., et al., Open air biocathode enables effective electricity generation with microbial fuel cells. *Environmental Science & Technology*, 2007. **41**(21): p. 7564-7569.

73. Nguyen, T.A., et al., Carbon and steel surfaces modified by Leptothrix discophora SP-6: Characterization and implications. *Environmental Science & Technology*, 2007. **41**(23): p. 7987-7996.

74. Zhang, J.N., et al., Electricity generation in a microbial fuel cell with a microbially catalyzed cathode. *Biotechnology Letters*, 2008. **30**(10): p. 1771-1776.

75. Aldrovandi, A., et al., Sustainable power production in a membrane-less and mediator-less synthetic wastewater microbial fuel cell. *Bioresource Technology*, 2009. **100**(13): p. 3252-3260.

76. Erable, B., et al., Marine aerobic biofilm as biocathode catalyst. *Bioelectrochemistry*, 2010. **78**(1): p. 51-56.

77. You, S.J., et al., Power generation and electrochemical analysis of biocathode microbial fuel cell using graphite fibre brush as cathode material. *Fuel Cells*, 2009. **9**(5): p. 588-596.

78. Rhoads, A., H. Beyenal, and Z. Lewandowski, Microbial fuel cell using anaerobic respiration as an anodic reaction and biomineralized manganese as a cathodic reactant. *Environmental Science & Technology*, 2005. **39**(12): p. 4666-4671.

79. Leduc, L.G. and G.D. Ferroni, The chemolithotrophic bacterium *Thiobacillus ferrooxidans. Fems Microbiology Reviews*, 1994. **14**(2): p. 103-119.

80. Huang, L.P., et al., Enhancement of hexavalent chromium reduction and electricity production from a biocathode microbial fuel cell. *Bioprocess and Biosystems Engineering*, 2010. **33**(8): p. 937-945.

81. Clauwaert, P., et al., Biological denitrification in microbial fuel cells. *Environmental Science & Technology*, 2007. **41**(9): p. 3354-3360.

82. Virdis, B., et al., Microbial fuel cells for simultaneous carbon and nitrogen removal. *Water Research*, 2008. **42**(12): p. 3013-3024.

83. Lefebvre, O., A. Al-Mamun, and H.Y. Ng, A microbial fuel cell equipped with a biocathode for organic removal and denitrification. *Water Science and Technology*, 2008. **58**(4): p. 881-885.

84. Shea, C., et al., Adapting a denitrifying biocathode for perchlorate reduction. *Water Science and Technology*, 2008. **58**(10): p. 1941-1946.

85. Aulenta, F., et al., Microbial reductive dechlorination of trichloroethene to ethene with electrodes serving as electron donors without the external addition of redox mediators. *Biotechnology and Bioengineering*, 2009. **103**(1): p. 85-91.

86. Aulenta, F., et al., Characterization of an electro-active biocathode capable of dechlorinating trichloroethene and cis-dichloroethene to ethene. *Biosensors & Bioelectronics*, 2010. **25**(7): p. 1796-1802.

87. Steinbusch, K.J.J., et al., Bioelectrochemical ethanol production through mediated acetate reduction by mixed cultures. *Environmental Science & Technology*, 2010. **44**(1): p. 513-517.

88. Lojou, E., et al., Hydrogenase activity control at *Desulfovibrio vulgaris* cell-coated carbon electrodes: biochemical and chemical factors influencing the mediated bioelectrocatalysis. *Electroanalysis*, 2002. **14**(13): p. 913-922.

89. Rozendal, R.A., et al., Hydrogen production with a microbial biocathode. *Environmental Science & Technology*, 2008. **42**(2): p. 629-634.

90. Jeremiasse, A.W., E.V.M. Hamelers, and C.J.N. Buisman, Microbial electrolysis cell with a microbial biocathode. *Bioelectrochemistry*, 2010. **78**(1): p. 39-43.

91. Cheng, K.Y., G. Ho, and R. Cord-Ruwisch, Anodophilic biofilm catalyzes cathodic oxygen reduction. *Environmental Science & Technology*, 2010. **44**(1): p. 518-525.

92. Powell, E.E., et al., Growth kinetics of *Chlorella vulgaris* and its use as a cathodic half cell. *Bioresource Technology*, 2009. **100**(1): p. 269-274.

93. Villano, M., et al., Bioelectrochemical reduction of CO_2 to CH_4 via direct and indirect extracellular electron transfer by a hydrogenophilic methanogenic culture. *Bioresource Technology*, 2010. **101**(9): p. 3085-3090.

94. Park, H.I., et al., Nitrate reduction using an electrode as direct electron donor in a biofilm-electrode reactor. *Process Biochemistry*, 2005. **40**(10): p. 3383-3388.

95. Chen, G.-W., et al., Application of biocathode in microbial fuel cells: cell performance and microbial community. *Applied Microbiology and Biotechnology*, 2008. **79**(3): p. 379-388.

96. Clauwaert, P., et al., Enhanced nitrogen removal in bio-electrochemical systems by pH control. *Biotechnology Letters*, 2009. **31**(10): p. 1537-1543.

97. Cheng, S., et al., Direct biological conversion of electrical current into methane by electromethanogenesis. *Environmental Science & Technology*, 2009. **43**(10): p. 3953-3958.

98. Nevin, K.P., et al., Electrosynthesis of organic compounds from carbon dioxide is catalyzed by a diversity of acetogenic microorganisms. *Applied and Environmental Microbiology*, 2011. **77**(9): p. 2882-2886.

99. Schwarz, W.H. and J.R. Gapes, Butanol - rediscovering a renewable fuel. *BioWorld Europe*, 2006. **01-2006**: p. 16-19.

100. Jones, D.T. and D.R. Woods, Acetone-butanol fermentation revisited. *Microbiological Reviews*, 1986. **50**(4): p. 484-524.

101. Beesch, S.C., Acetone-butanol fermentation of starches. *Applied Microbiology*, 1953. **1**(2): p. 85-95.

102. Davies, R. and M. Stephenson, Studies on the acetone-butyl alcohol fermentation I. nutritional and other factors involved in the preparation of active suspensions of *C. acetobutylicum. Biochemical Journal*, 1941. **35**: p. 1320-1331.

103. Prescott, S.G. and C.G. Dunn, Indusrtial microbiology, 3rd ed. 1959, New York: McGraw-Hill Book Co.

104. Thauer, R., et al., The reaction of the iron-sulfur protein hydrogenase with carbon monoxide. *European Journal of Biochemistry*, 1974(42): p. 447-452.

105. Monot, F., J.M. Engasser, and H. Petitdemange, Influence of ph and undissociated butyric-acid on the production of acetone and butanol in batch cultures of *Clostridium acetobutylicum*. *Applied Microbiology and Biotechnology*, 1984. **19**(6): p. 422-426.

106. Herrero, A.A., et al., Growth inhibition of *Clostridium thermocellum* by carboxylic acids: a mechanism based on uncoupling by weak acids. *Applied Microbiology and Biotechnology*, 1985. **22**(1): p. 53-62.

107. Jungerma.K, et al., Function of reduced pyridine nucleotide-ferredoxin oxidoreductases in saccharolytic clostridia. *Biochimica Et Biophysica Acta*, 1973. **305**(2): p. 268-280.

108. Gray, C.T. and H. Gest, Biological formation of molecular hydrogen. *Science*, 1965. **148**(3667): p. 186-&.

109. Kim, T.S. and B.H. Kim, Electron flow shift in *Clostridium acetobutylicum* fermentation by electrochemically introduced reducing equivalent. *Biotechnology Letters*, 1988. **10**(2): p. 123-128.

110. Song, J., et al., Microbes as electrochemical CO_2 conversion catalysts. *Chemsuschem*, 2011. **4**(5): p. 587-590.

111. Nolling, J., et al., Genome sequence and comparative analysis of the solvent-producing bacterium Clostridium acetobutylicum. *Journal of Bacteriology*, 2001. **183**(16): p. 4823-4838.

112. Ragsdale, S.W. and E. Pierce, Acetogenesis and the Wood-Ljungdahl pathway of CO_2 fixation. *Biochimica Et Biophysica Acta-Proteins and Proteomics*, 2008. **1784**(12): p. 1873-1898.

113. Kumar, M. and K. Gayen, Developments in biobutanol production: new insights. *Applied Energy*, 2011. **88**(6): p. 1999-2012.

114. Park, H.D., et al., Occurrence of ammonia-oxidizing archaea in wastewater treatment plant bioreactors. *Applied and Environmental Microbiology*, 2006. **72**(8): p. 5643-5647.

115. Strous, M., J.G. Kuenen, and M.S.M. Jetten, Key physiology of anaerobic ammonium oxidation. *Applied and Environmental Microbiology*, 1999. **65**(7): p. 3248-3250.

116. Strous, M., et al., Missing lithotroph identified as new planctomycete. *Nature*, 1999. **400**(6743): p. 446-449.

117. Arrigo, K.R., Marine microorganisms and global nutrient cycles. *Nature*, 2005. **437**(7057): p. 349-355.

118. Madigan, M.T., Martinko, J.M., Brock: biology of microorganisims. 11 ed. 2006: Upper Saddle River: Person Prentice Hall.

119. Hibiya, K., S. Tsuneda, and A. Hirata, Formation and characteristics of nitrifying biofilm on a membrane modified with positively-charged polymer chains. *Colloids and Surfaces B-Biointerfaces*, 2000. **18**(2): p. 105-112.

120. Lee, W., et al., Capture of microbial cells on brush-type polymeric materials bearing different functional groups. *Biotechnology and Bioengineering*, 1997. **53**(5): p. 523-528.

121. Tsuneda, S., et al., High-throughput processing of proteins using a porous and tentacle anion-exchange membrane. *Journal of Chromatography A*, 1995. **689**(2): p. 211-218.

122. Hibiya, K., et al., Simultaneous nitrification and denitrification by controlling vertical and horizontal microenvironment in a membrane-aerated biofilm reactor. *Journal of Biotechnology*, 2003. **100**(1): p. 23-32.

123. Terada, A., et al., Nitrogen removal characteristics and biofilm analysis of a membrane-aerated biofilm reactor applicable to high-strength nitrogenous wastewater treatment. *Journal of Bioscience and Bioengineering*, 2003. **95**(2): p. 170-178.

124. Groeneweg, J., B. Sellner, and W. Tappe, Ammonia oxidation in *nitrosomonas* at NH_3 concentrations near K_m: effects of pH and temperature. *Water Research*, 1994. **28**(12): p. 2561-2566.

125. Kim, J.R., et al., Analysis of ammonia loss mechanisms in microbial fuel cells treating animal wastewater. *Biotechnology and Bioengineering*, 2008. **99**(5): p. 1120-1127.

126. Min, B., et al., Electricity generation from swine wastewater using microbial fuel cells. *Water Research*, 2005. **39**(20): p. 4961-4968.

127. You, S.J., et al., Improving phosphate buffer-free cathode performance of microbial fuel cell based on biological nitrification. *Biosensors & Bioelectronics*, 2009. **24**(12): p. 3698-3701.

128. He, Z., et al., Electricity production coupled to ammonium in a microbial fuel cell. *Environmental Science & Technology*, 2009. **43**(9): p. 3391-3397.

129. Virdis, B., et al., Electron fluxes in a microbial fuel cell performing carbon and nitrogen removal. *Environmental Science & Technology*, 2009. **43**(13): p. 5144-5149.

130. Virdis, B., et al., Simultaneous nitrification, denitrification and carbon removal in microbial fuel cells. *Water Research*, 2010. **44**(9): p. 2970-2980.

131. Gregory, K.B., D.R. Bond, and D.R. Lovley, Graphite electrodes as electron donors for anaerobic respiration. *Environmental Microbiology*, 2004. **6**(6): p. 596-604.

132. Xie, S., et al., Simultaneous carbon and nitrogen removal using an oxic/anoxic-biocathode microbial fuel cells coupled system. *Bioresource Technology*, 2011. **102**(1): p. 348-354.

133. Yan, H., T. Saito, and J.M. Regan, Nitrogen removal in a single-chamber microbial fuel cell with nitrifying biofilm enriched at the air cathode. *Water Research*, 2012. **46**(7): p. 2215-2224.

134. Sharma, B. and R.C. Ahlert, Nitrification and nitrogen removal. *Water Research*, 1977. **11**(10): p. 897-925.

Chapter 3

Constant versus Dynamic Anode Potentials: Effects on Microbial Community Development and Composition

Abstract

Anode potentials in BESs may affect both the electrochemical performance and the microbial community structures of the system. The performances of MFCs under both potentiostatic operation and fixed external resistance have been studied. However, the comparative effect of constant versus dynamic MFC anode potential (resulting from fixed external resistance) on microbial communities has not been directly demonstrated. To investigate whether setting anode potentials will result in distinct microbial communities from dynamic anode potentials, we picked fixed anode potentials of -250 mV and -119 mV to match with the negative peak anode potential values obtained from MFCs operated with fixed external resistances of 1 kΩ and 47 Ω, respectively. Pyrosequence data from two-month time series samples showed hindered enrichment of *Geobacter* bacteria in a more diverse anode bacteria community at lower fixed anode potential (-250 mV) compared to 1 kΩ, though more comparable *Geobacter* abundances were found in anode biofilms from the -119 mV and 47 Ω reactors. Setting the anode potentials at the negative peak values of the dynamic reactors resulted in less energy extraction for microbial growth, which might slow down the evolution of the whole anode microbial community as well as the enrichment of exoelectrogenic bacteria. In addition, a possible limitation of potentiostatic operation with a volumetric anode is uncertainty in the actual anode potential due to variable proximity to the reference electrode. This study indicated that a

balance between screening exoelectrogenic bacteria and encouraging microbial growth needs to be considered when setting a low anode potential in BESs.

3.1 Introduction

MFCs have drawn wide attention for their potential of recovering energy from organics using microbes to catalyze electron transfer to the anode electrode. Investigating microbial community responses to bioelectrochemical changes will greatly benefit the development and operation of systems that promote highly electroactive and stable microbial communities in the anode biofilm. There are two distinctly different operational strategies with respect to the anode: potentiostatic operation and fixed external resistance, which allows a dynamic anode potential. The comparative effect of constant versus dynamic MFC anode potential on microbial communities has not been directly demonstrated.

Operating BESs with fixed anode potentials has often been used to isolate anode-related performance effects by removing the possible cathode limitation in systems operated with fixed external resistances [1]. Setting different anode potentials can affect both the electrochemical performance and the microbial community structures in BESs, though the reported effects are sometimes inconsistent with each other. Lower fixed anode potentials lead to lower current production [2-5] but higher maximum power densities [6, 7]. Most studies have found that lower anode potentials enriched more known exoelectrogenic bacteria (e.g. *Geobacter sulfurreducens* and *Geobacter psychrophilus*) [7-9] in the anode biofilm, required longer reactor startup times [2, 3, 6, 9, 10], and supported thinner biofilms [2, 3, 11, 12].

The potential difference between the anode and the electron-donor substrate controls the theoretical maximum energy gain ($\Delta G^{o\prime}$) that exoelectrogenic bacteria can extract for microbial maintenance and growth (eq. 3-1) [13]:

$$\Delta G^{o\prime} = -nF(E^{o\prime}{}_{a} - E^{o\prime}{}_{donor}) \quad \text{(eq. 3-1)}$$

where ($E^{o\prime}$ represents the respective biological standard potential of the electron donor or the anode, $\Delta G^{o\prime}$ denotes the change of Gibbs free energy at pH 7 and 25 °C, n is the number of electrons involved, and F the Faraday constant (96,485 C mol^{-1} e^-). The *actual* energy gain would depend on the potential of the terminal electron donor of the bacterium [2]. As the anode potential (E_a) decreases, microbes that cannot respire at the low potential might gradually be outcompeted from the anode biofilm. Meanwhile, since lower energy gain will lead to less biomass accumulation [2, 11], the microbial community in the anode biofilm might evolve more slowly at low anode potentials, delaying the selection process on the community. For example, with acetate as the organic electron donor ($E^{o\prime}{}_{donor}$ = -296 mV, [14]), the theoretical energy gain for the bacteria in an MFC with a fixed E_a of -250 mV is only -27 kJ mol^{-1} acetate, and -128 kJ mol^{-1} acetate with a fixed E_a of -119 mV. Compared to fixed-resistance MFCs with dynamic anode potentials that pass through higher potentials and peak negatively at -250 mV and -119 mV, constant anode potentials might affect the microbial community differently (Figure 3-1). There might be a critical potential value at which the enrichment preference of exoelectrogenic bacteria is negated by the inhibition on microbial community evolvement.

The objective of this study was to investigate whether microbial community development differs between reactors with constant anode potentials and those with fixed resistances and the resultant dynamic anode potentials. We operated two sets of MFC reactors, each with a pair of duplicates running at a fixed anode potential (-250 mV or -119 mV) corresponding to the negative peak values obtained from the corresponding fixed external-resistance reactors. The external resistances (1 kΩ and 47 Ω) were selected to represent both sides of the power density curve, based on extensive previous data with these MFC configurations. MFCs were used instead of microbial electrolysis cells (MECs) to avoid the possible enrichment of methanogens in a

single-chamber MEC [15], especially with an anaerobic digester effluent inoculum. The evolution of the microbial communities in the anode biofilms was determined by 16S rRNA gene pyrosequencing.

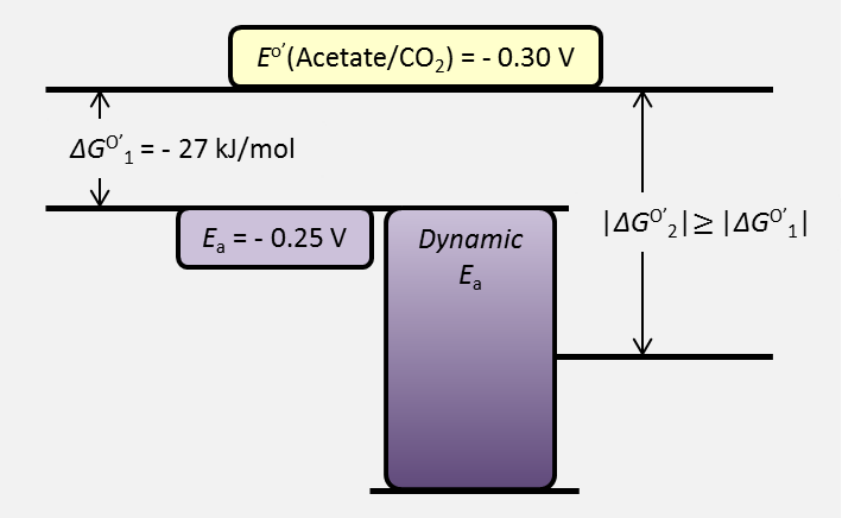

Figure 3-1. The theoretical maximum energy gain for exoelectrogenic bacteria using an anode with dynamic potentials is larger than for a potentiostatic anode set at the corresponding negative peak potential value (e.g., -0.25 V in this schematic).

3.2 Materials and methods

3.2.1 Reactor setup and operation

Single-chamber air-cathode MFC reactors were constructed from Plexiglas cubes to form a cylindrical chamber 4 cm long by 3 cm in diameter (empty bed volume of 28 mL) [16]. Anodes were made from a graphite fiber brush (PANEX33 160k, ZOLTEK, St Louis, MO, USA) with a 2.5 cm outer diameter and a 3 cm effective length. Air cathodes (0.5 mg-Pt/cm^2) made from carbon cloth (type B, E-TEK, Somerset, NJ, USA) with four PTFE layers [17] were pressed against a cation-exchange membrane (CEM) (Selemion CMV, AGC Engineering, Chiba, Japan) with two holes (Figure 3-2) to reduce excess oxygen intrusion to anodes while allowing ion

exchange. Reactors were first autoclaved and then inoculated with 10% (v:v) primary anaerobic digester effluent from the Pennsylvania State University Wastewater Treatment Plant (PSU WWTP). The feed medium contained 1 g L^{-1} sodium acetate and Wolfe's vitamins (5 ml L^{-1}) and minerals (12.5 ml L^{-1}) (Balch et al., 1979) in 50 mM phosphate buffer (Na_2HPO_4, 4.56 g L^{-1}; NaH_2PO_4 monohydrate, 2.45 g L^{-1}; NH_4Cl, 0.31 g L^{-1}; KCl, 0.13 g L^{-1}). Reactors were kept in a 30 °C thermostatic chamber and covered to prevent light intrusion into the reactors.

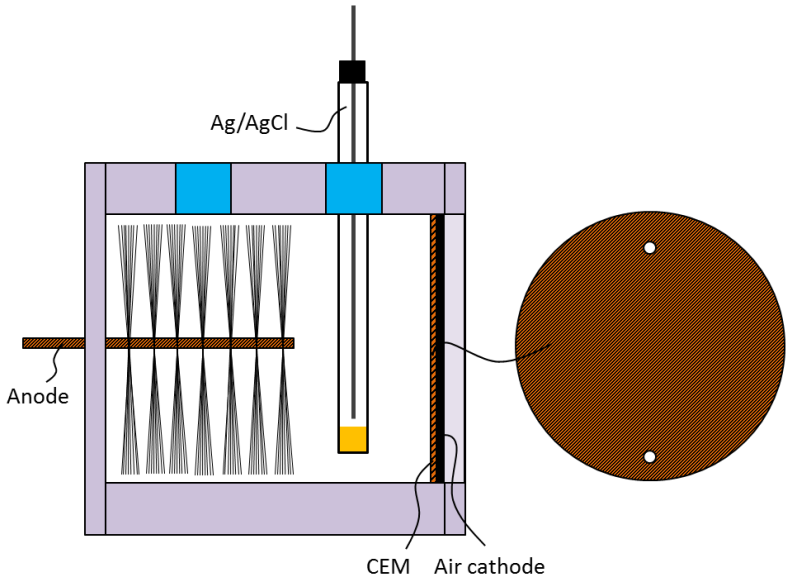

Figure 3-2. The schematic of MFC configuration with a brush anode, an air cathode, a Selemion CEM, and a Ag/AgCl reference electrode. Two holes (~ 2 mm ID) were drilled through the CEM to help proton transfer across the membrane.

Duplicate MFCs were operated under each of the four different electrochemical conditions: fixed external resistance at 1 kΩ (R-1k), fixed anode potential at -250 mV (P-250), fixed external resistance at 47 Ω (R-47), and fixed anode potential at -119 mV (P-119). Pre-tests established that when the external resistances were set at 1 kΩ and 47 Ω, the corresponding anode potentials reached negative plateaus of -250 and -119 mV. All reactors were operated in batch mode and re-fed with fresh medium when cell voltage outputs (E_{cell}) dropped below 50 mV (for R-1k and R-47) or current generation (I) went below 40 μA (for P-250 and P-119).

3.2.2 Electrochemical monitoring and calculation

Ag/AgCl reference electrodes (211 mV versus SHE) (RE-5B, Bioanalytical Systems, Mount Vernon, IN) were inserted into reactors (Figure 3-2) for potential setting and measurement. For reactors P-250 and P-119, current (I) and cathode potential (E_c) were measured by a potentiostat (VMP3, BioLogic, Knoxville, TN). The cell voltages of P-250 and P-119 were calculated as $E_{cell} = E_c - E_a$. For R-1k and R-47 with fixed external resistances (R), E_a and E_{cell} were monitored via a multimeter (Keithley, Cleveland, OH, USA), and I and E_c were calculated as $I = E_{cell}/R$ and $E_c = E_{cell} + E_a$. Coulombic recovery (CR) during a cycle was calculated based on the electrons transferred to the anode and the total electrons available from the complete oxidation of the sodium acetate in the medium:

$$CR = \frac{\int_0^t I dt}{(1/82)\cdot 0.026 \cdot 8 \cdot F}, \qquad \text{(eq. 3-2)}$$

where $1/82$ is the mole number of 1 g L^{-1} sodium acetate, 0.026 L is the solution volume, and 8 is the moles of electrons released per mol of sodium acetate oxidized.

3.2.3 Sample collection and DNA extraction

A volume of 0.25 ml inocula samples for the two sets of experiments, R-1k/P-250 and R-47/P-119, were taken for DNA extraction on day 0. Anode samples from reactors R-1k and P-250 were taken on days 12, 24, 41, and 54, and days 9, 18, 26, 41, and 58 for reactor R-47 and P-119, by cutting ~ 4% (v/v) anode graphite fibers from the end closest to the cathode using ethanol-wiped and flame-sterilized scissors. Regardless of the different cycle times of reactors under each condition, the samples were taken mid-cycle during peak electrochemical activity. This degree of anode removal (approximately 16-20% total) should not affect performance based on previous tests with single-chamber air-cathode MFCs showing that up to 75% of the anode brush can be

removed without adversely affecting voltage or power generation [18]. Anode samples taken from different locations on graphite fiber brushes were assumed to represent the whole anode bacterial community according to a recent finding that the dominant bacterial groups in an anode biofilm were homogenously distributed throughout the graphite fiber brush [19]. Genomic DNA from the inocula, the time-series anode samples, and the cathode biofilms at the end of the experiments was extracted right after each sampling using the PowerSoil DNA Isolation Kit (MO-BIO Laboratories, Carlsbad, CA, USA) and stored at -20 °C. The final DNA concentrations in the extractions were quantified on a UV-Vis spectrophotometer (Nanodrop 2000, Thermo Scientific, USA).

3.2.4 Pyrosequencing and data preprocessing

Forty-five DNA extraction samples were amplified for pyrosequencing using 16S rRNA gene-targeting forward and reverse fusion primers. (Reactors P-119 only had one sample taken from one of the duplicates on day 26.) The forward primer was constructed (5'-3') with the Roche A linker (CCATCTCATCCCTGCGTGTCTCCGACTCAG), an 8 - 10 bp barcode, and the 28F primer (GAGTTTGATCNTGGCTCAG). The reverse fusion primer was constructed (5'-3') with a biotin molecule, the Roche B linker (CCTATCCCCTGTGTGCCTTGGCAGTCTCAG), and the 519R primer (GTNTTACNGCGGCKGCTG) [20-22]. Amplification products were then pooled, cleaned, and size selected following Roche 454 protocols (454 Life Sciences, Branford, Connecticut). Sequencing was performed on a 454 GS-FLX sequencer (Roche Diagnostics Corporation, Indianapolis, IN) utilizing the Titanium Sequencing Kit (Roche) to generate 400-bp sequence reads (Supplementary materials).

Raw sequences from 45 DNA samples were pre-processed using the mothur program (http://www.mothur.org) before data analysis. First, to minimize the effect of random sequencing

errors, low-quality sequences (i.e., those with mismatches to the forward primer (> 2 bp) or barcodes (> 1 bp) and those with a homopolymer longer than 8 bp or a sequence length shorter than 200 bp) were eliminated. Second, primers and barcodes were trimmed and unique sequences were pulled out for further quality check via alignment with a reference dataset downloaded from SILVA (http://www.arb-silva.de/). Third, sequences that were close to more abundant sequences (< 2 mismatches per 100 bp) were preclustered to its nearest abundant sequences (because abundant sequences are more likely to generate erroneous sequences than rare sequences) and chimeric sequences from all the unique sequences were removed. Finally, sequences were classified according to SILVA SSU non-redundant reference database.

3.2.5 Data analysis

Pre-processed sequences were clustered into operational taxonomic units (OTUs) by setting a 0.03 or 0.05 distance limit, and rarefaction curves were generated using the mothur program. Sequences were phylogenetically assigned to taxonomic classifications using an RDP naïve Bayesian rRNA classifier (http://rdp.cme.msu.edu/classifier/classifier.jsp) with a confidence threshold of 80%. Sequences with confidence values below this to any know taxonomies were categorized as unclassified. Relative abundance of a given phylogenetic group was calculated as the number of sequences affiliated with that group divided by the total number of sequences per sample. Principal component analysis (PCA) was conducted using mothur for 44 samples, which excluding one anomaly (one duplicate of R-47 at day 9 had an abnormally high second primary variance value relative to the other samples).

3.3 Results

3.3.1 Constant and dynamic anode potentials have divergent effects on the electrochemical performances of MFCs

During the 13 fed-batch cycles with a fixed external resistance of 1 kΩ, the R-1k MFCs had dynamic anode potentials ranging from a mean positive peak value ($E_{a,mean,pk,+}$) (mean of 13 batches) of 421 ± 51 mV to a mean negative peak value ($E_{a,mean,pk-}$) of -237 ± 11 mV, and relatively constant peak current ($I_{mean,pk,H}$) of 0.42 ± 0.05 mA (Figure 3-3A, B). With a fixed anode potential similar to the negative peak anode potentials of R-1k MFCs, duplicate P-250 MFCs produced much less and unstable peak current during their 11-batch operation, ranging from 0.06 ± 0.05 (minimum) to 0.48 ± 0.01 mA (maximum). The cathode potential of P-250 MFCs was constantly higher than R-1k, with lower mean peak values ($E_{cathode,mean,pk}$) of 221 ± 58 mV and 117 ± 32 mV for P-250 and R-1k, respectively (Figure 3-4). The current production showed that the electrochemical performance of P-250 was unstable over the operation time; however, the duplicate reactors of P-250 (P-250-1 and P-250-2) showed nearly identical current production patterns after 30 days (Figure 3-5).

With a lower fixed external resistance or a correspondingly higher fixed anode potential, MFCs R-47 and P-119 had about one order of magnitude greater current production than the reactor set of R-1k and P-250 (Figure 3-3C, D). Although MFC P-119 had higher current production ($I_{mean,pk,H}$= 3.13 ± 0.51 mA) than MFC R-47 ($I_{mean,pk,H}$ = 2.47 ± 0.31 mA), their current patterns and batch durations (an average of 2.5 day) were similar. MFC R-47 had dynamic anode potentials during each batch ($E_{a,mean,pk+}$= 293 ± 37 mV and $E_{a,mean,pk-}$ = -149 ± 57 mV), with $E_{a,mean,pk-}$ gradually drifting below the fixed anode potential of P-119 after

three weeks. Unfortunately, the cathode potentials of only the MFC R-47 reactors were measured ($E_{cathode,mean,pk-}$ = -62 ± 23 mV) during this set of reactors (Figure 3-4).

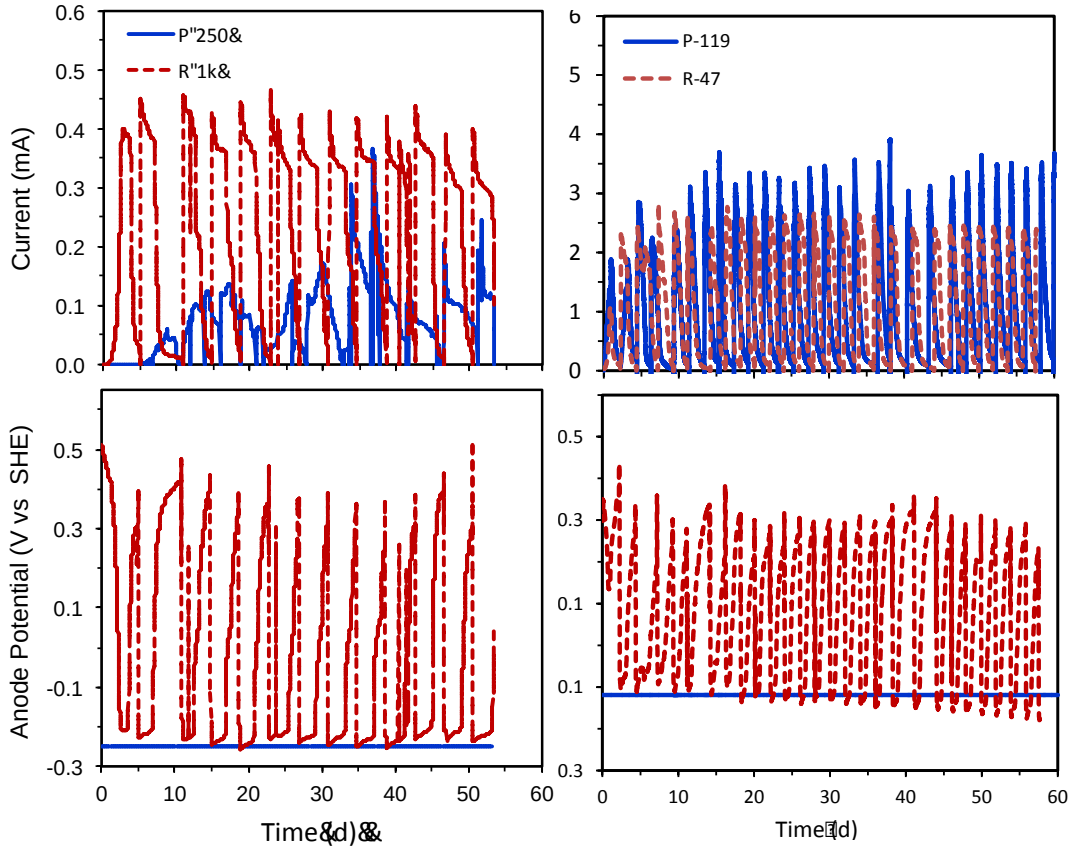

Figure 3-3. Current production of R-1k and P-250 (A) and R-47 and P-119 (C), and anode potential of R-1k and P-250 (B) and R-47 and P-119 (D).

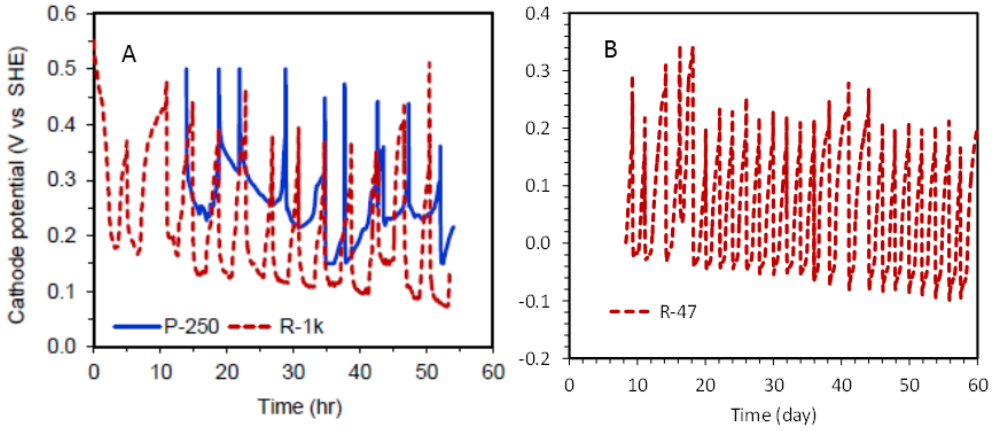

Figure 3-4. Cathode potentials of MFC P-250, R-1k, and R-47. (Cathode potentials of P-119 were not recorded.)

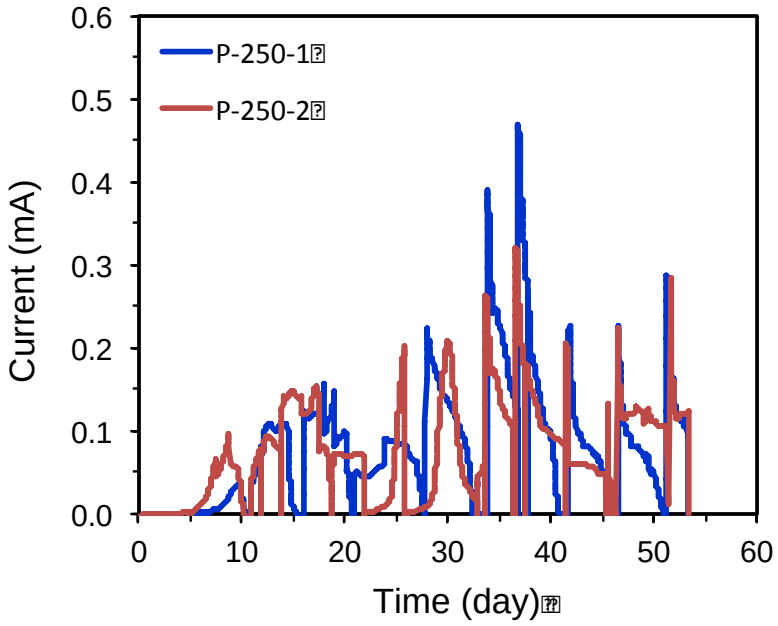

Figure 3-5. The current production of the duplicate P-250 reactors.

3.3.2 More diverse bacterial communities were observed at lower anode potentials

A total of 95,171 high quality reads were obtained from pyrosequencing after filtering and trimming. After further alignment, clustering, and chimera filtering, a subgroup of 1,221 sequences was pulled out from each sample for species richness analysis and classification. The rarefaction curves showed that although the inoculum for reactors R-1k and P-250 had fewer bacterial OTUs (3% distance) than the inoculum for R-47 and P-119, their bacterial communities were constantly more diverse than those from R-47 and P-119 (Figure 3-6). For the lower current systems, the potentiostatic P-250 duplicates had more diverse anode and cathode bacterial communities than the R-1k reactors. However, this trend was not observed among the R-47 and P-119 reactors.

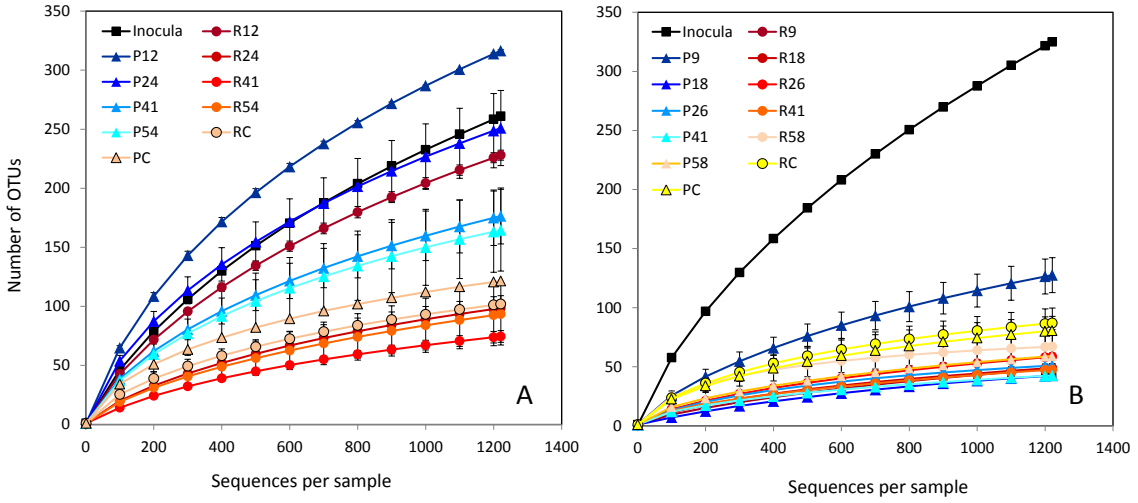

Figure 3-6. Rarefaction curves based on the pyrosequencing of 45 samples from (A) P-250 and R-1k and (B) P-119 and R-47 at a 3% distance. "P" and "R" refer to "potentiostatic" and "fixed external resistance", respectively. Numbers after "P" or "R" refer to the sampling time (day), and "C" refers to the cathode sample. Error bars at each data point are from duplicates.

3.3.3 Emergence of Geobacter-dominated communities varied with anode potentials

The *Geobacter* genus was not abundant in the two inocula from the primary anaerobic digester effluent (8.3% and 0.1% relative abundance) (Figure 3-7), which were collected several months apart. After 41 days of MFC operation with sodium acetate as the substrate, *Geobacter* gradually dominated the anode biofilm communities in reactors R-1k (85 ± 1 %). However, this enrichment process was significantly prolonged in the P-250 reactors (48 ± 7 % maximum after 54 days) and never reached stable performance and community composition. The enrichment of *Geobacter* was much more rapid in the anode biofilms of the higher-current systems R-47 and P-119 (Figure 3-7). A decrease of *Geobacter* abundance in the communities at the end of operation was detected in the R-1k (only one of the duplicates), R-47, and P-119 systems (but not P-250) and was most pronounced in the higher-current systems, though the performances of these systems remained stable. This decline in *Geobacter* relative abundance was accompanied by

increased representation of unclassified sequences, *Bacteroidetes*, *Chlorobi*, or *Actinobacteria* phyla.

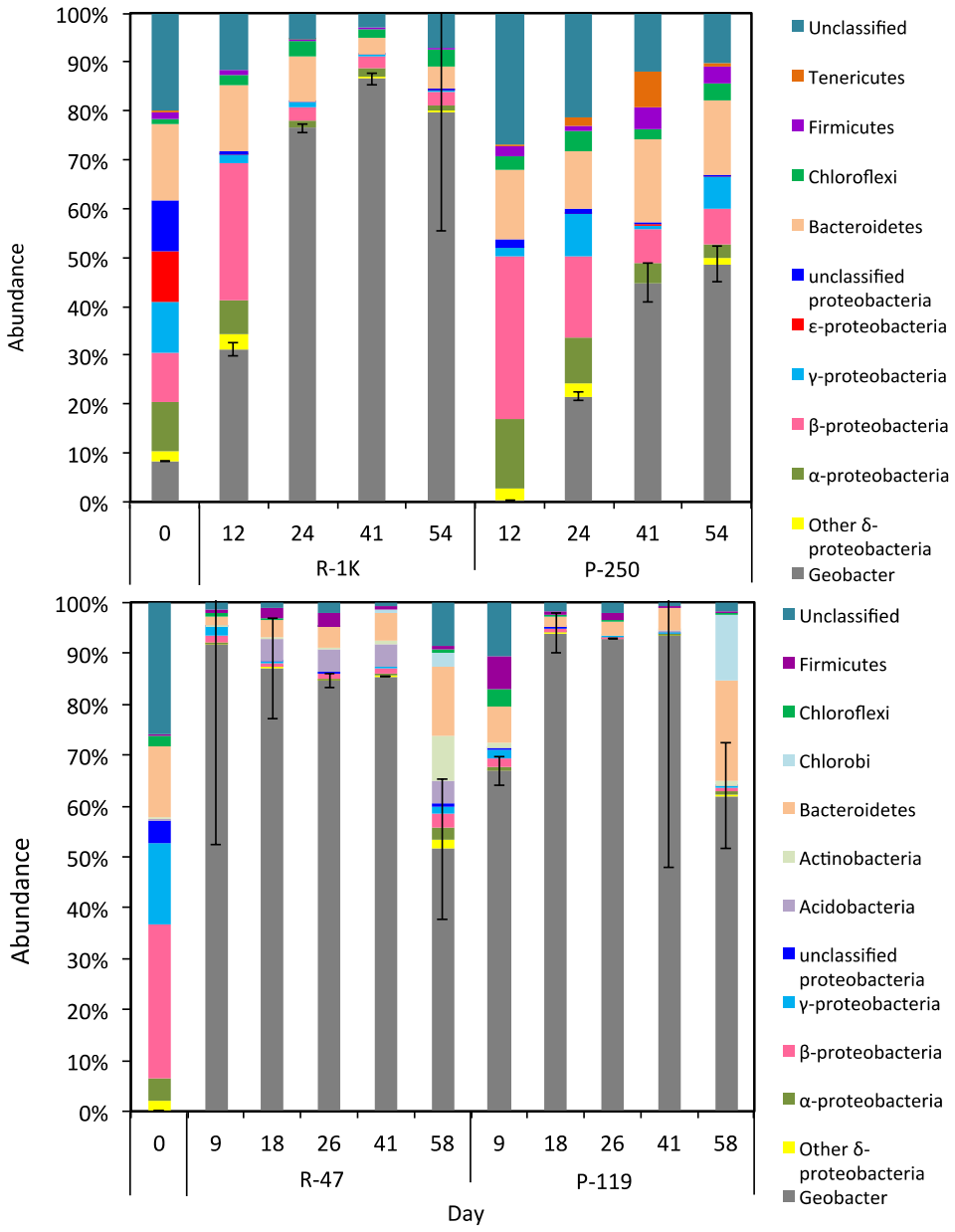

Figure 3-7. Abundance of *Geobacter* genus (singled out because it was the most abundant known exoelectrogen detected), classes from Proteobacteria, and other dominating phyla in the anode time series biofilm samples of P-250 and R-1k (A), and P-119 and R-47 (B). Taxonomies with < 2% maximum relative abundance in the bacterial community were not shown, and their total abundance was less than 2%. Day 0 samples were from the two inocula. Error bars for *Geobacter* genus are shown.

3.3.4 Air cathodes enriched aerobic and facultative bacterial populations

Started with the same inocula, the cathode biofilms had significantly distinct bacterial community structures from the corresponding anodes at the end of MFC operation (Figure 3-8). In the cathode biofilm of all MFC reactors, bacteria from the *Comamonadaceae* family, mainly common aerobic soil bacteria from the *Acidovorax* genus, were outcompeted by the enrichment of *Thauera* and *Dechloromonas* genera from the *Rhodocyclaceae* family. *Dechloromonas* species might be denitrifiers or perchlorate-reducing bacteria living facultatively on the air cathode [23, 24]. Significant enrichment of *Actinobacteria* that were all from the *Mycobacterium* genus were found in R-47 and P-119, but not the lower-current R-1k or P-250 reactors.

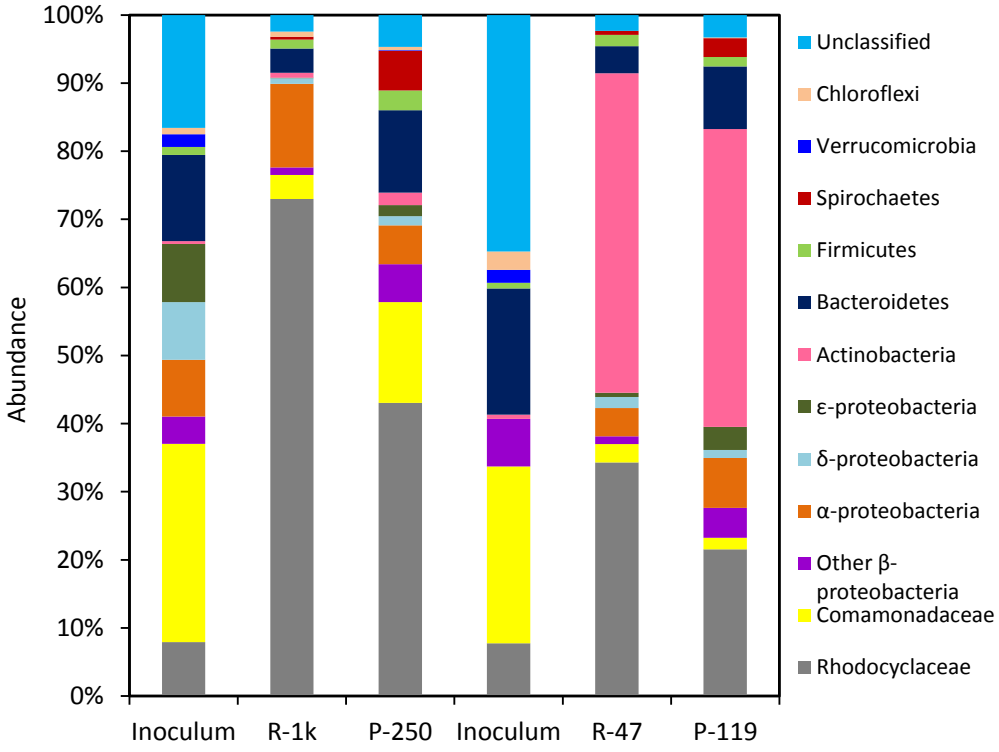

Figure 3-8. The abundance of dominating family, class, and phylum in the cathode biofilm at the end of the operation of P-250, R-1k, P-119, and R-47. Taxonomies with < 2% maximum relative abundance in the bacterial community were not included, and their total abundance was less than 2%.

3.3.5 Comparative analysis of bacterial communities in anode and cathode biofilms

The results from principle component analysis (PCA) (Figure 3-9) showed that the development of the anode bacterial community in P-250 was slower and had a different path from that in R-1k MFCs (Figure 3-9B). Whereas the time-series communities from R-1k quickly converged to the same principle component location, the successive P-250 communities were different from the R-1k communities and never converged over the duration of the sampling. The development paths of the anode bacterial communities from R-47 and P-119 (Figure 3-9C) had both overlaps and differences, with all four systems initially developing similarly from the common inoculum, but then one of the P-119 communities showing little change in the last few weeks of operation while the other three systems continued to change to similar locations on the PCA coordinates. The communities from the different anode potential reactors (Figure 3-9D) developed differently, except that the community in one of the P-119 reactors was more similar to the P-250 communities on the last two sampling events. The PCA plots also show that the bacterial communities of the air-cathode biofilms developed differently from the anode biofilms from identical inocula.

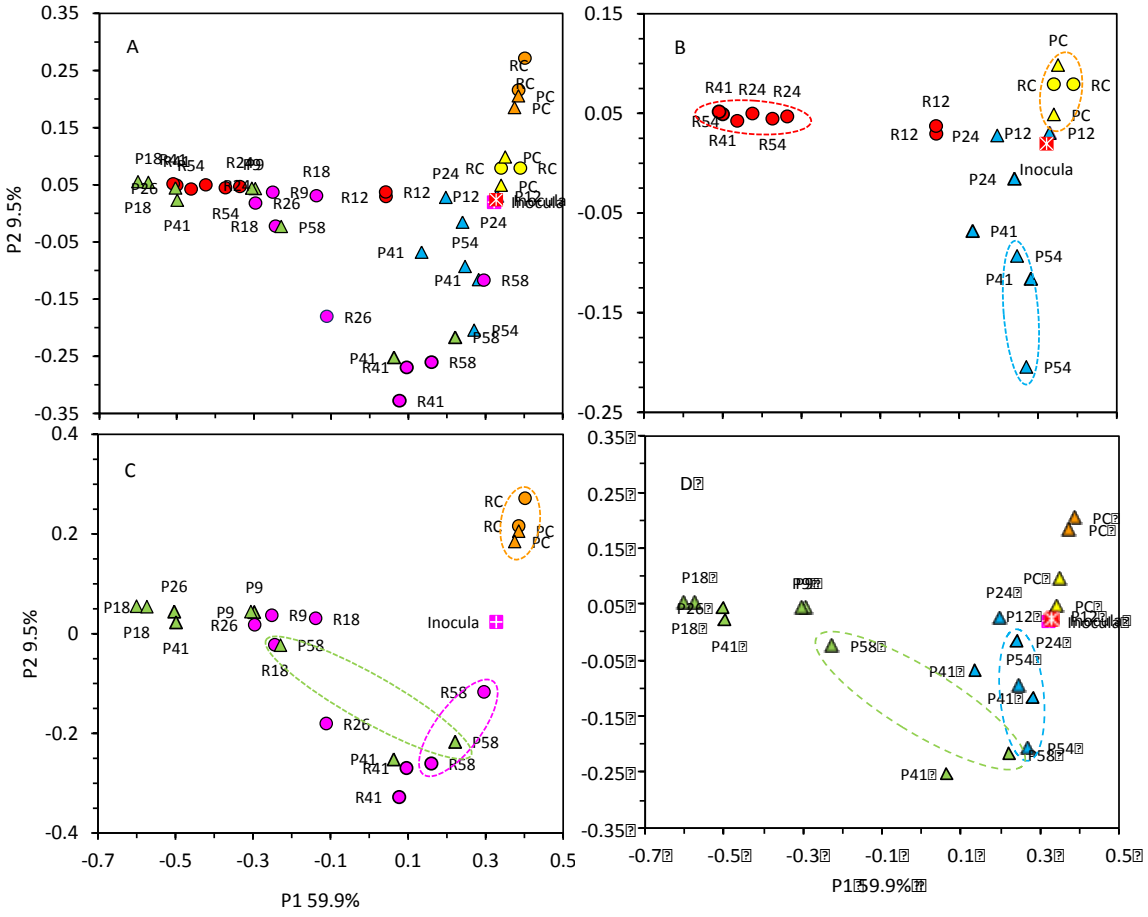

Figure 3-9. Principle component analysis (PCA) plots of two inocula, the anode time series biofilm samples, and air-cathode biofilm samples at the end of the operation (A) in all MFCs, excluding one anomaly (one duplicate of R-47 at day 9 had a significantly off-scale P2 value). Comparative plots for (B) P-250 and R-1k, (C) P-119 and R-47, and (D) P-250 and P-119 are also shown here. Duplicated samples are shown as individual data points in the plots. Clusters of the convergent terminal bacterial community from each MFC are circled. Labels follow the same notation as **Figure 3-6**.

3.4 Discussion

3.4.1 Setting anode potential: stricter screening or faster growth?

In BESs for current production, it is preferred in simple substrate conditions to have more exoelectrogenic bacteria dominating the anode microbial community. Setting lower anode

potentials (down to -150 mV) was previously found to lead to more *Geobacter sulfurreducens* enriched in the anode biofilm after more than 25-day operation [7, 8]. In one of our experiment sets, R-47 and P-119, slightly higher abundance of *Geobacter* species (by 8%) was found with fixed anode potentials than with the corresponding fixed external resistance after 18-day operation (Figure 3-7). However, time series sampling showed that setting the anode potential at the negative peak value prolonged the enrichment of *Geobacter* species, compared to that with dynamic anode potentials (Figure 3-7). This delayed enrichment effect was even more significant when the anode potential was set at a lower value (-250 mV). This might be related to the low biomass yield in the anode biofilm of P-250, which was visually apparent relative to that of R-1k, and much less than that of R-47 and P-119. This is in accord with the previous finding that anode biomass production increases with increased possible metabolic energy gain [2, 11], which is proportional to the difference between the anode potential and the redox potential of the substrate or terminal electron donor of the bacterium (eq. 3-1). Therefore, although setting the anode potential at the negative peak value of the corresponding fixed-resistance system tends to screen bacteria that are capable of obtaining energy at lower anode potentials, it also leaves less energy over the course of a batch cycle that can be extracted for microbial growth, thus slowing down the development of the whole anode microbial community as well as the enrichment of exoelectrogenic bacteria.

3.4.2 Anode community diversity distributed spatially along brush anodes

As explained in the materials and method section, sampling at any position of the anode brush was assumed to represent the whole anode biofilm community, because previously the dominant bacterial groups in an anode biofilm were found homogenously distributed among the identical graphite fiber brush anodes [19]. However, the microbial fuel cells in Vargas et al

(2013) were operated with an external resistance of 1 kΩ, which allows a relatively small current. In this study, a decline in abundance of *Geobacter* species was found at the end of the operation of R-1k (only one of the duplicates), R-47, and P-119, with the decline being significantly pronounced in the higher-current reactors. As the anode biofilms were sampled from the anode brush beginning on the cathode end, the apparent reverse enrichment of *Geobacter* spp. could have been community variance along the anode electrode in our case, perhaps due to uneven current distribution along the brush anode, as reported by Zhang *et al* [25]. However, Zhang *et al*'s study was performed on a scaled MFC (1.87 liter) in which the unevenness of the current distribution was more obvious with larger current production (up to 123 mA). Interestingly, we found this apparent reverse enrichment effect was less obvious in the potentiostatic reactors in each MFC pair (i.e., P-250 compared to R-1k, and P-119 compared to R-47). This might indicate that setting anode potential could partially relieve the unevenness of the current and microbial distribution spatially along the anode brush.

3.4.3 Possible effect on cathodic microbial community from pH gradient due to the addition of CEM

The addition of the selemion CEM partially prevented excessive oxygen intrusion to the anode biofilm, as the CE (28% - 41%) for MFC R-1k (Table 3-1) was considerably higher than the CE from the same MFC design without any membranes (20% -27%) [17]. Although two holes were cut in the CEM to relieve the proton transfer resistance (Figure 3-2), the effectiveness of this modification was not verified and the addition of the CEM might still increase the pH gradient in the anolytic bulk solution and especially in the narrow cathodic space between the membrane and the air cathode. We found that the cathode microbial community in MFC R-1k and P-250 still had similar dominating bacterial groups with air-cathode biofilms in single-chamber MFCs lacking

membranes [26], however, with greater current density, the cathode biofilm in R-47 and P-119 were largely dominated by *Mycobacterium* genus, which has a unique cell wall and can survive long exposure to acids and alkalis [27, 28].

Table 3-1. Accumulated coulombs per cycle (*Q*, C) (maximum, minimum, and average) and coulombic recovery (*CR*, %) (maximum, minimum, and average) of each MFC condition.

	P-250	**R-1k**	**P-119**	**R-47**
Max/Min *Q* (C)	64 / 11	101 / 65	203 / 96	202 / 62
Average *Q* (C)	40 ± 16	85 ± 9	182 ± 23	182 ± 26
Max/Min *CR* (%)	26 / 5	41 / 28	83 / 39	82 / 25
Average *CR* (%)	17 ± 6	35 ± 4	75 ± 9	74 ± 10
Total batches	10	13	29	27

3.4.4 Comparative discussion with other findings

Setting lower anode potentials down to -150 mV was previously found to lead to more *G. sulfurreducens* enriched in the anode biofilm after more than 25-day operation [7, 8]. Formic acid-fed anodic communities with a fixed anode potential of -150 mV enriched more *Geobacter* spp. than with an external resistance of 1 kΩ [7], though the fixed anode potential was approximately 100 mV higher than the minimum anode potentials of reactors with the 1 kΩ external resistance. However, in our study, anodic communities with a fixed anode potential of -250 mV had a significantly lower composition of *Geobacter* spp. than with an external resistance of 1 kΩ after almost two months operation. The electrochemical performance in the P-250 reactors never stabilized over 54 day operation and had lower current production than the R-1k systems. Another study reported that an air-cathode MFC with a fixed anode potential of -200 mV and without an ion exchange membrane took about 20 to 40 days to start up, and its current density went from smaller than to greater than a system with fixed resistance (1 kΩ) after 10 to 15 day operation [6]. However, a single-chamber MEC with no oxygen intrusion and operated with

an anode potential of -250 mV [5] had a similar current production level with the P-250 reactors in this study.

The apparent off-trend behavior of the P-250 reactors in this study at selecting *Geobacter* spp. might be due to the extra low potential used here and the addition of a cation exchange membrane at the cathode to reduce oxygen intrusion into the medium. With marginal theoretical energy gain and limited oxygen as an alternative terminal electron acceptor, the anodic community and current production in the P-250 systems developed very slowly and had not reached steady state at the conclusion of these experiments (Figures 3-5 and 3-9). Previous community analyses using PCA to interpret DGGE patterns showed that the acetate-fed anodic community with a 1 kΩ external resistance did not stabilize until 40 days [29]. Another explanation of these results is a possible limitation of potentiostatic operation with a volumetric anode because of uncertainty in the actual anode potential caused by variable proximity to the reference electrode. This might lead to even lower actual anode potentials being applied to the system that exaggerated this difference by allowing negligible energy gain from acetate oxidation and anode reduction.

3.5 Acknowledgements

We acknowledge Dr. Justin Tokash's advice on potentiostatic operation and Matt Yates's help with the initial adaptation to mothur program. Financial support under King Abdullah University of Science and Technology (KAUST) KUS-I1-003-13 and Army Research Office Equipment Grant W911NF-11-1-0410 are gratefully acknowledged.

3.6 Literature cited

1. Logan, B.E., Exoelectrogenic bacteria that power microbial fuel cells. *Nature Reviews Microbiology*, 2009. **7**(5): p. 375-381.
2. Wei, J.C., et al., A new insight into potential regulation on growth and power generation of *Geobacter sulfurreducens* in microbial fuel cells based on energy viewpoint. *Environmental Science & Technology*, 2010. **44**(8): p. 3187-3191.
3. Busalmen, J.P., A. Esteve-Nunez, and J.M. Feliu, Whole cell electrochemistry of electricity-producing microorganisms evidence an adaptation for optimal exocellular electron transport. *Environmental Science & Technology*, 2008. **42**(7): p. 2445-2450.
4. Finkelstein, D.A., L.M. Tender, and J.G. Zeikus, Effect of electrode potential on electrode-reducing microbiota. *Environmental Science & Technology*, 2006. **40**(22): p. 6990-6995.
5. Zhu, X.P., M.D. Yates, and B.E. Logan, Set potential regulation reveals additional oxidation peaks of *Geobacter sulfurreducens* anodic biofilms. *Electrochemistry Communications*, 2012. **22**: p. 116-119.
6. Zhang, F., et al., Improving startup performance with carbon mesh anodes in separator electrode assembly microbial fuel cells. *Bioresource Technology*, 2013. **133**: p. 74-81.
7. Sun, D., et al., Syntrophic interactions improve power production in formic acid fed MFCs operated with set anode potentials or fixed resistances. *Biotechnology and Bioengineering*, 2012. **109**(2): p. 405-414.
8. Torres, C.I., et al., Selecting anode-respiring bacteria based on anode potential: phylogenetic, electrochemical, and microscopic characterization. *Environmental Science & Technology*, 2009. **43**(24): p. 9519-9524.

9. Commault, A.S., et al., Influence of anode potentials on selection of *Geobacter* strains in microbial electrolysis cells. *Bioresource Technology*, 2013. **139C**: p. 226-234. DOI: 10.1016/j.biortech.2013.04.047.

10. Cho, E.J. and A.D. Ellington, Optimization of the biological component of a bioelectrochemical cell. *Bioelectrochemistry*, 2007. **70**(1): p. 165-172.

11. Aelterman, P., et al., The anode potential regulates bacterial activity in microbial fuel cells. *Applied Microbiology and Biotechnology*, 2008. **78**(3): p. 409-418.

12. Parot, S., M.L. Delia, and A. Bergel, Forming electrochemically active biofilms from garden compost under chronoamperometry. *Bioresource Technology*, 2008. **99**(11): p. 4809-4816.

13. Schroder, U., Anodic electron transfer mechanisms in microbial fuel cells and their energy efficiency. *Physical Chemistry Chemical Physics*, 2007. **9**(21): p. 2619-2629.

14. Logan, B.E., et al., Microbial fuel cells: Methodology and technology. *Environmental Science & Technology*, 2006. **40**(17): p. 5181-5192.

15. Clauwaert, P. and W. Verstraete, Methanogenesis in membraneless microbial electrolysis cells. *Applied Microbiology and Biotechnology*, 2009. **82**(5): p. 829-836.

16. Liu, H. and B.E. Logan, Electricity generation using an air-cathode single chamber microbial fuel cell in the presence and absence of a proton exchange membrane. *Environmental Science & Technology*, 2004. **38**(14): p. 4040-4046.

17. Cheng, S., H. Liu, and B.E. Logan, Increased performance of single-chamber microbial fuel cells using an improved cathode structure. *Electrochemistry Communications*, 2006. **8**(3): p. 489-494.

18. Hutchinson, A.J., J.C. Tokash, and B.E. Logan, Analysis of carbon fiber brush loading in anodes on startup and performance of microbial fuel cells. *Journal of Power Sources*, 2011. **196**(22): p. 9213-9219.

19. Vargas, I.T., I.U. Albert, and J.M. Regan, Spatial distribution of bacterial communities on volumetric and planar anodes in single-chamber air-cathode microbial fuel cells. *Biotechnology and Bioengineering*, 2013. doi: 10.1002/bit.24949.

20. Dowd, S.E., et al., Evaluation of the bacterial diversity in the feces of cattle using 16S rDNA bacterial tag-encoded FLX amplicon pyrosequencing (bTEFAP). *Bmc Microbiology*, 2008. **8**.

21. Ishak, H.D., et al., Bacterial diversity in Solenopsis invicta and Solenopsis geminata ant colonies characterized by 16S amplicon 454 pyrosequencing. *Microbial Ecology*, 2011. **61**(4): p. 821-831.

22. Medina, R.F., P. Nachappa, and C. Tamborindeguy, Differences in bacterial diversity of host-associated populations of *Phylloxera notabilis* Pergande (Hemiptera: Phylloxeridae) in pecan and water hickory. *Journal of Evolutionary Biology*, 2011. **24**(4): p. 761-771.

23. Horn, M.A., et al., *Dechloromonas denitrificans* sp nov., *Flavobacterium denitrificans* sp nov., *Paenibacillus anaericanus* sp. nov and *Paenibacillus terrae* strain MH72, N2O-producing bacteria isolated from the gut of the earthworm *Aporrectodea caliginosa*. *International Journal of Systematic and Evolutionary Microbiology*, 2005. **55**: p. 1255-1265.

24. Wolterink, A., et al., *Dechloromonas hortensis* sp nov and strain ASK-1, two novel (per)chlorate-reducing bacteria, and taxonomic description of strain GR-1. *International Journal of Systematic and Evolutionary Microbiology*, 2005. **55**: p. 2063-2068.

25. Zhang, L., et al., Anodic current distribution in a liter-scale microbial fuel cell with electrode arrays. *Chemical Engineering Journal*, 2013. **223**: p. 623-631.

26. Shehab, N., et al., Characterization of bacterial and archaeal communities in air-cathode microbial fuel cells, open circuit and sealed-off reactors. *Applied Microbiology and Biotechnology*, 2013: p. doi:10.1007/s00253-013-5025-4.

27. Cole, S.T., et al., Deciphering the biology of *Mycobacterium tuberculosis* from the complete genome sequence. *Nature*, 1998. **393**(6685): p. 537-544.

28. Young, R.A., et al., Genes for the major protein antigens of the leprosy parasite mycobacterium-leprae. *Nature*, 1985. **316**(6027): p. 450-452.

29. Xing, D., et al., Isolation of the exoelectrogenic denitrifying bacterium Comamonas denitrificans based on dilution to extinction. *Applied Microbiology and Biotechnology*, 2010. **85**: p. 1575-1587.

Chapter 4

Metabolic Flux Change With Cathode-Derived Electron Supplement in *Clostridium acetobutylicum* Biocathode

Abstract

In this study, we tested the possibility of using electrical energy *without* exogenous mediator addition to influence the distribution of valuable extracellular products, such as hydrogen, butanol, and ethanol, using *C. acetobutylicum* as the cathode biocatalyst. We demonstrated that *C. acetobutylicum* is exoelectrotrophic by fixing a cathode potential at -400 mV and providing organic carbon sources. *C. acetobutylicum* achieved a current uptake of up to 83 mA/m^2, with a decreasing trend over time that electrochemical impedance spectroscopy showed was probably due to an increased cathode charge transfer resistance. Negative control experiments and cyclic voltammetry tests ruled out abiotic electrochemical hydrogen evolution and electron shuttles for electron transfer, suggesting that the cells directly derived electrons from the cathode electrode. Increased yields of more energy dense products (hydrogen and butanol) and decreased yields of butyrate, acetate, and ethanol were found with current uptake by *C. acetobutylicum*. The electron balance indicated that current uptake might have also reduced the biomass production of *C. acetobutylicum*, which was not directly measured. This study demonstrated that a solventogenic bacterium can be exoelectrotrophic. The metabolic flux shift with current uptake found in this study provides a primary guidance for the potential utilization of a *C. acetobutylicum* biocathode in a bioelectrochemical system.

4.1 Introduction

Clostridium acetobutylicum has been the most extensively studied and utilized clostridia species due to its acetone-butanol-ethanol (ABE) production pathways [1]. With carbohydrates as the substrate, *C. acetobutylicum* can produce hydrogen, carbon dioxide, acetate, and butyrate during the acidogenic fermentation phase. With the resultant pH decrease, the metabolism of *C. acetobutylicum* can then shift to solventogenic pathways, which produce acetone, butanol, and ethanol [1]. In industrial ABE fermentation plants, the produced acetone and butanol were separated from the liquor through a serious distillation processes. The produced carbon dioxide and hydrogen were also recovered and separated for further use [2, 3]. However, the traditional ABE fermentation processes relied on the use of conventional starch (maize, wheat, millet, rye, etc.) or sugar (molasses), which greatly affected the economic viability of the ABE fermentation and caused it to gradually lose its market due to competition with petrochemical solvent production [4, 5]. Although alternative fermentation substrates, such as xylose and arabinose hydrolyzed from corn cob, have been demonstrated to be fermented by *C. acetobutylicum* [6], new technologies that assist *C. acetobutylicum* to convert more diverse renewable biomass into biofuels would help provide a more sustainable solvent production process.

Altered electron flow has previously been found in *C. acetobutylicum* (ATCC 4259) fermentation using electrochemical energy as a source of reducing equivalents in the presence of the exogenous electron mediator methyl viologen [7]. Cathode-donated electrons were used to reduce $NAD(P)^+$:ferredoxin oxidoreductase, which affected the main electron pathways in the branched fermentation of *C. acetobutylicum*, resulting in increased yields of the more reduced butanol (up to 26%) and decreased yields of less reduced acetone (up to 25%) [7]. Also, *C. acetobutylicum* was demonstrated to produce exclusively hydrogen using cathode-derived electrons under organic-free conditions in the presence of methyl viologen [8]. Recently, *C.*

acetobutylicum (ATCC 824) was demonstrated to generate current by anode reduction in glucose-fed MFCs without the addition of redox mediators [9], with the current profile indicating the change from acidogenesis to solventogenesis. These results led us to speculate whether *C. acetobutylicum* can directly accept electrons from a cathode without exogenous mediator addition and achieve altered fermentation product distribution.

It was recently demonstrated that acetogens could synthesize acetate from CO_2 on a cathode electrode by consuming electrical current [10, 11]. The use of microbes as biocatalysts for synthesis reactions in electrochemical cells has been called microbial electrosynthesis (MES) [12]. Unlike acetogens, most solventogenic bacteria, including *C. acetobutylicum*, do not have the Wood-Ljungdahl pathway for CO_2 fixation [13, 14]. This indicates that even if they can receive electrons directly from a cathode, they would still have to grow heterotrophically for bioproduction. Therefore, organic substrates would still need to be supplied as a carbon source for *C. acetobutylicum* at the cathode, but the metabolic products yield might be altered through the exogenous provision of additional reducing equivalents.

Therefore, in this study, we first tested whether *C. acetobutylicum* is exoelectrotrophic by supplying a cathode potential of -400 mV and glucose as the organic carbon source. Negative control experiments and cyclic voltammetry tests were performed to assess the possible presence of electron shuttles in original YTG medium and investigate the electron transfer mechanism between *C. acetobutylicum* and the cathode. Second, we monitored the metabolic flux change in *C. acetobutylicum* with current uptake from the cathode, including the production of hydrogen, butanol, ethanol, acetone, butyrate, and acetate. Finally, an electron balance was performed to evaluate the contributions from the cathodic current and glucose to the fermentation products.

4.2 Materials and methods

4.2.1 Reactor configuration and operation

Glass-bottle, two-chamber H-type MECs (Glasstron In., Vineland, NJ) were used for all the following tests (Figure 4-1). Each MEC chamber was 180 ml and filled with 110 ml N_2-degassed medium. The chambers were connected by two sidearm joints of 2.5 cm inner diameter and a cation exchange membrane (Nafion 117, FuelCellStore). Both anode and cathode electrodes were graphite carbon plates (surface areas of 18.82 cm^2) (GraphiteStore.com Inc., Buffalo Grove, IL) polished using sandpaper (grit type 400 and 1500), sonicated to remove debris, cleaned by soaking in 1 N hydrochloric acid overnight, and rinsed three times in Milli-Q water [15].

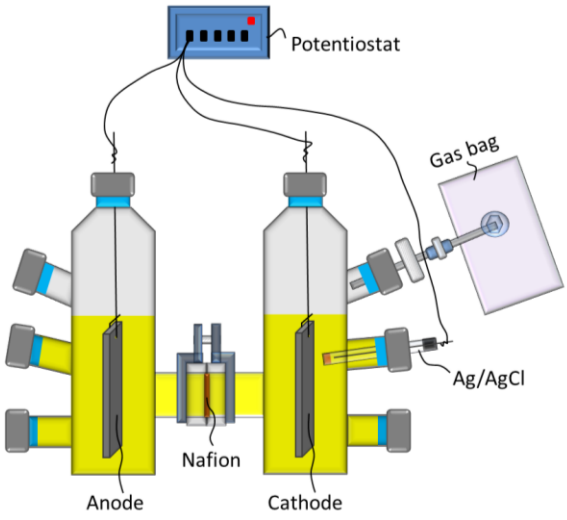

Figure 4-1. Schematic of reactor configuration.

The cathode chamber was inoculated with 10% *C. acetobutylicum* (ATCC 824) suspended culture, which had been grown anaerobically at 37 °C in YTG medium (pH = 6.7) containing 5 g L^{-1} glucose (28 mM), 16 g L^{-1} Bacto tryptone, 10 g L^{-1} yeast extract, and 8 g L^{-1} NaCl. The cathode potential (E_c) was maintained at -611 mV versus a Ag/AgCl reference

electrode (+ 211 mV versus SHE) (RE-5B, Bioanalytical Systems, Mount Vernon, IN), equivalent to -400 mV versus SHE, to avoid the abiotic electrochemical evolution of hydrogen. Gas produced in the cathode chamber was vented through a 22-gauge syringe needle inserted through a silicone septum and connected with a 0.2-μm sterile Polyethersulfone syringe filter (VWR International, Radnor, PA). The filtered gas was then transferred through a gas valve and a short length of Teflon tubing and collected in a gas bag (Calibrated Instruments, McHenry, MD) (Figures 4-1, 4-2).

Figure 4-2. Reactor setup of four MECs.

4.2.2 Long-term current-uptake experiment

Duplicate MECs (MEC1 and MEC2) were operated for two months to assess the ability of *C. acetobutylicum* pure culture to draw current from a cathode electrode without exogenous electron mediators. The anode chamber and the cathode chamber were filled with pure water and YTG medium, respectively. Before the inoculation of *C. acetobutylicum* to the cathode chamber, MECs with sterile medium were operated at E_c = -400 mV to exclude the possibility of abiotic hydrogen production. MECs with *C. acetobutylicum* biocathodes were operated for 8 batches, each approximately one week long, then left in open circuit during batch 9, and changed back to

closed circuit in batch 10. MECs during batches 5 to 10 were fed YTG with a reduced glucose concentration (1 g L^{-1} or 5.5 mM).

4.2.3 Metabolic flux comparison test

To monitor the possible metabolic flux changes in *C. acetobutylicum* associated with current uptake, two groups of duplicated MECs were operated for 4 batches, with group C in closed circuit for all four batches and group C-O in closed circuit for batches 1 and 2 and open circuit for batches 3 and 4. Electrodes were transferred to clean MEC reactors at the end of batch 2 and batch 3 to reduce effects from suspended cells. The anode chambers were filled with sterile YTG medium without glucose, and the cathode chambers were fed YTG medium with the addition of an oxygen scavenger (5 g L^{-1} L-cysteine) based on headspace oxygen detection in the latter batches of the long-term tests and a reduced glucose concentration (12 mM for batches 1 and 2 and 7.5 mM for batches 3 and 4) to reduce the effects from suspended growth. To assess the contribution of non-biological electrochemical reactions and suspended cells to the current uptake, cyclic voltammetry (CV) tests were performed with a potentiostat (VMP3, BioLogic, Knoxville, TX) on the abiotic cathode before inoculation and *C. acetobutylicum* biocathodes and cathode effluent (separately) at the end of batch 4.

4.2.4 Electrochemical monitoring and experiments

Cathode potential setting, anode potential and current-uptake monitoring, CV, and Electrochemical Impedance Spectroscopy (EIS) tests were all conducted using a potentiostat (VMP3, BioLogic, Knoxville, TX). Current density was calculated by normalizing current by the cathode electrode surface area (18.82 cm^2). Cell voltages were calculated as $E_{cell} = E_c - E_a$.

During the CV tests, cathode potential was scanned from +0.15 to -0.7 V vs Ag/AgCl at a scan rate of 1 mV s^{-1} for the abiotic cathode in sterile medium, and 0.1 mV s^{-1} for both the biocathode in fresh medium and a new cathode in the cathode effluent from batch 4 of the metabolic flux comparison test. To identify the changes of solution resistance, anode charge transfer resistance, and cathode charge transfer resistance over time, EIS was conducted during batches 1 and 4 on MECs at each of the following conditions (all versus SHE): E_c = -400 mV (the fixed cathode potential in all experiments in this study), E_a = -50 mV (the average anode potential when E_c was set at -400 mV and the current uptake was the maximum), and E_{cell} = -350 mV (the corresponding cell voltage to E_c = -400 mV and E_a = -50 mV. The MECs for EIS tests were operated under the same condition as the group C reactors and had current uptake comparable to the group C reactors (data not shown). The frequency of EIS ranged from 100 kHz to 100 mHz, with a sinusoidal perturbation of 10 mV amplitude. Charge transfer resistances were obtained by fitting semi-circles to spectra in Nyquist plots [16].

4.2.5 Analytical methods

Gas samples (250 µl) were drawn twice from each gas bag for composition analysis on a gas chromatograph (GC; SRI 310C and 8610B). Gas production volume (V_{prod}) was quantified using a calibrated glass syringe. The total net moles of produced hydrogen (n_{H_2}) and carbon dioxide (n_{CO_2}) were calculated based on their gas composition fraction (α_{H_2} and α_{CO_2}, v/v) and the total gas volume ($V_{tot} = V_{prod} + V_{head}$, where V_{head} is the cathode headspace volume of 70 ml) (eq. 4-1, 4-2).

$$n_{H_2} = \alpha_{H_2} \cdot V_{tot} \quad \text{(eq. 4-1)}$$

$$n_{CO_2} = \alpha_{CO_2} \cdot V_{tot} \quad \text{(eq. 4-2)}$$

Fermentation products including butyrate, acetate, butanol, ethanol, and acetone were quantified using a GC (GC-2010 Plus, Shimadzu, Kyoto, Japan) with a 30 m × 0.32 mm × 0.5 µm Stabilwax-DA column (Cat. # 11039, Restek, Bellefonte, PA) and helium as the carrier gas. At several points during the MEC batch operation, 1.5 ml aliquots were withdrawn from the cathode chambers and filtered through a 0.2-µm sterile Polyethersulfone syringe filter. Part of the filtered sample (0.4 ml) was diluted to 1 ml with Milli-Q water and stored in a GC vial at -20 °C pending GC analysis; part (0.5 ml) was diluted to 2 ml for glucose concentration measurement using the Dubios method [17]; and the remainder was used for measuring pH using a pH meter (Fisher Scientific, AB15).

4.3 Results

4.3.1 Current uptake by glucose-fermenting Clostridium acetobutylicum

With the cathode potentiostatically maintained at -400 mV, MECs with sterile YTG medium had current uptake less than 1 mA/m^2 (data not shown). However, after the inoculation of *C. acetobutylicum* pure culture to the cathode chamber, a cathodic current of up to -82 mA/m^2 was measured and current uptake was constantly detected for two months of operation with periodic medium changes (Figure 4-3). Although substantial biomass growth occurred in the cathode chambers during each batch, the cathodic current uptake decreased significantly from batch 1 to 5. After being disconnected from the potentiostat and left in open circuit during batch 9, one of the duplicate biocathodes failed to recover its electroactivity when switched back to closed-circuit mode in batch 10 (Figure 4-4). Both an abnormal increase of current uptake with time in one MEC and the presence of oxygen in the headspace were detected in batch 7.

With a lower substrate concentration in the metabolic flux comparison tests, the cathodic current uptake in the two sets of MECs had a smaller magnitude (Figure 4-5, up to -14 mA/m^2) than in the beginning of long-term operation. However, a similar trend of decreasing current uptake with time was observed in both cases. The current uptake in the C and C-O reactors were comparable during batch 1 and 2 (Figure 4-5).

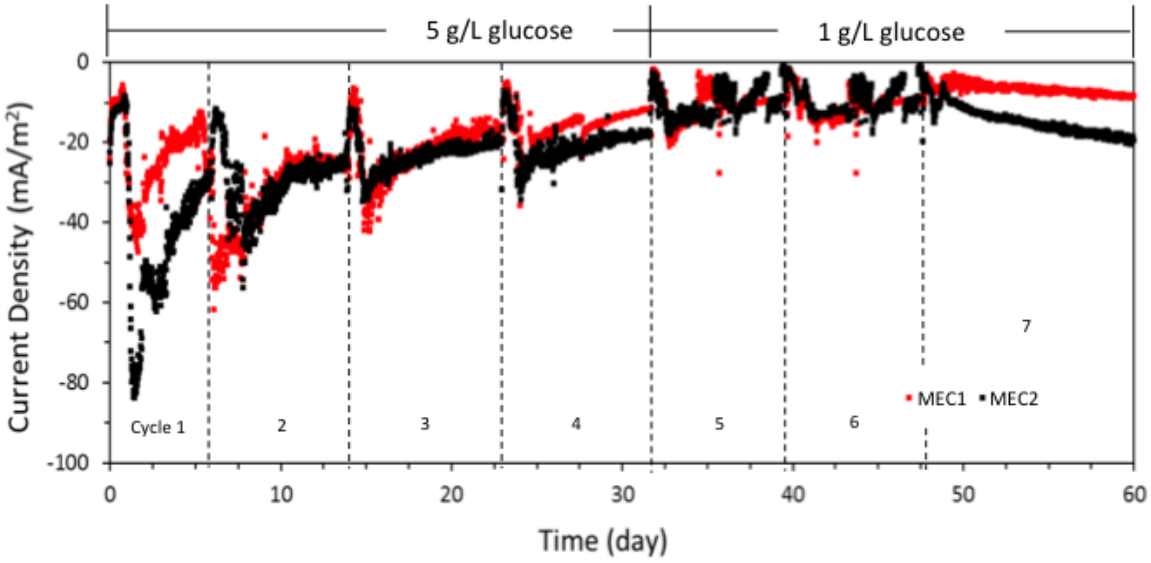

Figure 4-3. Current uptake in long-term experiments demonstrated that *C. acetobutylicum* is exoelectrotrophic.

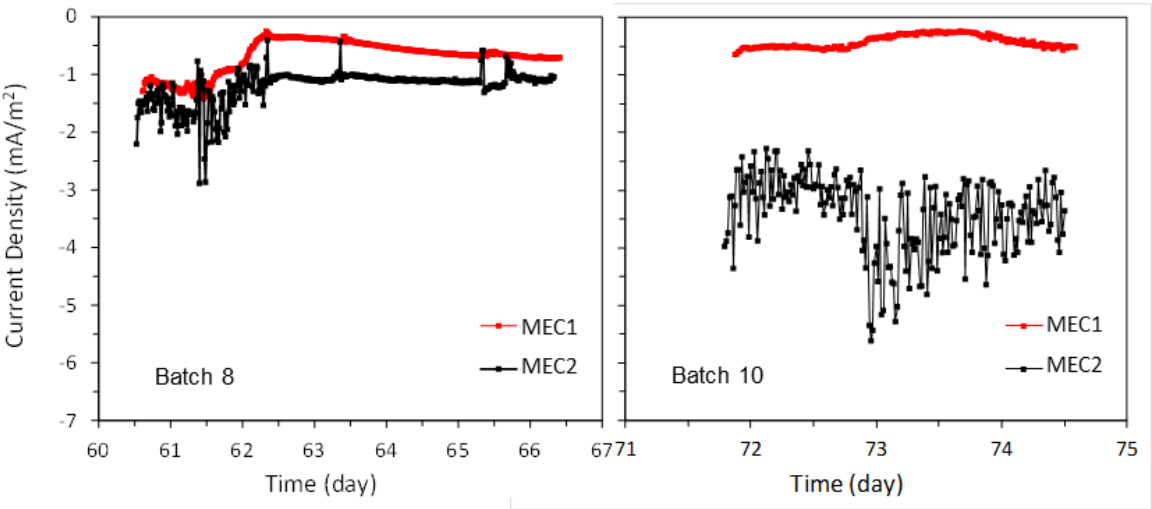

Figure 4-4. Current uptake in batches 8 and 10. After batch 9 in open circuit, one of the duplicate biocathodes failed to recovery its electroactivity.

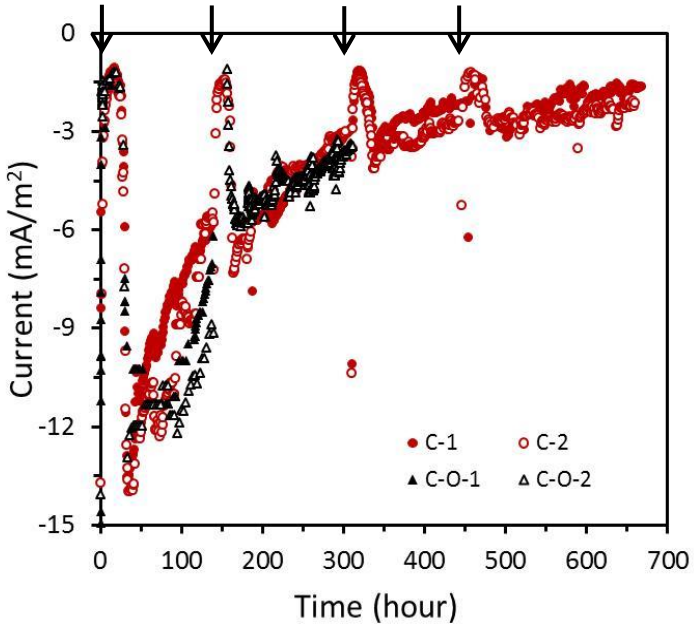

Figure 4-5.Current uptake in metabolic flux comparison test demonstrated that *C. acetobutylicum* is exoelectrotrophic. Reactors C were closed circuit for all four batches, and reactors C-O were closed circuit for batches 1 and 2 and open circuit for batches 3 and 4. Arrows show the times of medium changes.

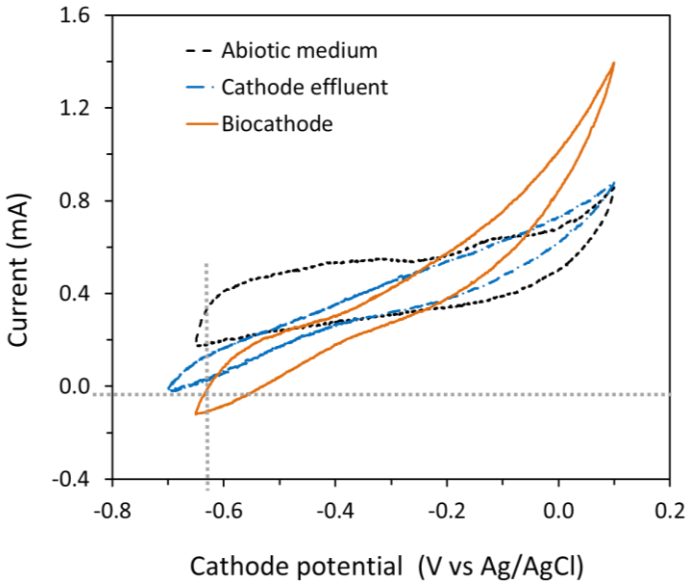

Figure 4-6. Cyclic voltammetry tests of abiotic medium before inoculation (scan rate 1 mV/s), cathode effluent from MECs after the fourth cycle in the metabolic flux comparison test (0.1 mV/s), and the biocathode after four cycles in the metabolic flux comparison test in fresh medium (0.1 mV/s).

CV tests showed no current uptake with either the sterile YTG medium or the cathode effluent containing substantial *C. acetobutylicum* cells from the fourth batch of the MECs in the metabolic flux comparison test (Figure 4-6). The biocathode from the same reactors, however, showed cathodic electroactivity in fresh YTG medium with a negative current around -610 mV vs Ag/AgCl (-400 mV) (Figure 4-6).

4.3.2 Hydrogen production change with current uptake by *Clostridium acetobutylicum*

Prior to the inoculation of *C. acetobutylicum* to the cathode chamber, no hydrogen gas was detected in the headspace of the MECs operated for 24 hours with E_c = -400 mV and the sterile YTG medium. Inoculated MECs had both hydrogen and carbon dioxide production along with current uptake during each batch (Figures 4-7, 4-8). Methane was below detection level during all the batches in all MECs. Net hydrogen oxidation was commonly seen in open-circuit conditions towards the end of the batch based on declining hydrogen composition in the headspace gas, e.g., in batch 3-4 of C-O MECs or batch 9 of MEC 1&2 (Figures 4-7, 4-8), but this was not observed in closed-circuit biocathode systems during either long-term operation or the metabolic flux comparison tests (Figures 4-7, 4-8). Therefore, while net hydrogen production was comparable at the beginning of the batch between open- and closed-circuit reactors, the hydrogen composition at the end of the batch was slightly higher (29%) in closed-circuit conditions (Figure 4-7). The carbon dioxide production was not affected by current uptake (Figure 4-7).

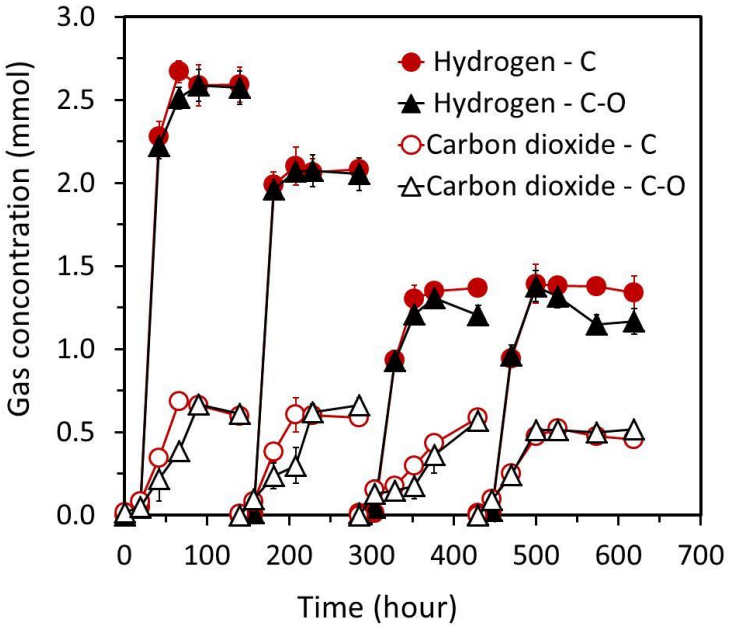

Figure 4-7. Hydrogen and carbon dioxide composition in cathode headspaces during metabolic flux comparison test. Reactors C were closed circuit for all four batches, and reactors C-O were closed circuit for batches 1 and 2 and open circuit for batches 3 and 4.

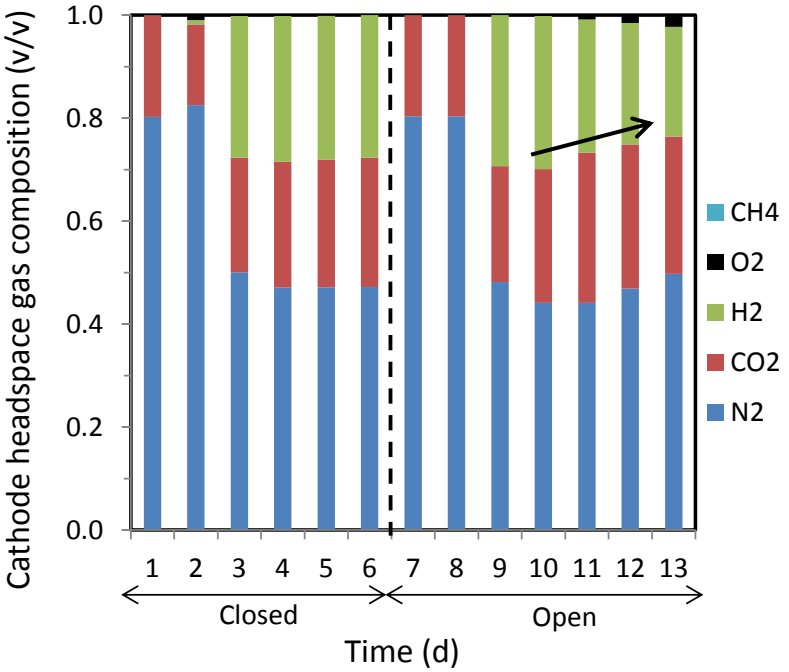

Figure 4-8. Hydrogen production by *C. acetobutylicum* in the cathode chamber with closed (batch 8) and open circuits (batch 9). The arrow points out the net hydrogen oxidation in the open circuit condition.

4.3.3 Fermentation products, glucose consumption, and pH change in the metabolic flux comparison test

With current uptake, decreased butyrate production (by up to 26 ± 6%) and increased butanol production (by up to 53 ± 19%) were detected, based on the batch endpoint differences between group C and group C-O MECs (Figure 4-9A). The occurrence of this metabolic change was similar to the net hydrogen production trend, in that the difference of butyrate production became more pronounced as the batch progressed, with more butyrate consumed but less hydrogen oxidized in group C MECs with current uptake. Decreased ethanol production (by up to 48 ± 12%) and acetate production (by up to 32 ± 3%) were also found with current uptake; however, the initial acetate production in group C MECs was higher than in open-circuit group C-O and the obvious acetate production decrease was only detected in batch 4 (Figures 4-9B, 4-9C). The productions of acetone were not significantly different between group C and C-O MECs (Figure 4-9B). In all cases, the solvent concentrations were significantly lower than the acid products.

Serving as both the organic carbon source and the primary electron donor, glucose was only partially removed during each batch at an average removal efficiency of 49 ± 13%. There was no correlation between glucose removal and current uptake (Figure 4-10). The final solution pH in all MECs was above 5, but the acidification due to the fermentation was slightly relieved in the cathode chamber of the closed-circuit MECs (Figure 4-10).

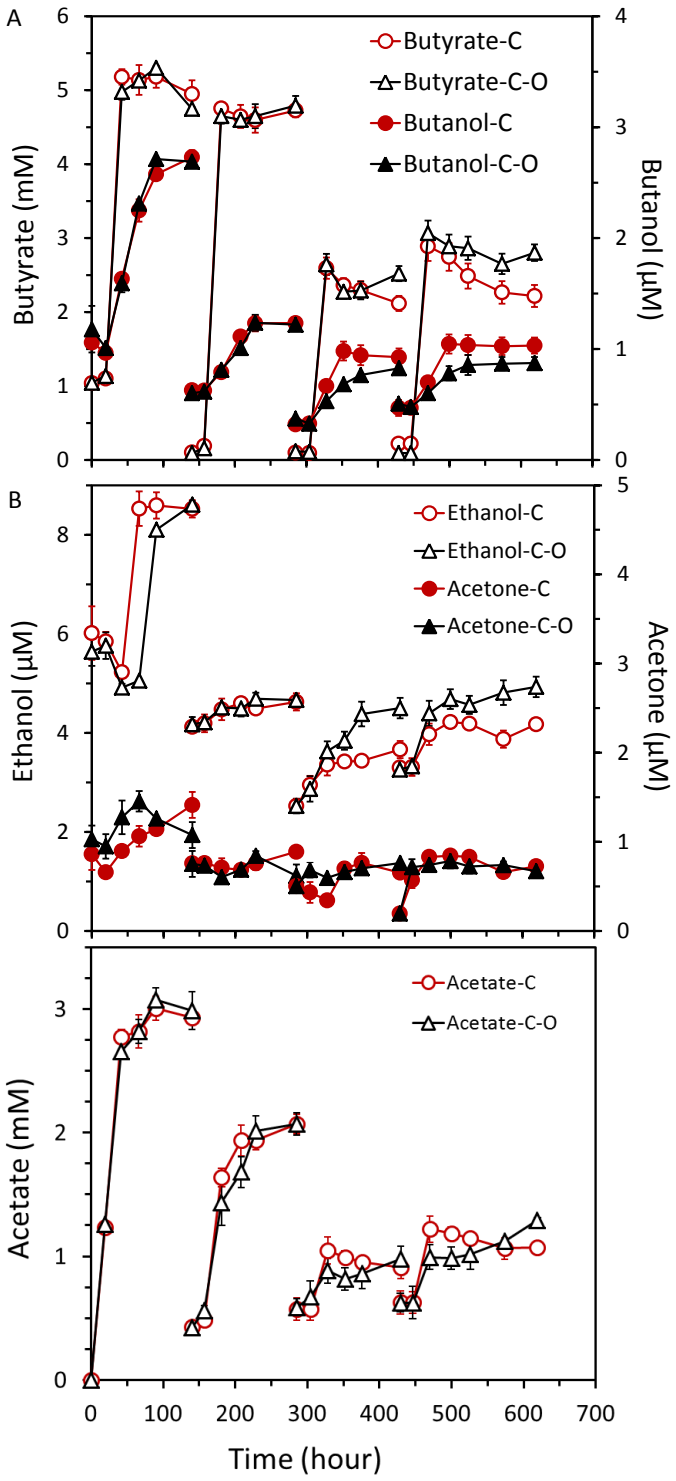

Figure 4-9. Fermentation products with and without current uptake. Reactors C were closed circuit for all four batches, and reactors C-O were closed circuit for batches 1 and 2 and open circuit for batches 3 and 4.

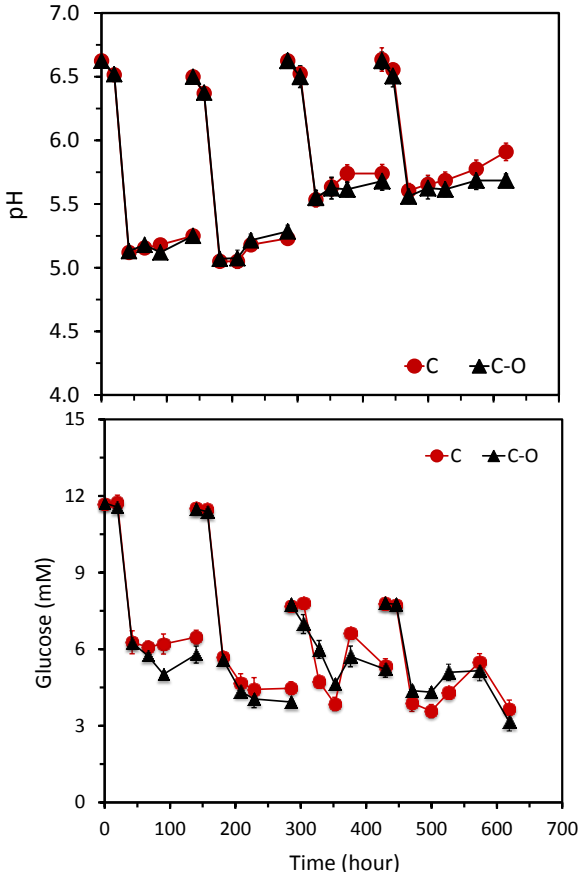

Figure 4-10. Substrate consumption and pH change in metabolic flux comparison test. Reactors C were closed circuit for all four batches, and reactors C-O were closed circuit for batches 1 and 2 and open circuit for batches 3 and 4.

4.3.4 EIS test of resistance changes over time

Whole-cell and cathode EIS results were fitted by an equivalent circuit of $R_1 + C_2/(R_2+Wd_2) + C_3/(R_3+Wd_3)$ and $R_1 + C_2/(R_2+Wd_2)$, respectively (shown graphically in Figure 4-11). In these equivalent circuits, R_1 was assumed to represent ohmic resistance, which refers to solution resistance and membrane resistance in this study. R_2 and R_3 in the equivalent circuit for whole-cell EIS were assumed to correspond to the charge transfer resistance on the anode and cathode electrodes, and R_2 in the equivalent circuit for cathode EIS was assumed to represent the charge transfer resistance on cathode electrodes. The fitted results from those equivalent circuits

showed that the ohmic resistance in *C. acetobutylicum* MECs did not change much after 4 batches, with 104 Ω for cycle 1 and 100 Ω for cycle 4 (Figure 4-11). However, the whole-cell EIS showed that the charge transfer resistance on both the anode and cathode electrodes increased from cycle 1 to cycle 4, with R_2 increasing from 0 to 29 Ω and R_3 increasing from 7 to 72 Ω. The increase in cathode charge transfer resistance from cycle 1 to cycle 4 was also supported by cathode EIS results, with R_2 increasing from 0 to 34 Ω (Figure 4-11). Anode EIS tests were not performed because the cathode potential was fixed by a potentiostat to avoid anode limitation in both the long-term and comparison tests.

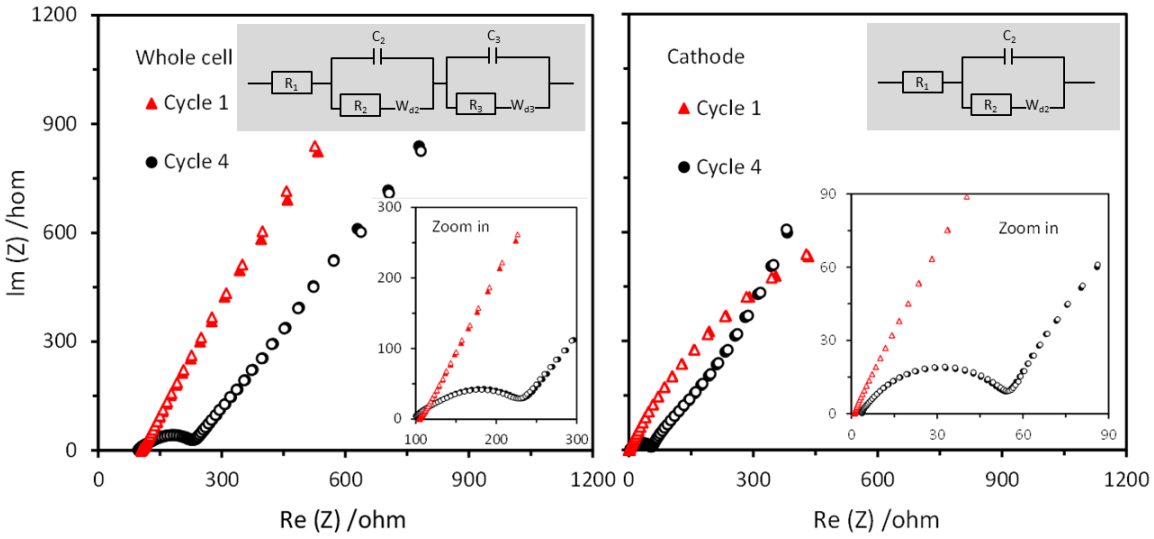

Figure 4-11. EIS tests on whole cell and cathode indicated that the decrease of current uptake was not due to membrane fouling but probably increased cathode charge transfer resistance. Inset figures share the same x and y-axis units as the larger figures. Corresponding equivalent circuits were embeded in each plot.

4.4 Discussion

4.4.1 Exoelectrotrophic C. acetobutylicum serving as a biocatalyst for butanol production

With sterile YTG medium, no negative current was found in either the CV tests or when the cathode potential was set at -400 mV and no hydrogen was produced, indicating that *C. acetobutylicum* served as a biocatalyst for current uptake on the cathode. CV tests of the cathode effluent, which contained substantial suspended *C. acetobutylicum* cells and fermentation products, also showed no negative current at -400 mV, further suggesting that the current uptake by *C. acetobutylicum* occurred in the biocathode but not suspended cells. The absence of reversible redox peaks in the CV showed that cathodic electron transfer did not depend on electron shuttles for electron transfer, but rather the direct contact between the cells and the electrode. The possibility of feeding a mixed-culture biocathode with electrons for the production of various fermentation products including a small fraction of ethanol and butyrate was recently demonstrated and a relationship between the *Clostridium* population with valerate production was reported [18]. However, no specific evidence of *C. acetobutylicum* taking current was reported in that study.

The current uptake by *C. acetobutylicum* reached up to 82 mA/cm^2 at -400 mV with 5 g L^{-1} glucose. This current density would likely be greater if we used a higher glucose concentration (> 10 g L^{-1}), which was widely applied in traditional fermentation experiments [1] and even in MFCs [8]. However, the current densities we obtained in this study were already higher than those induced by the five acetogens previously reported for the electrosynthesis of acetate and 2-oxobutyrate (*i.e. Clostridium ljungdahlii*, *Clostridium aceticum*, *Moorella thermoacetica*, *Sporomusa sphaeroides*, and *Sporomusa silvacetica*) [10]. The current densities

from Nevin *et al* were calculated here based on the consumed coulombs, time durations, and electrode areas provided.

4.4.2 Metabolic flux change in C. acetobutylicum with current uptake

The total electron recovery in metabolic products compared to the total electrons consumed ranged between 68% and 120% (Table 4-1). Electron recoveries went greater than 100% in some batches, which might be due to that some electrons were derived from other YTG medium components that were not accounted for in the calculation. Current uptake in group C MECs resulted in increased hydrogen and butanol production, but decreased ethanol, butyrate, and acetate accumulation compared to group C-O in open circuit (Figure 4-12). The hydrogen yields in the MECs (from 2.1 to 2.7 mol H_2 / mol glucose) were higher or comparable to that in other fermentation studies [19, 20]. The butanol production, however, was 3 orders of magnitude lower than regular fermentation processes [21]. This was mainly due to the high solution pH in MECs (Figure 4-6), as it was reported that the solventogenesis process usually takes place when the pH is below 5 and the optimum pH for butanol and acetone production is 4.3 [22]. Therefore, a low medium pH (< 5) would need to be maintained by adding more acids or glucose (to produce more acids) for more comparable butanol production, as well as other metabolic flux changes.

To investigate the mechanism of the metabolic flux change found with current uptake, a detailed electron balance of group C and C-O MECs during the comparison test was calculated (Table 4-1). However, the results showed that though the metabolic products changed with current uptake, the actual electrons that *C. acetobutylicum* derived from the cathode were less than 1% of that from glucose oxidation, and the electrons derived from the cathode during batch 3 and 4 in group C MECs were not comparable to the increased electrons saved in their products,

when compared to group C-O MECs (Table 4-1). This indicated that current uptake might have also affected biomass production of *C. acetobutylicum*. Therefore, a detailed carbon balance of all carbon products and biomass accumulation (suspended and attached) should be included in a future experiment for better understanding of the metabolic flux shift. Also, a galvanostatic experimental condition with a greater fixed current instead of potentiostatic operation might be helpful to increase the ratio of electrons from current uptake compared to glucose.

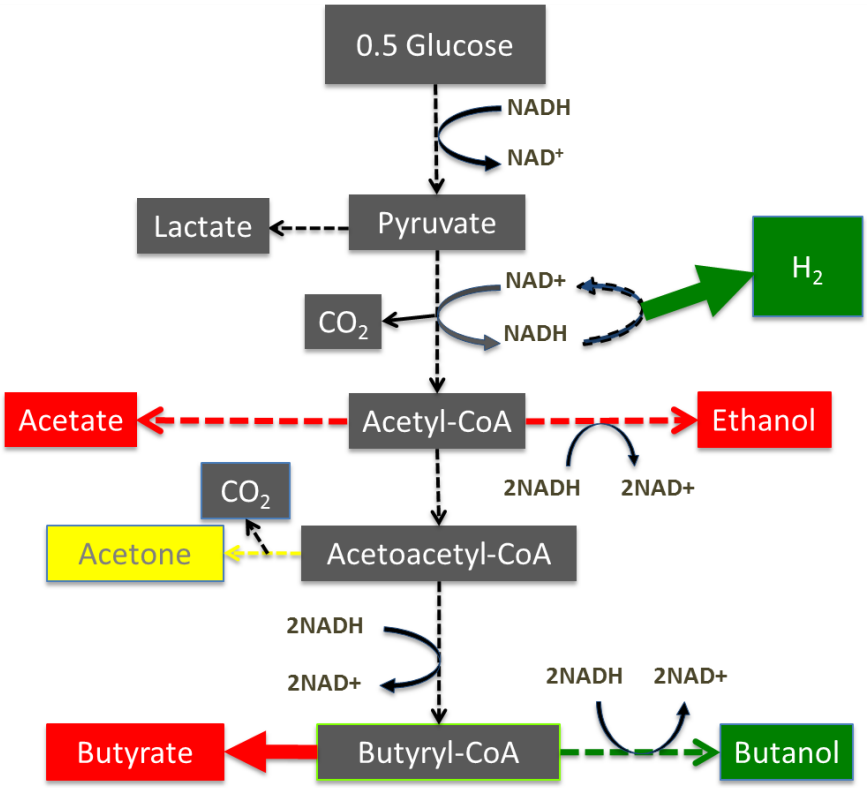

Figure 4-12. Summary of metabolic flux change in *Clostridium acetobutylicum* with current uptake in C reactors relative to open-circuit C-O reactors (green means increased yields of the product, red decreased yields, and yellow no change)

Table 4-1. Electron balance of group C and C-O MECs in the metabolic flux comparison test. Calculation of electrons (unit: C) consumed that came from the cathode and glucose transformation, electrons conserved in organic products, and the energy recovery efficiency for organic matter production are listed below.

Group	Cycle	e^- consumed from		e^- conserved in products						Electron recovery eff[e] (%)	Cathodic e^- contribution[g](%)
		Cathode [a]	Glucose [b]	H_2 [c]	Butanol [d]	Butyrate [d]	Ethanol [d]	Acetate[d]	Acetone[d]		
C	1	**8.7** ± 0.2	**1330** ± 69	**500** ± 21	**0.43** ± 0.02	**830** ± 79	**0.32** ± 0.02	**249** ± 9	**0.07** ± 0.02	118[f]	0.7
	2	**4.1** ± 0.6	**1797** ± 64	**402** ± 1	**0.15** ± 0.01	**981** ± 19	**0.06** ± 0.02	**139** ± 7	**0.02** ± 0.0	85	0.2
	3	**2.4** ± 0.3	**600** ± 75	**262** ± 4	**0.15** ± 0.02	**428** ± 33	**0.15** ± 0.02	**29** ± 7	**0.02** ± 0.0	119	0.4
	4	**3.1** ± 0.3	**1050** ± 89	**257** ± 19	**0.14** ± 0.02	**424** ± 4	**0.11** ± 0.00	**38** ± 7	**0.07** ± 0.00	68	0.3
C-O	1	**8.4** ± 0.6	**1512** ± 85	**497** ± 20	**0.38** ± 0.02	**786** ± 48	**0.38** ± 0.01	**253** ± 13	**0.01** ± 0.00	101	0.6
	2	**3.4** ± 0.7	**1925** ± 54	**396** ± 19	**0.16** ± 0.01	**997** ± 16	**0.06** ± 0.00	**140** ± 8	**0.00** ± 0.00	80	0.2
	3	**0**	**647** ± 79	**230** ± 11	**0.12** ± 0.04	**510** ± 20	**0.25** ± 0.03	**33** ± 8	**0.03** ± 0.00	120	0.0
	4	**0**	**1186** ± 90	**225** ± 15	**0.09** ± 0.01	**575** ± 24	**0.21** ± 0.03	**56** ± 2	**0.06** ± 0.00	72	0.0

[a] e^- from cathode was calculated by integrating current versus time $Q = \int_0^t Idt = \sum_{i=0}^{n}(I_i \Delta t_i)$

[b] e^- from glucose was calculated based on glucose oxidation: $\text{glucose} + 6H_2O \rightarrow 6CO_2 + 24H^+ + 24e^-$

[c] e^- saved in hydrogen was calculated based on hydrogen oxidation: $H_2 \rightarrow 2H^+ + 2e^-$

[d] e^- saved in butyrate, butanol, ethanol, acetate and, acetone were 20 mol e^- / mol butyrate, 24 mol e^- / mol butanol, 12 mol e^- / mol ethanol, and 8 mol e^- / mol acetate and 16 mol e^- / mol acetone.

[e] Electron recovery efficiency refers to value of total e^-conserved in products divided by to the total e^- consumed.

[f] Some values are greater than 100% due to the experiment errors brought by sample dilution for GC analysis.

[g] Cathodic e^- contribution refers to the value of e^- consumed from the cathode and e^- consumed from glucose.

4.4.3 Current uptake decreased over time due to the increase of cathode charge transfer

Decreased current uptake in both the long-term operation and comparison tests suggested that increased electrochemical impedances developed over time in the system. Relatively constant ohmic resistances during the four-batch operation precluded an increased resistance contributed by fouling of the Nafion membrane (Figure 4-11). However, increased charge transfer resistance was found in both whole cell (R_2+R_3) and cathode (R_2) EIS, indicating that the charge permeability of the cathode biofilm decreased over time. One possibility is that the electrochemical condition and low glucose concentration stimulated *C. acetobutylicum* to sporulate over time [23], in which case cells were becoming less active and more inactive cells were insulating the cathode surface.

4.5 Acknowledgment

We acknowledge Dr. Xiuping Zhu and David Jones for help with the GC analysis. Zehra Zaybak and Dr. John M. Pisciotta provided advice on reactor construction.

Financial support under King Abdullah University of Science and Technology (KAUST) KUS-I1-003-13 and Army Research Office Equipment Grant W911NF-11-1-0410 are gratefully acknowledged.

4.6 Literature cited

1. Jones, D.T. and D.R. Woods, Acetone-butanol fermentation revisited. *Microbiological Reviews*, 1986. **50**(4): p. 484-524.

2. Pinto Mariano, A., et al., Butanol production in a first-generation Brazilian sugarcane biorefinery: Technical aspects and economics of greenfield projects. *Bioresource Technology*, 2013. **135**: p. 316-323.

3. Killeffer, D.H., Butanol and acetone from corn - a description of the fermentation process. *Industrial and Engineering Chemistry*, 1927. **19**(1): p. 46-50.

4. Lenz, T.G. and A.R. Moreira, Economic-evaluation of the acetone-butanol fermentation. *Industrial & Engineering Chemistry Product Research and Development*, 1980. **19**(4): p. 478-483.

5. Marlatt, J.A. and R. Datta, Acetone-butanol fermentation process-development and economic-evaluation. *Biotechnology Progress*, 1986. **2**(1): p. 23-28.

6. Nakhmanovich, B.M. and N.A. Shcheblykina. Fermentation of pentoses of corn cob hyrolyzates by *Clostridium acetobutylicum*. *Mikrobiologiya*, 1959. **28**: p. 99-104

7. Kim, T.S. and B.H. Kim, Electron flow shift in *Clostridium acetobutylicum* fermentation by electrochemically introduced reducing equivalent. *Biotechnology Letters*, 1988. **10**(2): p. 123-128.

8. Song, J., et al., Microbes as electrochemical CO_2 conversion catalysts. *Chemsuschem*, 2011. **4**(5): p. 587-590.

9. Finch, A.S., et al., Metabolite analysis of clostridium acetobutylicum: fermentation in a microbial fuel cell. *Bioresource Technology*, 2011. **102**(1): p. 312-315.

10. Nevin, K.P., et al., Microbial electrosynthesis: feeding microbes electricity to convert carbon dioxide and water to multicarbon extracellular organic compounds. *Mbio*, 2010. **1**(2).

11. Nevin, K.P., et al., Electrosynthesis of organic compounds from carbon dioxide is catalyzed by a diversity of acetogenic microorganisms. *Applied and Environmental Microbiology*, 2011. **77**(9): p. 2882-2886.

12. Rabaey, K., G. Peter, and L.K. Nielsen, Metabolic and practical considerations on microbial electrosynthesis. *Current Opinion in Biotechnology*, 2011. **22**(3): p. 371-377.

13. Ragsdale, S.W. and E. Pierce, Acetogenesis and the Wood-Ljungdahl pathway of CO_2 fixation. *Biochimica Et Biophysica Acta-Proteins and Proteomics*, 2008. **1784**(12): p. 1873-1898.

14. Nolling, J., et al., Genome sequence and comparative analysis of the solvent-producing bacterium Clostridium acetobutylicum. *Journal of Bacteriology*, 2001. **183**(16): p. 4823-4838.

15. Call, D.F. and B.E. Logan, A method for high throughput bioelectrochemical research based on small scale microbial electrolysis cells. *Biosensors & Bioelectronics*, 2011. **26**(11): p. 4526-4531.

16. Hutchinson, A.J., J.C. Tokash, and B.E. Logan, Analysis of carbon fiber brush loading in anodes on startup and performance of microbial fuel cells. *Journal of Power Sources*, 2011. **196**(22): p. 9213-9219.

17. Dubois, M., et al., Colormetric method for determination of sugars and related substances. *Analytical Chemistry*, 1956. **28**(3): p. 350-356.

18. Dennis, P.G., et al., Dynamics of cathode-associated microbial communities and metabolite profiles in a glycerol-fed bioelectrochemical system. *Applied and Environmental Microbiology*, 2013: p. doi: 10.1128/AEM.00569-13.

19. Zhang, H.S., M.A. Bruns, and B.E. Logan, Biological hydrogen production by *Clostridium acetobutylicum* in an unsaturated flow reactor. *Water Research*, 2006. **40**(4): p. 728-734.

20. Cappelletti, B.M., et al., Fermentative production of hydrogen from cassava processing wastewater by Clostridium acetobutylicum. *Renewable Energy*, 2011. **36**(12): p. 3367-3372.

21. Kim, B.H., et al., Control of carbond and electron flow in *Clostridium acetobutylicum* fermentations - utilization of carbon monoxide to inhibit hydrogen production and to enhance butanol yields. *Applied and Environmental Microbiology*, 1984. **48**(4): p. 764-770.

22. Bahl, H., et al., Effect of pH and butyrate concentration on the production of acetone and butanol by *Clostridium acetobutylicum* grown in continuous culture. *European Journal of Applied Microbiology and Biotechnology*, 1982. **14**(1): p. 17-20.

23. Alsaker, K.V. and E.T. Papoutsakis, Transcriptional program of early sporulation and stationary-phase events in *Clostridium acetobutylicum*. *Journal of Bacteriology*, 2005. **187**(20): p. 7103-7118.

Chapter 5

Enhanced Nitrogen Removal in Single-Chamber MFCs with Increased Gas Diffusion Areas

Abstract

Single-chamber MFCs with nitrifiers pre-enriched at the air cathodes have previously been demonstrated as a passive strategy for integrating nitrogen removal into current-generating BESs. To further define system design parameters for this strategy, we investigated in this study the effects of oxygen diffusion area and COD/N ratio in continuous-flow reactors. Doubling the gas diffusion area by adding an additional air cathode or a diffusion cloth significantly increased the ammonia and COD removal rates (by up to 115% and 39%), ammonia removal efficiency (by up to 134%), the cell voltage and cathode potentials, and the power densities (by a factor of approximately two). When the COD/N ratio was lowered from 13 to 3, we found up to 244% higher ammonia removal rate but at least 19% lower ammonia removal efficiency. An increase of COD removal rate by up to 27% was also found when the COD/N ratio was lowered from 11 to 3. The CE was not affected by the additional air cathode, but decreased an average of 11% with the addition of a diffusion cloth. Ammonia removal by assimilation was also estimated to understand the ammonia removal mechanism in these systems. These results show that the doubling of gas diffusion area enhanced N and COD removal rates without compromising electrochemical performance.[1]

[1] Materials presented in this chapter were published in the following paper: Yan, H. and Regan. J.M., Enhance nitrogen removal in single-chamber microbial fuel cells with increased gas diffusion areas. *Biotechnology and Bioengineering* **2013**, *110*, (3): 785-91.

5.1 Introduction

Nitrogen removal is one of the key goals of wastewater treatment plants (WWTPs) to reduce eutrophication in freshwater systems induced by anthropogenic discharges of N and P [1]. In the development of MFCs for wastewater treatment, recent studies have looked at adding this nitrogen removal goal to the primary MFC objective of converting chemical oxygen demand (COD) into electrical current [2]. Phosphate recovery as struvite in both MFCs and microbial electrolysis cells (MECs) has also been demonstrated [3, 4].

In nitrogen-removing MFC designs, influent ammonia (referring to NH_3 or NH_4^+ in this paper) was usually nitrified to nitrite and nitrate with oxygen supplied either by aeration in some part of the MFC system [5-9] or by passive diffusion into the solution through an air cathode [7, 10, 11]. This latter approach avoids the energy requirements of active aeration to support nitrification, thereby improving the net system energy recovery potential of MFC implementation. The nitrification-produced nitrite and nitrate could be removed in MFC systems by denitrification in conjunction with soluble electron donor oxidation or cathode oxidation in biocathodes [12, 13], and several designs have explicitly incorporated this function in the MFC system [5, 6, 8], while in other systems denitrification occurs fortuitously [11].

In our previous demonstration of single-chamber air-cathode MFCs for simultaneous nitrogen and COD removal, the adoption of a pre-enriched nitrifying biofilm on the air cathode and the use of diethylamine-functionalized polymer (DEA) as the binder successfully enhanced the system's ammonia removal efficiency to 98% [11]. However, this was observed in fed-batch systems with 2 to 4 day batches, whereas the hydraulic retention time (HRT) in aeration tanks of WWTPs usually ranges from 3 - 8 hours [14], and may be somewhat higher with high COD wastewaters. Therefore, modifications are required that provide a suitable biofilm microenvironment to preferentially retain a higher abundance of the slow-growing nitrifiers. The

goal of this research was to enhance the ammonia removal rate in an air-cathode MFC system without impairing exoelectrogenic performance. Since the ammonia-oxidation reaction in the nitrification process has a strict demand for oxygen [15], increasing the oxygen diffusion area with preacclimation of a nitrifying biofilm should support more nitrifying bacteria and accelerate the ammonia removal rate. The oxygen diffusion area could be increased by the addition of a second air cathode, which might enhance electrochemical performance in these typically cathode-limited systems, or the addition of a non-platinized gas-permeable material. With the potential for distinct effects of these two options on nitrifiers and heterotrophs (on the anode and the cathode), a practical design consideration is whether the change of the oxygen diffusion area will affect the range of influent COD/N ratios that can be effectively treated. In addition, these modified designs might also affect other pathways of ammonia removal, such as ammonia assimilation and ammonia volatilization.

Therefore, the hypothesis of this study was that increasing gas diffusion areas will increase the nitrogen removal ability as well as the electrical performance of single-chamber air-cathode MFCs. Single-chamber air-cathode MFCs were assembled with an extra air cathode or an identical area non-platinized diffusion cloth to double oxygen diffusion areas. Together with the regular design as a control, three MFC designs were tested at different COD/N ratios (3, 5, 7, 9, 11, and 13) and their performances were compared.

5.2 Materials and methods

5.2.1 Reactor setup

Three designs of MFC reactors were constructed in duplicate. Control reactors (C1 & C2) were single-chamber MFCs consisting of an air cathode placed on one end of a plastic

(Plexiglass) cylindrical chamber 6 cm long by 3 cm in diameter (empty bed volume of 42 mL) and a brush anode vertically secured in the middle of the cylindrical chamber (Figure 5-1). The air cathode and brush anode were made identically to our previous research [11]. The other two reactor designs differed from the control only in the addition of a second gas-diffusion area, which was either a diffusion cloth (CD1 & CD2) or a second air cathode (CC1 & CC2) placed on the other end of the cylindrical chamber (Figure 5-1). The diffusion cloth was made identically to the air cathode except that no Pt catalyst layer was added to the DEA binder, which was coated on the solution-side of air cathodes [11]. Also, the diffusion cloth was not connected to the electric circuit. For all three designs, brush anodes were inserted to these reactors after the nitrifier enrichment stage was finished.

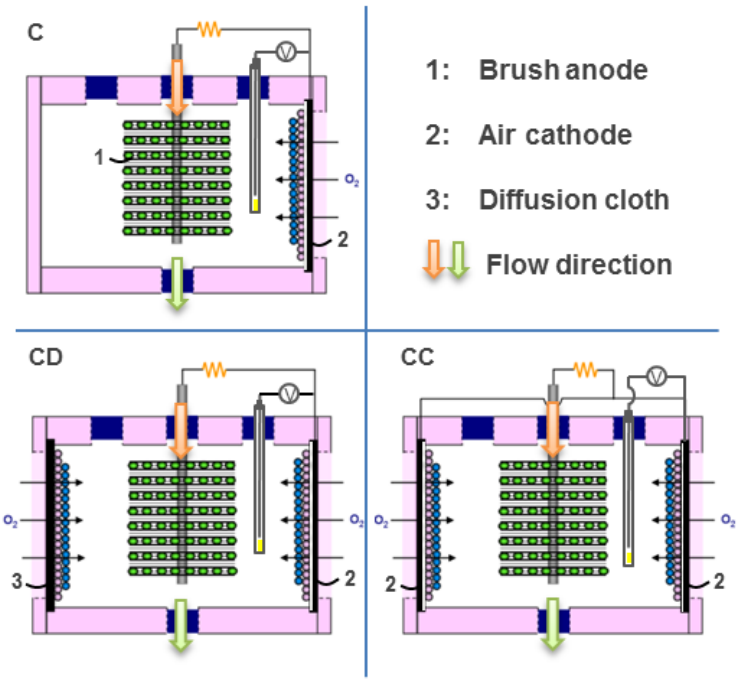

Figure 5-1. Schematics of the continuous-flow control MFC (C), MFCs with the addition of a diffusion cloth (CD), and MFCs with an extra air cathode (CC).

5.2.2 Inoculation and operation

5.2.2.1 Enrichment stage

At the beginning of nitrifier enrichment, each reactor was inoculated with 3 mL of mixed liquor taken from the aerated nitrification tank of the Pennsylvania State University Wastewater Treatment Plant and 5 mL cultured suspension of *Nitrosomonas europaea* (ATCC 19718). All reactors were operated in a 30 °C thermostatic chamber in fed-batch mode, with autoclaved medium containing 0.382 g L^{-1} NH_4Cl (100 mg N L^{-1}) and the following basal components (pH 7.28): 1.78×10^{-3} g L^{-1} Na_2CO_3, 3.12×10^{-3} g L^{-1} $MgCl_2$, 0.79×10^{-3} g L^{-1} $CaCl_2$, 4.26×10^{-5} g L^{-1} $FeSO_4$, 3.76×10^{-6} g L^{-1} $CuSO_4$, 2.452 g L^{-1} $NaH_2PO_4 \cdot H_2O$, 4.576 g L^{-1} Na_2HPO_4, and 0.13 g L^{-1} KCl. This medium contained 50 mM phosphate to buffer proton production or consumption induced by anode and cathode reactions as well as nitrification and denitrification processes, and sodium carbonate to support autotrophic growth. Reactors were covered to prevent the growth of photosynthetic organisms and UV inhibition of ammonia-oxidizing bacteria. When there was above 90% ammonia removal in any reactor, all of the reactors were refilled with fresh sterile medium. The enrichment lasted 20 days (six batches).

5.2.2.2 Fed-batch MFC stage

To move into MFC status, the nitrifier-enriched reactors were then inoculated with 21 mL of a suspended exoelectrogenic microbial consortium taken from a sodium acetate-fed air-cathode MFC that had been running for more than half a year [16]. MFCs were operated in batch mode with medium containing 1 g L^{-1} CH_3COONa, 0.382 g L^{-1} NH_4Cl (100 mg N L^{-1}), trace minerals and vitamins [17], and the basal components described in section 3.2.2.1. The COD/N ratio of this medium was about 7.8. Reactors were also covered to prevent light effects except during

medium changes. MFCs were operated with an external resistor of 1000 Ω to balance the fast COD removal and the relatively slow ammonia removal and re-fed with complete replacement of the medium when the voltage decreased below 10 mV, giving batch durations of two to four days. The batch-mode MFC stage lasted 37 days (15 batches).

5.2.2.3 Continuous-flow MFC stage

After they obtained stable performances in batch mode, MFCs were moved to continuous-flow mode with a HRT of 12.8 hours, which was confirmed by a tracer analysis test. The medium was introduced into the system near the axial position of the brush anode and removed from the center of the opposite wall (Figure 5-1), thus preferentially providing COD for exoelectrogens on the anode electrode. During the continuous-flow mode, the COD/N ratio of the medium was varied from 13 to 3 by adjusting the ammonia concentration from 30 to 130 mg N L^{-1}. Besides ammonium chloride, the medium also contained fixed concentrations of 0.5 g L^{-1} CH_3COONa, trace minerals and vitamins, and the basal components described in section 2.2.1. Due to the increase of ammonia chloride concentration, the medium conductivity increased from 7.00 mS cm^{-1} to 8.01 mS cm^{-1} when the COD/N ratio decreased from 13 to 3. The conductivity of our feed was higher than most sewage. To increase the conductivity in a real nitrogen-removing system, one might recirculate anaerobic digester supernatant (conductivity between 5 to 6 mS cm^{-1} for the Penn State secondary digester). MFCs were operated with an external resistor of 1000 Ω for 1 day at each COD/N ratio in a randomly selected order of 7, 11, 9, 13, 3, and 5. We also re-ran the COD/N ratio of 13 to investigate an apparent anomaly in the data for this condition, and then the COD/N ratio of 7 again to assess the stability of the system over the one-week test duration. The nitrification inhibitor nitrapyrin was added at the end of the operation (final concentration 25 mg L^{-1}) to eliminate ammonia oxidation and allow a measurement of the

combined contribution of ammonia volatilization and assimilation to ammonia removal in these systems.

5.2.3 Analysis

5.2.3.1 Chemical analysis

During the enrichment stage, 0.4 ml samples were taken from each reactor every two or three days using 3 mL syringes (VWR International, LLC.) and filtered immediately through a 0.2-μm pore diameter PTFE syringe filter (VWR International, LLC.). The concentration of the ammonia was measured using Standard Methods 10031 [18] (HACH Company, Loveland. CO). Nitrite (NO_2^--N) and nitrate (NO_3^--N) concentrations were quantified by ion chromatography (Dionex DX-120, Dionex Co., Sunnyvale, CA) using an AS16 4-mm column with 1.0 mM NaOH eluent. Bulk solution pH in each MFC was tested before and after each batch using a calomel pH electrode (VWR International, LLC.) and pH meter (Fisher Scientific, AB15). In MFC mode, 1.0 ml samples were taken from reactors before and after each batch, and pH was simultaneously measured. In addition to NH_4^+-N/NH_3-N, NO_2^--N, and NO_3^--N, soluble COD (sCOD) was also measured using Standard Methods 5220 [18] (HACH COD system). In continuous-flow MFC status, samples were collected from the MFC effluent after each reactor had been operated for 1 day at each COD/N ratio. The analyses of nitrogen compounds, sCOD, and pH were the same as that of batch-mode MFCs.

5.2.3.2 Electrochemical analysis

The voltage drop (*E*) across the external resistor (1000 Ω) in the circuit was measured at 10-min intervals using a multimeter (Keithley Instruments, Cleveland, OH), and current (*I*) was calculated using Ohm's Law. Cathode potentials were measured by the same multimeter relative to a Ag/AgCl reference electrode (RE-5B, Bioanalytical Systems Inc.) inserted into the system near the cathode (Figure 5-1), and then converted to the value versus SHE by adding 211 mV to the relative potential values. Anode potentials were calculated by subtracting cell voltages from cathode potentials. The two cathodes of CC reactors were connected with a short copper wire and assumed to have the same potential. At the conclusion of the COD/N ratio experiments, we conducted continuous-flow polarization tests by applying external resistances of 5k, 1k, 500, 250, 125, 80, 40, 20, 10, and 5 Ω for two HRTs each. To prevent the failure of ammonia removal without full recovery as we reported in our previous work [11], polarization experiments were not performed.

5.2.3.3 Statistical analysis

Two-way ANOVA with replication was used for determining if the effects of oxygen diffusion area and COD/N ratio on MFC performance were significant (p-value < 0.05). The analysis was done in Microsoft Office Excel 2007 and five MFC performance parameters were considered: ammonia removal rate, ammonia removal efficiency, COD removal rate, cell potential, and CE.

5.2.4 Calculations

CE was calculated based on integrated current, sCOD removal (to exclude the influence by biomass in bulk solution), and flow rate (eq. 5-1), where t = time of sample collection, F = Faraday's constant, and the flow rate Q = 84 mL d^{-1}. The ammonia removal efficiency ($\eta_{NH_4^+-N}$) depended on the influent and effluent ammonia concentrations $[NH_4^+-N]_{in}$ and $[NH_4^+-N]_{eff}$ (eq. 5-2). The ammonia removal rate ($r_{NH_4^+-N}$) and the sCOD removal rate (r_{COD}) were determined by the ammonia and sCOD removal and an HRT of 12.8 hr. (eq. 5-3, 5-4).

$$CE = \frac{8\int_0^t \frac{E}{R}dt}{FQt\Delta COD} \qquad \text{[eq. 5-1]}$$

$$\eta_{NH_4^+-N} = \frac{[NH_4^+-N]_{In} - [NH_4^+-N]_{Eff}}{[NH_4^+-N]_{In}} \times 100\% \qquad \text{[eq. 5-2]}$$

$$r_{NH_4^+-N} = \frac{\Delta NH_4^+-N}{HRT} \qquad \text{[eq. 5-3]}$$

$$r_{COD} = \frac{\Delta COD}{HRT} \qquad \text{[eq. 5-4]}$$

5.3 Results

5.3.1 Nitrogen removal

5.3.1.1 Enrichment and fed-batch MFC stages

The ammonia removal was consistently more rapid in CD and CC reactors than in C reactors during the enrichment (Figure 5-2). Nitrate production, indicative of ammonia and nitrite

oxidation, was observed in all reactors. No net nitrite production was detected. The amount of nitrate production accounted for 80% of ammonia removal at the end of the enrichment stage for all reactors (data not shown).

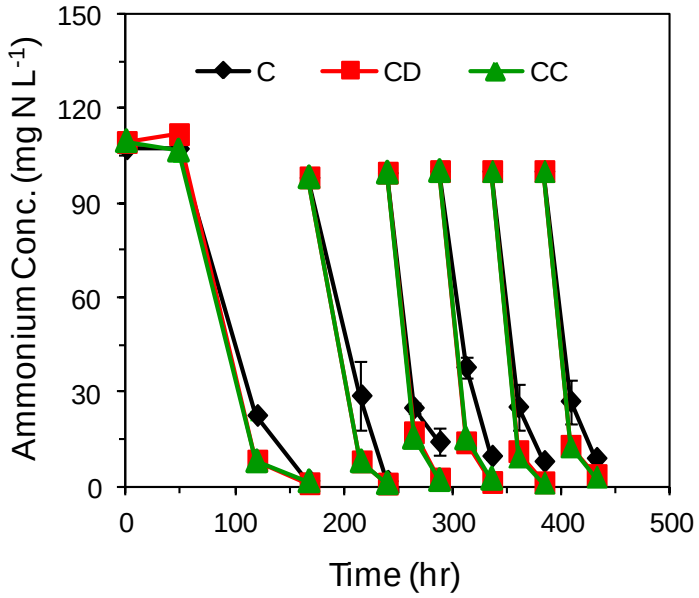

Figure 5-2. Ammonia concentrations during the enrichment stage.

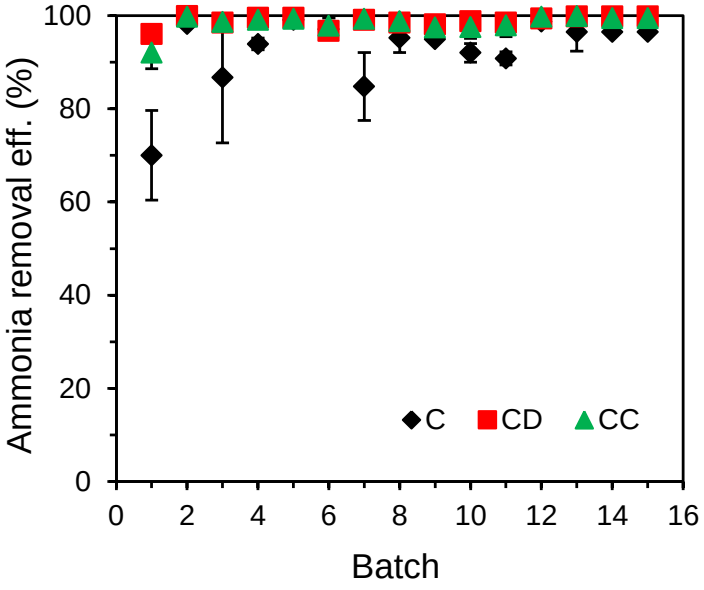

Figure 5-3. Ammonia removal efficiencies in C, CD, and CC reactors during fed-batch mode.

During the 15 cycles of fed-batch MFC operation, ammonia removal efficiencies in all reactors eventually exceeded 99%, with the C reactors taking longer to attain this performance (Figure 5-3). No nitrite was detected and the nitrate concentration was low, from 1.7 to 15.2 mg N L^{-1} when the ammonia concentration was 100 mg N L^{-1} in the MFCs. The low nitrate concentrations were presumably due to reduction by simultaneous denitrification in the single-chamber systems. However, when there was an ammonia shock (265 mg N L^{-1}) in the medium in batch 7, which was to detect if there was still effective nitrification in the system, significant net nitrate production (50.0 to 73.2 mg N L^{-1}) was detected in all MFC reactors.

5.3.1.2 Continuous-flow MFC stage

With varied influent ammonia concentrations during the continuous-flow MFC operation, the reactors with two gas-diffusion areas showed a clear and consistent trend of increasing ammonia removal rate with increasing ammonia concentration (i.e., decreasing COD/N ratio) ($p = 0.000$). Ammonia removal rates in CD reactors increased from 43 to 148 g N m^{-3} d^{-1} as the COD/N ratio decreased from 13 to 3 (Figure 5-4). The ammonia removal rates of CC reactors showed minimal difference with CD reactors ($p = 0.915$). Both of these modified reactor designs had significantly higher ammonia removal rates than C reactors (28 to 69 g N m^{-3} d^{-1}) at all COD/N ratios ($p = 0.015$ and 0.012 for C/CD and C/CC, respectively). The C reactors exhibited a maximum ammonia removal rate plateau at a COD/N ratio of 5, with no increase at the highest ammonia load. The effluent ammonia concentration in all reactors increased with the decrease of COD/N ratios, as the ammonia loading rate increased. With the increase of the influent ammonia concentration, ammonia removal efficiencies decreased ($p = 0.000$) (Figure 5-4). Nitrite and nitrate were not detected in any of the reactors. When nitrapyrin was added at the end of the

operation, a reduction of ammonia removal rate by 15%, 44%, and 42% was detected in C, CD, and CC reactors (Figure 5-5).

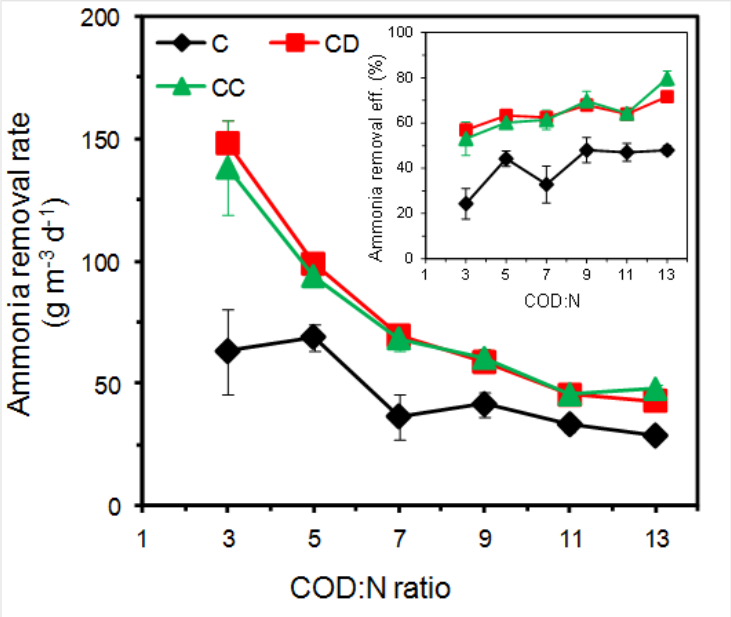

Figure 5-4. Ammonia removal rates and efficiencies (inset) in C, CD, and CC MFCs

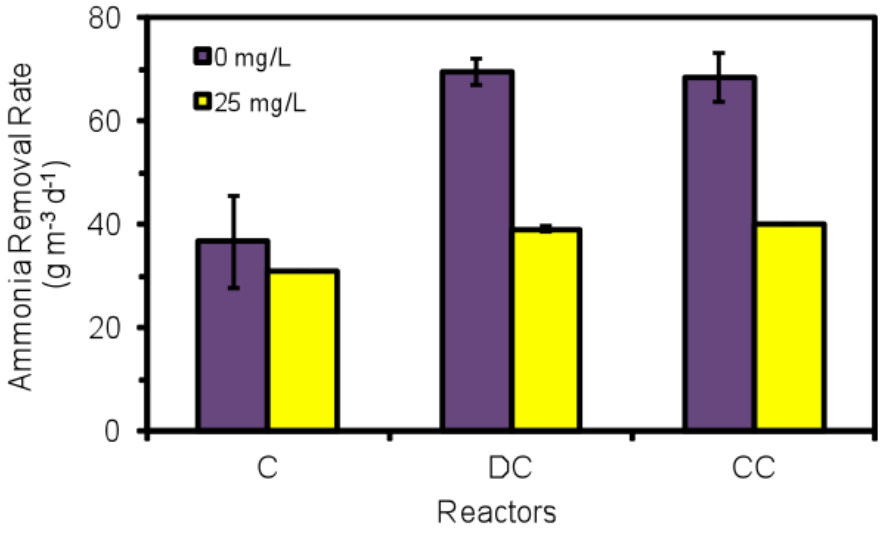

Figure 5-5. Reduction of ammonia removal rates with 25 mg L^{-1} nitrapyrin at COD/N of 7.

5.3.2 COD removal and CE

The average COD removal efficiencies of the three MFC designs were nearly the same (94.0 ± 0.3 %) during fed-batch operation. During the continuous-flow MFC stage, COD removal rate in the CD and CC reactors was consistently faster than that in C reactors ($p = 0.000$ for C/CD and C/CC, and 0.422 for CD/CC) (Figure 5-6). Although the influent COD concentration was fixed, COD removal rates in C, CD, and CC reactors still increased by 21%, 9%, and 27%, respectively, when the COD/N ratio decreased from 11 to 3 ($p = 0.001$) (Figure 5-5). At a COD/N of 13, COD removal rates in C and CC reactors increased compared to a COD/N of 11. The same result was obtained again when all MFCs were re-run at a COD/N of 13 after the first-round experiments at each COD/N ratio. It is possible that the increased COD removal rates were actually a result of continued biofilm development over the course of this study beyond the 37 days of batch-mode operation, because the higher rates coincide with the latter COD/N ratios tested.

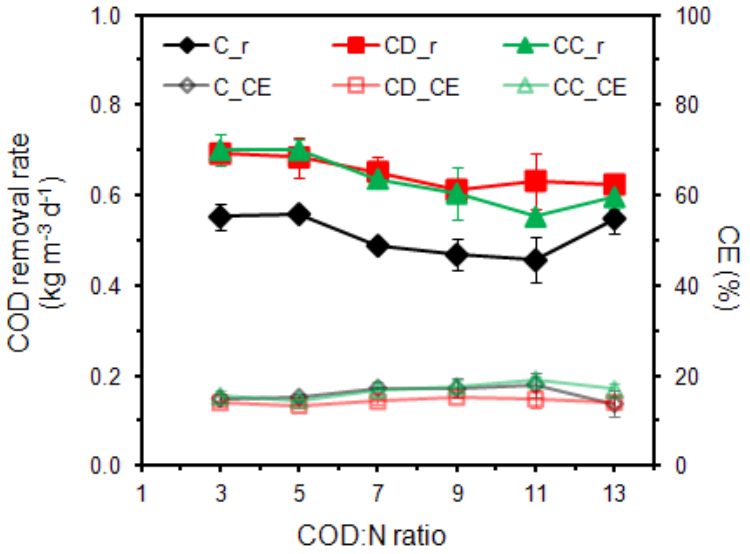

Figure 5-6. COD removal rates (solid symbols) and CEs (hollow symbols) in C, CD, and CC reactors.

Compared to fed-batch mode, MFCs in continuous-flow mode achieved higher CEs, with maximum values of 18%, 15%, and 19% for C, CD, and CC reactors, respectively (Figure 5-6). Maximum CEs in C, CD, and CC reactors in fed-batch mode were 17%, 10%, and 11%, respectively. CEs in C and CC reactors showed a slight decreasing trend when the COD/N ratio decreased from 11 to 3 ($p = 0.010$). Through all the COD/N ratios, CD reactors had the lowest CE among the three designs ($p = 0.012$, 0.000, and 0.378 for CD/C, CD/CC, and C/CC respectively) (Figure 5-6).

5.3.3 pH change

In the enrichment stage, there was a pH decrease during each batch from 7.20 to 6.87 ± 0.04 in all reactors. However, effluent pH in the MFCs during both fed-batch and continuous-flow modes showed slight increases within 0.2 from the influent pH. The change of pH was not affected by the additional air cathode or diffusion cloth ($p = 0.761$ and 0.797 for C/CD and C/CC, respectively).

5.4 Discussion

5.4.1 Effects of gas diffusion areas on MFC performance

By comparing the CD and CC designs with the C reactors, we found that doubling the gas diffusion area boosted the ammonia removal rate in MFCs by up to 134%. This could be explained by faster substrate uptake due to having more nitrifier biomass previously enriched on the extra air cathode in CC reactors or on the diffusion cloth in CD reactors (Figure 5-2), and also by increased ammonia volatilization through the increased gas diffusion area [10, 11]. The

ammonia removal rate in the doubled gas diffusion area designs (reactors CD and CC) increased to 148 g N m^{-3} d^{-1} at the COD:N of 3, which was higher than the ammonia removal rate reported previously (33 – 104 g N m^{-3} d^{-1}) by controlling the dissolved oxygen of aerated catholyte [5]. However, due to the leakage of oxygen from cathode to anode in these single-chamber MFCs, CEs in our three systems were similar or lower than MFC designs with membranes [5-9].

The CD and CC reactors achieved up to 39% greater COD removal rates than C reactors (Figure 5-6), probably due to larger oxygen flux introduced to CD and CC. The additional air cathode and diffusion cloth also increased the cell voltage by 29% and 12%, respectively, relative to C reactors. This indicated that the system was cathode limited even at the high external resistance (1000 Ω) used in these experiments relative to the internal resistance, which is approximately 100 Ω for similar reactors [11]. The increased power densities in CC and CD reactors observed during continuous-flow polarization tests (Figure 5-7) further suggested that increasing gas diffusion area will enhance not only nitrogen and COD removal but also electrical performance of the MFCs. The addition of a diffusion cloth, even though it was not connected to the electrical circuit, increased the cathode potential and thus the cell voltage (Figure 5-8). Presumably this was due to a higher dissolved oxygen concentration at the Pt side of the cathode in CD reactors compared to C reactors. The dissolved oxygen near the diffusion cloth in CD reactors might migrate to the air cathode, which might explain the higher anode potential and lower CE in CD reactors than C reactors (Figures 5-8, 5-7). The dissolved oxygen might also pass through the gap between the end of the anode brush and the reactor inner wall (Figure 5-1). It was reported that higher oxygen concentrations could reduce the polarization resistance and the overpotential of the oxygen reduction reaction on platinized cathodes [19, 20].

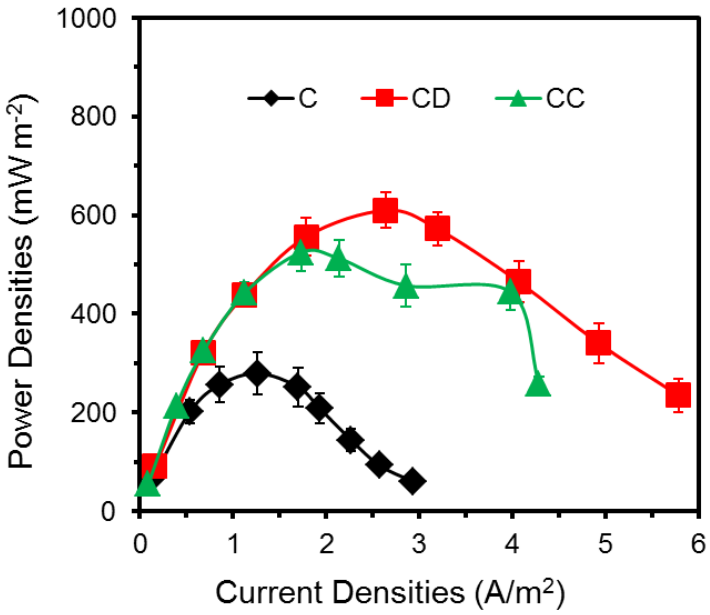

Figure 5-7. Continuous-flow polarization test showed increased power densities in CD and CC reactors relative to C.

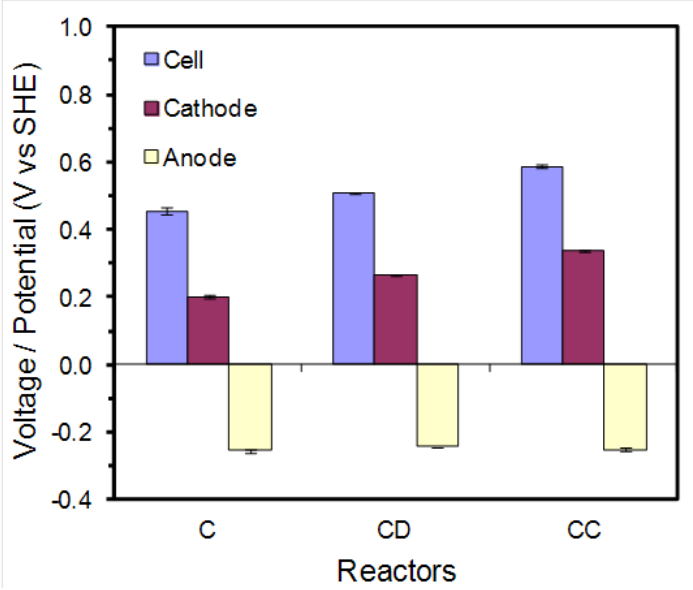

Figure 5-8. Cell voltage and electrode potentials of C, CD, and CC MFCs at COD/N = 7.

The two strategies for increasing oxygen diffusion area had divergent effects on CE, which increased in CC reactors and decreased in CD reactors relative to C reactors (Figure 5-6). This was likely due to the fact that the additional air cathode in CC reactors was connected to the electrical circuit and involved in electrochemical oxygen reduction, while the diffusion cloth was

not. Without the electrochemical oxygen consumption, aerobes and microaerophiles on the diffusion cloth had a greater possibility to take up the oxygen that diffused into CD reactors than in CC reactors, leading to a higher organic substrate utilization rate directed toward nonexoelectrogenic pathways in CD reactors. However, the material cost of the non-platinized diffusion cloth is only 21% of an air cathode [21], so the slight increase in CE might not be justified.

5.4.2 Effects of COD/N ratios on MFC performance

In CD and CC reactors, the ammonia removal rate was directly proportional to its loading rate (R^2 = 0.995 and 0.992 for CD and CC, respectively) (Figure 5-9), which suggested that the growth of nitrifiers might be under substrate limitation. However, the ammonia removal rate in C reactors plateaued at an ammonia loading rate of 156 g N m^{-3} d^{-1} (Figure 5-9), indicating it to be the maximum ammonia removal rate in this single air-cathode MFC design under the evaluated acclimation conditions. The ammonia removal rates of C, CD, and CC reactors at COD/N of 7 did not vary significantly (variation < 5%) after one week of operation, indicating the relative stability of the systems during a single round test of variable COD/N ratios. Extended operation at each condition might have resulted in nitrifier acclimation to the different ammonia loading.

5.4.3 Ammonia removal mechanisms

The ammonia removal mechanisms in these single-chamber air-cathode designs include simultaneous nitrification and denitrification, volatilization, and assimilation. Due to the volatilization of ammonia and gaseous nitrification and denitrification intermediates (nitrous oxide) and products across the gas diffusion areas, it is not possible to perform a strict nitrogen

balance in these systems. Based on previous discussions about ammonia removal in single-chamber, single air-cathode MFCs, 50% or more ammonia removal might be contributed by ammonia volatilization and assimilation in the system [10, 11]. Our estimates for the COD:N ratio of 13 (Appendix) show that the maximum ammonia assimilation rates that could occur in C, CD, and CC reactors were 25.9, 30.1, and 28.3 g N m^{-3} d^{-1}, respectively, which did not vary significantly since they are based on yields from identical substrate loadings and very similar COD removal rates at this highest COD/N ratio. It was expected that the gas diffusion area could also increase the ammonia volatilization rate. However, calculating the nitrification extent at each COD/N ratio would require further research involving the addition of specific inhibitors and comparable control conditions.

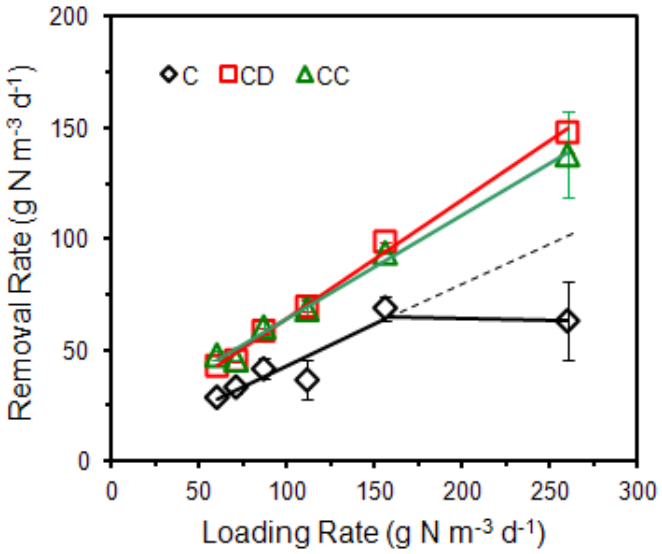

Figure 5-9. Ammonia removal rates versus ammonia loading rates, and their linear regression relationship.

5.5 Acknowledgment

This research was supported by Award KUS-I1-003-13 from the King Abdullah University of Science and Technology (KAUST).

5.6 Literature cited

1. Dodds, W.K., et al., Eutrophication of US freshwaters: analysis of potential economic damages. *Environmental Science & Technology*, 2009. **43**(1): p. 12-19.
2. Liu, H. and B.E. Logan, Electricity generation using an air-cathode single chamber microbial fuel cell in the presence and absence of a proton exchange membrane. *Environmental Science & Technology*, 2004. **38**(14): p. 4040-4046.
3. Cusick, R.D. and B.E. Logan, Phosphate recovery as struvite within a single chamber microbial electrolysis cell. *Bioresource Technology*, 2012. **107**: p. 110-115.
4. Fischer, F., et al., Microbial fuel cell enables phosphate recovery from digested sewage sludge as struvite. *Bioresource Technology*, 2011. **102**(10): p. 5824-5830.
5. Kim, J.R., et al., Analysis of ammonia loss mechanisms in microbial fuel cells treating animal wastewater. *Biotechnology and Bioengineering*, 2008. **99**(5): p. 1120-1127.
6. Min, B., et al., Electricity generation from swine wastewater using microbial fuel cells. *Water Research*, 2005. **39**(20): p. 4961-4968.
7. You, S.J., et al., Improving phosphate buffer-free cathode performance of microbial fuel cell based on biological nitrification. *Biosensors & Bioelectronics*, 2009. **24**(12): p. 3698-3701.
8. Virdis, B., et al., Microbial fuel cells for simultaneous carbon and nitrogen removal. *Water Research*, 2008. **42**(12): p. 3013-3024.

9. Virdis, B., et al., Simultaneous nitrification, denitrification and carbon removal in microbial fuel cells. *Water Research*, 2010. **44**(9): p. 2970-2980.

10. Yan, H., T. Saito, and J. Regan, Nitrogen removal in a single-chamber microbial fuel cell with nitrifying biofilm enriched at the air cathode. *Water Research*, 2012.

11. Clauwaert, P., et al., Biological denitrification in microbial fuel cells. *Environmental Science & Technology*, 2007. **41**(9): p. 3354-3360.

12. Gregory, K.B., D.R. Bond, and D.R. Lovley, Graphite electrodes as electron donors for anaerobic respiration. *Environmental Microbiology*, 2004. **6**(6): p. 596-604.

13. Xie, S., et al., Simultaneous carbon and nitrogen removal using an oxic/anoxic-biocathode microbial fuel cells coupled system. *Bioresource Technology*, 2011. **102**(1): p. 348-354.

14. Rittmann, B.E. and P.L. McCarty, eds. Environmental biotechnology: principles and applications. 2001, McGraw-Hill Companies, Inc.

15. Sharma, B. and R.C. Ahlert, Nitrification and nitrogen removal. *Water Research*, 1977. **11**(10): p. 897-925.

16. Zhang, F., D. Pant, and B.E. Logan, Long-term performance of activated carbon air cathodes with different diffusion layer porosities in microbial fuel cells. *Biosensors and Bioelectronics*, 2011. **30**(2011): p. 49-55.

17. Lovley, D.R. and E.J.P. Phillips, Novel mode of microbial energy metabolism: organic carbon oxidation coupled to dissimilatory reduction of iron or manganese. *Applied and Environmental Microbiology*, 1988. **54**(6): p. 1472-1480.

18. APHA, Standard methodes fo the examination of water and wastewater (19^{th} ed). 1995, Washington DC, USA: American Public Health Association, American Water Works Association.

19. Antoine, O., Y. Bultel, and R. Durand, Oxygen reduction reaction kinetics and mechanism on platinum nanoparticles inside Nafion (R). *Journal of Electroanalytical Chemistry*, 2001. **499**(1): p. 85-94.

20. Norskov, J.K., et al., Origin of the overpotential for oxygen reduction at a fuel-cell cathode. *Journal of Physical Chemistry B*, 2004. **108**(46): p. 17886-17892.

21. Tokash, J.C. and B.E. Logan, Electrochemical evaluation of molybdenum disulfide as a catalyst for hydrogen evolution in microbial electrolysis cells. *International Journal of Hydrogen Energy*, 2011. **36**(16): p. 9439-9445.

Chapter 6

Future Work

In my PhD dissertation, I investigated anode community behaviors corresponding to different anode potential patterns, demonstrated the exoelectrotrophic capability of *C. acetobutylicum* and its metabolic flux change with cathodic current, and improved combined nutrient treatment in MFCs with increased gas diffusion area for a nitrifier-enriched mixed community. These studies have provided a better understanding of microbial behaviors and potentials in BESs. However, there are still opportunities and challenges to be addressed for further understanding and employment of microbial performance for bioenergy production:

1. Galvanostatic experiments supplying different magnitudes of cathodic current to *C. acetobutylicum* biocathodes in reactors with a high electrode-to-volume ratio might allow better control over the electron consumption from cathode current relative to that from glucose so that the metabolic flux change in *C. acetobutylicum* can be quantitatively controlled. Moreover, using a defined medium would allow a strict accounting of electron distribution, though the growth in such conditions in appreciably lower.
2. Biomass accumulation in both suspension and in the biofilm from a cathodic *C. acetobutylicum* culture biocathode could be quantified to draw a closed carbon and electron balance. As another possible metabolic product, lactate is also recommended to be quantified for the carbon and electron balance.
3. Alternative organic carbon sources such as pyruvate with less energy content than glucose are recommended for future metabolic flux change experiments on *C. acetobutylicum* with current uptake.

4. Exploration of solventogenic bacteria for the microbial electrosynthesis of solvents from carbon dioxide and water is recommended, though the major challenge lies on the screening of solventogenic bacteria with both Wood-Ljungdahl pathway and exoelectrotrophic capability.

Appendix A

Supplementary Information for Chapter 3

454 methods

Amplifications were performed in 25 ul reactions with Qiagen HotStar Taq master mix (Qiagen Inc, Valencia, California), 1ul of each 5uM primer, and 1ul of template. Reactions were performed on ABI Veriti thermocyclers (Applied Biosytems, Carlsbad, California) under the following thermal profile: 95°C for 5 min, then 35 cycles of 94°C for 30 sec, 54°C for 40 sec, 72°C for 1 min, followed by one cycle of 72°C for 10 min and 4°C hold.

Amplification products were visualized with eGels (Life Technologies, Grand Island, New York). Products were then pooled equimolar and each pool was cleaned with Diffinity RapidTip (Diffinity Genomics, West Henrietta, New York), and size selected using Agencourt AMPure XP (BeckmanCoulter, Indianapolis, Indiana) following Roche 454 protocols (454 Life Sciences, Branford, Connecticut). Size selected pools were then quantified and 150 ng of DNA were hybridized to Dynabeads M-270 (Life Technologies) to create single stranded DNA following Roche 454 protocols (454 Life Sciences). Single stranded DNA was diluted and used in emPCR reactions, which were performed and subsequently enriched. Sequencing following established manufacture protocols (454 Life Sciences).

Appendix B

Supplementary Information for Chapter 4

Table B-1. Abundances of phylum, classification, and genus in R-47 and P-119.

Inoculum		0	9	13	386	0	56	0	17	0	8
R-47		9	4.5	3.5	43.5	0	15.5	0	14	0	0
R-47		18	69	3.5	52.5	0	4	0	28	1	0
R-47		26	81	5.5	72	1	3	0	45.5	1	0
R-47		41	53.5	9.5	68.5	7.5	0	0	5.5	2	0
R-47		60	67	139.5	208	44	8.5	8.5	8.5	0	0.5
P-119		9	0.5	15.5	113	0	54.5	0	102.5	2.5	0
P-119		18	0.5	0	43	1	2.5	0	13	0	0
P-119		26	0	3	47	0	3	0	22	5	0
P-119		41	8.5	1	81	2.5	0	0	4.5	1	0
P-119		60	3	19	356.5	237	2.5	0	9	2	0
R-47-□cathode	R		2	1204	102.5	6.5	0	0	42.5	3	0

Table B-2. Abundances of phylum, classification, and genus in R-1k and P-250.

	1K ohm	Ea=-250	mV vs SHE							
		Acidobacte	Actinobac	Bacteroid	Chlorobi	Chlorofle	Cyanobac	Deferriba	Elusimicro	Firmicutes	Fusobacte
Inoculum	0	5	5	158	0	12	1	0	0	15	1
R-1K	12	9	7	349	0	47.5	0	0	0.5	35	0
R-1K	24	3	5.5	162	1.5	58	0	0	0	7	0.5
R-1K	41	1	6.5	55	5	28	0	0	0	4	0
R-1K	60	2	3	102.5	2	78	0	0	0	11.5	0
P-250	12	15	15.5	493	0.5	99	0	0	0	71	0
P-250	24	11	21	286	1	100	3	0.5	0	31	0
P-250	41	4	37	409	4.5	51	1	0	0	104	0
P-250	60	1	8	238	2	55.5	1.5	0.5	0	52.5	0.5
R-1K- cath	R	0	10	48	8.5	10	0	0	0	18	0
P-250-cath	P	0	24	159	17	6.5	0	12.5	0	38	0

Appendix C

Supplementary Information for Chapter 5

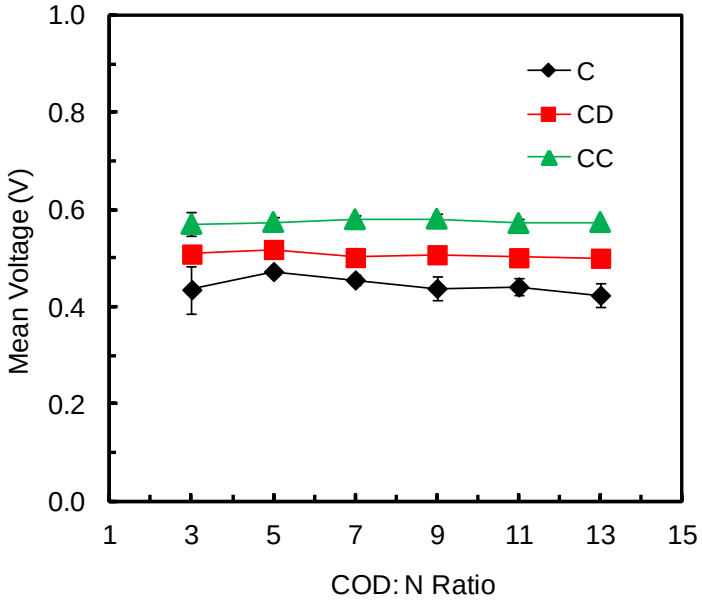

Figure C-1. Cell voltages (mean values at each COD/N ratio condition) of C, CD, and CC MFCs.

Estimation of ammonia assimilation rates using total redox reaction with cell synthesis for the combination of both non-exoelectrogens and exoelectrogens

We estimated the ammonia assimilation rate for the COD/N ratio of 13, assuming that autotrophic assimilation was minor in comparison with heterotrophic assimilation and that methanogenesis was negligible. The stoichiometric relation between ammonia assimilation and COD removal rates is shown in (eq. C-1), where M_N and $M_{CH_3COO^-}$ are the molecular weights of nitrogen and sodium acetate, respectively, $v_{NH_4^+-N}$ and $v_{CH_3COO^-}$ are the stoichiometric coefficients for ammonium and sodium acetate in the total redox reaction with cell synthesis for the combination of both non-exoelectrogens growing on the air cathode and exoelectrogens, and 0.78 is the mass conversion factor from COD to sodium acetate.

$$r_{NH_4^+\text{-N,assimilation}} = \frac{M_N}{M_{CH_3COO^-}} \cdot \frac{v_{NH_4^+\text{-N}}}{v_{CH_3COO^-}} \cdot \frac{r_{COD}}{0.78} \quad \text{[eq. C-1].}$$

The $\frac{v_{NH_4^+\text{-N}}}{v_{CH_3COO^-}}$ values for C, CD, and CC reactors are 0.216, 0.221, and 0.217, respectively. The detailed calculations are shown below.

Electron balance: in our mixed-culture single-chamber MFC system, we assume that fraction *a* from the total acetate-derived electrons was used by exoelectrogens, with f_{s1} of this fraction used for cell synthesis and f_{e1} transferred to the anode for energy generation (Figure C-4). Therefore, af_{e1} is simply the CE. Bacteria growing nonexoelectrogenically on the air cathode use the balance (i.e., 1-*a*) of the total acetate-derived electrons, with f_{s2} of this portion invested in cell synthesis and f_{e2} transferred to oxygen. f_{s2} and f_{e2} were adopted from empirical values for aerobic heterotrophs (f_{s2} = 0.6 and f_{e2} = 0.4).

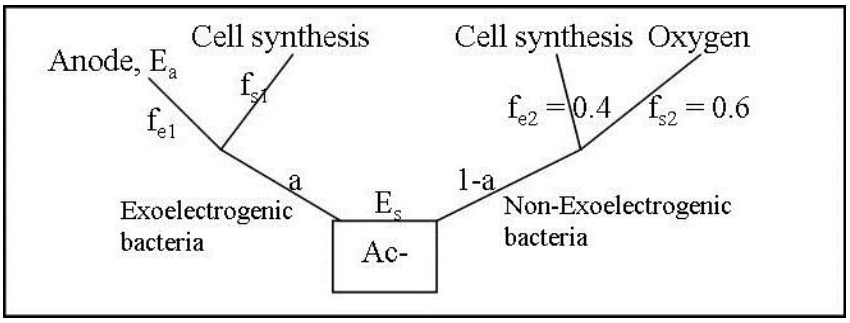

Figure C-2. Chart of electron flow from the substrate acetate to different pathways in MFC systems.

An energy balance between catabolism and anabolism was then coupled to the electron balance to calculate f_{s1}, f_{e1}, and *a* [1].

Energy balance

ΔG_p is the energy required to convert the sodium acetate to pyruvate, which is

$$\Delta G_p = 35.09 - 27.40 = 7.69\, kJ / e^{-} eq \qquad \text{[eq. C-2];}$$

ΔG_{pc} is the energy required to convert pyruvate to cellular carbon, estimated to be

$$\Delta G_{pc} = 18.8\, kJ / e^{-}\, eq \qquad \text{[eq. C-3];}$$

The term ε was used to account for energy–transfer efficiency. Therefore, the total energy requirement for cell synthesis (ΔG_s) is

$$\Delta G_s = \frac{\Delta G_p + \Delta G_{pc}}{\varepsilon} \qquad \text{[eq. C-4].}$$

ΔG_r is the free energy released per each equivalent of sodium acetate oxidized for energy generation. To supply the energy required for cell synthesis (ΔG_s), *A* equivalents of sodium acetate must be oxidized, which yields $A\Delta G_r$. Assuming the same energy transfer efficiency as cell synthesis (ε), the energy balance is

$$\varepsilon A \Delta G_r + \Delta G_s = 0 \qquad \text{[eq. C-5],}$$

$$\therefore A = -\frac{\Delta G_s}{\varepsilon \Delta G_r} = -\frac{\frac{\Delta G_p + \Delta G_{pc}}{\varepsilon}}{\varepsilon \Delta G_r} = -\frac{\Delta G_p + \Delta G_{pc}}{\varepsilon^2 \Delta G_r} = -\frac{73.58\, kJ / e^{-}\, eq}{\Delta G_r} \qquad \text{[eq. C-6].}$$

At the anode, sodium acetate was oxidized to carbon dioxide and the electrons went from sodium acetate to the anode electrode. The free energy released from this process (ΔG_r) could be calculated from the difference of the reduction potentials between the CO_2/acetate redox couple ($E_{CO_2 / acetate} = -0.28 V$) and the anode (E_{anode}) [2] as follows:

$$\Delta G_r = \Delta G_r^{0'} + RT \ln \frac{([CO_2])^{1/8}([HCO_3^-])^{1/8}[H^+]}{([Ac^-])^{1/8}}$$
$$= -nF\Delta E_0^{'} + RT \ln \frac{([CO_2])^{1/8}([HCO_3^-])^{1/8}[H^+]}{([Ac^-])^{1/8}}$$
$$= -nF(E_{anode} - E^{'}_{0_{CO_2/acetate}}) + RT \ln \frac{([CO_2])^{1/8}([HCO_3^-])^{1/8}[H^+]}{([Ac^-])^{1/8}}$$
$$= -1 \cdot (96485\,\text{C/mol}) \cdot (E_{anode} - (-0.28\,\text{V})) + (8.314\,\text{J/(mol}\cdot\text{K)}) \cdot (303.15\text{K}) \ln \frac{([CO_2])^{1/8}([HCO_3^-])^{1/8}[H^+]}{([Ac^-])^{1/8}}.$$

[eq. C-7]

The values of E_{anode}, sodium acetate effluent concentration $[Ac^-]$, CO_2 produced from the oxidation of the sodium acetate, $[CO_2]$, $[HCO_3^-]$, and pH for C, CD, and CC reactors at a COD/N ratio of 13 are shown below:

	C	CD	CC
E_{anode} (V)	-0.254	-0.244	-0.250
$[Ac^-]$ (mol/L)	0.146	0.064	0.072
*$[CO_2]$ (mol/L)	0.0040	0.0053	0.0053
$[HCO_3^-]$ (mol/L)	0.00048	0.00056	0.00054
pH	7.23	7.28	7.30

*The calculation of $[CO_2]$ and $[HCO_3^-]$: CO_2 is produced from sodium acetate. We assume a portion X of the sodium acetate removed was converted to CO_2 and HCO_3^-. Therefore,

$$X = a \cdot f_{e1} + (1-a) \cdot f_{e2} = CE + f_{e2} - a \cdot f_{e2} = CE + 0.4 - 0.4a$$ [eq. C-8].

Since there is no headspace, we further assume that all CO_2 was converted to H_2CO_3. Hence, we have at 30 °C:

$$p\text{Ka} = \frac{[HCO_3^-][H^+]}{[H_2CO_3]} = 5.01187 \times 10^{-7}$$

$[H_2CO_3] + [HCO_3^-] = 2X(\Delta Ac^-)$ [eq. C-9, 10]

We used the trial and error method to solve this problem for *a* and the $[CO_2]$ and $[HCO_3^-]$ values.

Using the relationships $f_{e1} = \frac{A}{1+A}$, $f_{s1} = \frac{1}{1+A}$, and $a = CE / f_{e1}$, the ΔG_r, A, f_{e1}, f_{s1}, and a values of C, CD, and CC reactors were calculated as the following:

	C	CD	CC
ΔG_r (kJ/e$^-$ eq)	-46.60	-47.72	-47.20
A	1.579	1.542	1.556
f_{e1}	0.612	0.607	0.609
f_{s1}	0.388	0.393	0.391
a	0.282	0.235	0.278

The $v'_{NH_4^+}$ in the following cell synthesis reaction is $\frac{1}{20}$:

$\frac{1}{5}CO_2 + \frac{1}{20}HCO_3^- + \frac{1}{20}NH_4^+ + H^+ + e^- = \frac{1}{20}C_5H_7O_2N + \frac{9}{20}H_2O$, and the $v'_{CH_3COO^-}$ in the following reduction reaction is $\frac{1}{8}$:

$\frac{1}{8}CO_2 + \frac{1}{8}HCO_3^- + H^+ + e^- = \frac{1}{8}CH_3COO^- + \frac{3}{8}H_2O$.

Therefore, the stoichiometric relationship between NH_4^+ and CH_3COO^- in the system is

$\frac{v_{NH_4^+}}{v_{CH_3COO^-}} = a \cdot \frac{f_{s1} \cdot v'_{NH_4^+}}{v'_{CH_3COO^-}} + (1-a) \cdot \frac{f_{s2} \cdot v'_{NH_4^+}}{v'_{CH_3COO^-}}$, and the values were calculated as below:

	C	CD	CC

$v_{NH_4^+} / v_{CH_3COO^-}$	0.216	0.221	0.217

Literature cited

1. Bruce E. Rittmann, P.L.M., ed. Environmental biotechnology: principles and applications. 2001, McGraw-Hill Companies, Inc.

2. Madigan, M.T., Martinko, J.M., Brock: biology of microorganisims. 11 ed. 2006: Upper Saddle River: Person Prentice Hall.

Vita

Hengjing Yan was born in Hunan Province, China. After completing her high school study in 2004, she entered the Department of Environmental Science and Engineering of Tsinghua University, Beijing, China, and received the degree of Bachelor of Science there in July 2008. She attended Pennsylvania State University at University Park since August 2008 and obtained the degree of Master of Science there in the major of Environmental Engineering, in August 2010. She continued her graduate study in the same institution as a Ph.D. candidate since August 2010.

Permanent Email: yhjiris@gmail.com

This dissertation was typed by the author.